Eco-physiological study of the marine benthic diatom Amphora sp. : optimization of culture conditions for health, cosmetic and food applications

Mary Arnaldo

COLLEGE VEGETAL
DOCTORAL ANIMAL, ALIMENT
PAYS DE LA LOIRE MER, ENVIRONNEMENT

Nantes Université

THESE DE DOCTORAT

NANTES UNIVERSITÉ

ECOLE DOCTORALE N° 642
Ecole doctorale Végétal, Animal, Aliment, Mer, Environnement
Spécialité : Biologie et écologie marine

Par

Mary Dianne Grace ARNALDO

Eco-physiological study of the marine benthic diatom *Amphora* sp. : optimization of culture conditions for health, cosmetic and food applications

Thèse présentée et soutenue à Nantes, le 4 décembre 2023
Unité de recherche : ISOMer - UR 21 60

Rapporteurs avant soutenance :

Philippe Soudant	Directeur de Recherche CNRS, Université de Bretagne Occidentale
Jean-François Briand	MCU-HDR, Université de Toulon

Composition du Jury :

Président :	Olivier Gonçalves	Professeur, Nantes Université
Examinateurs :	Freddy Guihéneuf	Directeur Scientifique (CSO), SAS inalve
Dir. de thèse :	Gaëtane Wielgosz-Collin	Professeure, Nantes Université
Co-dir. de thèse :	Vona Méléder	Professeure, Nantes Université

Invité(s)

Co-encadrante	Aurélie Mossion	MCU, Nantes Université

Our greatest glory is not in never falling, but in rising every time we fall.

-Confucius

Acknowledgements

I would like to thank all the members of the jury for having done me the honor of agreeing to evaluate this work, Dr. Philippe Soudant and Dr. Jean-François Briand as rapporteurs and Dr. Olivier Gonçalves and Dr. Freddy Guihéneuf as examiners.

I would like to thank all the people who helped me carry out this work, in particular my thesis supervisors Gaëtane Wielgosz-Collin, Vona Méléder, and Aurélie MOSSION, who gave me the opportunity to carry out this research and who went above and beyond in supporting me through these years until the end of my PhD.

I thank all the members of the ISOMer laboratory, who have been really helpful to me in any way they can. To Vony Rabesaotra for her technical help in lipid extraction analysis, Alexandra Petit and Philippe Rosa for always making sure I have what I need for my experiments, Dr. Paul Déléris for his help and expertise in genetics, and Dr. Bruno Jesus for helping me with my fluorescence analysis. Very big thanks to my interns, most especially Agathe Jaffrenou and Nadeeshani Dehel Gamage, who have been instrumental to my data gathering.

I would equally like to thank the Synoxis team, Thierry, Hugo, and Amélie who welcomed me to their facilities with open arms to build and improve the PSBR.

I also would like to dedicate this manuscript to my family and friends, who have been my rock during this challenging period. To my husband, Ronan, for always being there for me through it all, thank you. To my mom, and grandma whose love, faith, and support have brought me to where I am today. To my cousins Clyde and Carlin for taking care of everyone while I'm away reaching for my dreams. To my Bahuaud family, especially to Françoise and Jacques, who always treat me lovingly and kindly. To nang Cheche and family for welcoming me with open arms. Last but not the least, to my angels in heaven (nonoy Carl, Papa, and Erick) whom I painfully miss every day. I love you all very much. I hope I make you proud.

Table of Contents

List of Publications and Communications

Publications

2023 – Book chapter (awaiting publication) – Arnaldo MDG, Mossion A, Beignon T, Vuillemin H, Guihéneuf F, Wielgosz-Collin G, Méléder V. Diatom biofilm: ecology and cultivation from laboratory to industrial level, in *Diatom Photosynthesis: From Primary Production to High Value Molecules.* (eds.Goessling, J.W., Serôdio, J., and Lavaud, J.), Wiley Scrivener, Beverly, Mass.

2023 – Publication – Arnaldo, M.D.G., Gamage, N.D., Jaffrenou, A., Rabesaotra, V., Mossion, A., Wielgosz-Collin, G., Méléder, V., 2024. Comparison of different small-scale cultivation methods towards the valorization of a marine benthic diatom strain for lipid production. Algal Research 77, 103327.

2023 – Publication (in writing) – Arnaldo MDG, Rabesaotra V, Mossion A, Wielgosz-Collin G, Méléder V. Effect of light quality on *Amphora* sp. NCC169 biomass and total lipid rate in porous substrate photobioreactor.

Scientific communications

2023 – Poster – Biofilm Porous Substrate Photobioreactor. Arnaldo MDG, Gamage DGND, Mossion A, Wielgosz-Collin G, Beignon T, Vuillemin H, Méléder V. 8th European Phycological Congress, 20-26 August 2023, Brest, France.

2023 – Oral Communication– Arnaldo MDG, Gamage DGND, Mossion A, Wielgosz-Collin G, Méléder V. Culture en biofilm et approche écophysiologique pour l'optimisation de la production lipidique de souches de diatomées benthiques ligériennes. Journée de restitution des travaux d'etudes, 9 juin 2023, Saint-Nazaire, France.

2022 – E-Poster – Arnaldo MDG, Mossion A, Cointet E, Gamage DGND, Beignon T, Vuillemin H, Wielgosz-Collin G, Méléder V. Optimizing high value lipid production of *Amphora* sp. NCC169 from North-East Atlantic mudflats using porous substrate photobioreactor. Young Algaeneers Symposium, 19 June 2022, online.

2022 – Oral Communication – Arnaldo MDG, Mossion A, Cointet E, Gamage DGND, Beignon T, Vuillemin H, Wielgosz-Collin G, Méléder V. Optimizing high value lipid production of *Amphora* sp. NCC169 from North-East Atlantic mudflats using porous substrate photobioreactor. 29èmes journées de la Réunion annuelle de l'Association des Enseignants Chercheurs de Chimie Physique et Chimie Minérale des Facultés de Pharmacie, 9-10 June 2022, Lille, France.

2022 – Communication Orale – Arnaldo MDG, Mossion A, Cointet E, Gamage DGND, Beignon T, Vuillemin H, Wielgosz-Collin G, Méléder V. Optimizing high value lipid production of *Amphora* sp. NCC169 from North-East Atlantic mudflats using porous substrate photobioreactor. Les Journées Scientifiques, 3 June 2022, Nantes, France.

2021 – E-Poster – Arnaldo MDG, Mossion A, Cointet E, Gamage DGND, Beignon T, Vuillemin H, Wielgosz-Collin G, Méléder V. Optimizing high value lipid production of *Amphora* sp. NCC169 from North-East Atlantic mudflats using porous substrate photobioreactor. AlgaEurope, 7-10 December 2021, online.

2021 – Oral Communication– Arnaldo MDG, Mossion A, Cointet E, Gamage DGND, Beignon T, Vuillemin H, Wielgosz-Collin G, Méléder V. Optimizing high value lipid production of *Amphora* sp. NCC169 from North-East Atlantic mudflats using porous substrate photobioreactor. Lipids in the Ocean, 5-7 July 2021, online.

List of Figures

Introduction and Objectives of the Study

What are diatoms?

Eukaryotic marine and freshwater microalgae (i.e., phytoplankton, microphytobentos or periphyton, depending of their life-growth (Borowitzka, 2018; Wehr et al., 2015)) are crucial in driving key biogeochemical cycles (e.g., oxygen generation, nutrient recycling, atmospheric CO_2 removal, calcification) and in the provision of organic biomass for nearly all aquatic life (Benoiston et al., 2017). Amongst different groups of microalgae, diatoms, dinoflagellates, and coccolithophores primarily dominate the eutrophic coastal and continental shelf waters (Not et al., 2012).

Diatoms are a type of unicellular microalgae belonging to the phylum Bacillariophyta. They are postulated to have emerged during the late Permian to early Mesozoic era roughly 150 to 200 million years ago (Guillou et al., 1999; Kooistra et al., 2007; Medlin, 2016). The Cretaceous period represents a crucial time in the evolutionary history of diatoms, during which their diversification led to the emergence of three major clades that had a significant impact on their phylogenetic development: Coscinodiscophyceae which emerged during the Jurassic period, Mediophyceae which emerged in the early Cretaceous period, and Bacillariophyceae which emerged in the late Cretaceous period (Kooistra et al., 2007; Medlin, 2016). Interestingly, the major extinction event that occurred at the K-T boundary did not have a significant negative impact on diatoms, as they continued to diversify thereafter into well over 250 extant genera (Kooistra et al., 2007; Mann and Vanormelingen, 2013).

Diatoms are distinguished from other heterokonts by several unique characteristics, such as their ability to thrive in both marine and freshwater environments, their two overlapping cell structure, the lack of transitional helix in flagellum, their ring-shaped chloroplast DNA, and their diplontic life cycle in sexually reproducible species (Kumar et al., 2015). Most importantly, they are recognizable for their unique, glass-like exoskeletons made up of silica.

Diatoms flourish in virtually every aquatic environment. In lotic (e.g., rivers, streams, creeks, brooks) and lentic (e.g., lakes, ponds) freshwater systems, both plankton and periphyton play important roles, and the species composition changes in response to seasonal and anthropogenic changes in environmental parameters. In the marine environment, diatoms are mainly found in the upper layers of

water where photosynthesis is more conducive. Coastal and upwelling regions are dominated by diatoms where they play a crucial role in supporting productive fisheries. This is evidenced by extensive deposits of siliceous mud and oozes that have accumulated in these regions over geological time (Koizumi and Yamamoto, 2018).

Diatoms have adapted well to survive in conditions of limited resources, which makes them one of the pivotal groups of aquatic microalgae (Medlin, 2014; Rimet et al., 2019). The distribution and community structure of approximately 200,000 diatom species (Gordon et al., 2008; Mann and Droop, 1996) are manifestations of their evolutionary adjustments to particular ecological niches . For example, certain diatoms have acquired the ability to regulate their buoyancy, thereby enabling them to manipulate their position in the water column and optimize their access to light and nutrients (Du Clos et al., 2021). Conversely, other species have developed survival strategies to thrive in dimly lit conditions, such as in deep and/or murky waters (Hofmann et al., 2020; Shi et al., 2016). High latitude and polar environments are heavily reliant on diatoms for primary production due to the scarcity of resilient species (Dutkiewicz et al., 2015). On the other hand, despite their resilience towards variations in environmental conditions, diatoms are actually very sensitive to environmental changes. This trait makes them valuable bioindicators in monitoring water quality and assessing the overall health of aquatic ecosystems (Lobo et al., 2016; Salmaso et al., 2019).

Morphology

Diatoms possess distinct and complex silica cell walls termed ‘frustules’ that set them apart from other photosynthetic microorganisms. The species-specific morphology of these frustules characterizes the diversity and complexity of diatoms, making them the cornerstone of diatom taxonomy (McNair et al., 2018; Zimmermann et al., 2014) (Figure 1). Diatoms exhibit a wide variation in cell size, encompassing both small species (e.g., *Minidiscus* spp., 1.5 µm) and larger ones (e.g., *Ethmodiscus* spp., 2 mm) (Leblanc et al., 2018; Snoeijs et al., 2002).

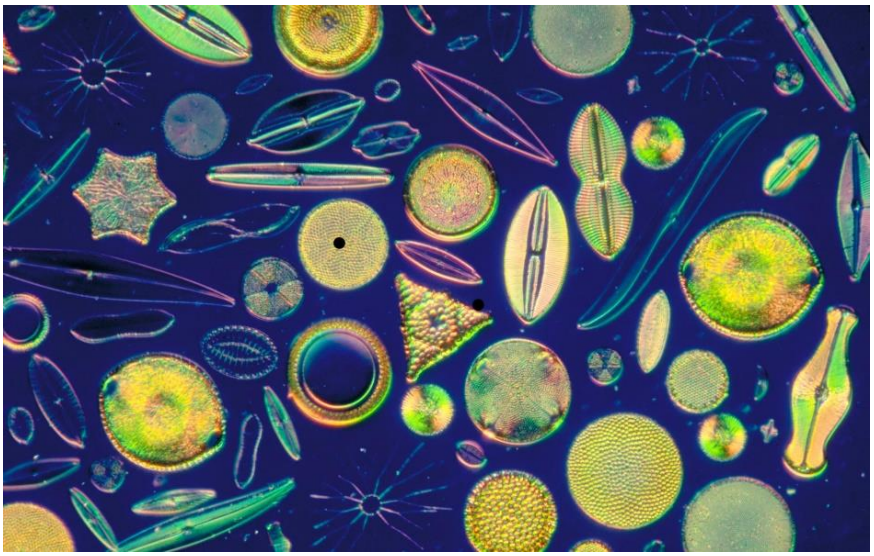

Figure 1 Diatom frustules exhibit a remarkable diversity in shape and structure, reflecting the vast array of species within the group (Carolina Biological Supply Company, n.d.).

Diatoms directly uptake soluble monosilicic acid [($Si(OH_4)$] from the surrounding environment and polymerizes it to form siliceous (SiO_2) frustules (Kolbe and Brunner, 2022). A frustule consists of two overlapping valves (thecae) called the epitheca (bigger upper half) and the hypotheca (smaller lower half) in a Petri dish-like fashion (Figure 2). These valves are connected by a number of hoop-like or segmental girdle bands which allow for the expansion of the rigid frustule during cell division (Goessling et al., 2019). The valve surfaces are lined with a stria of pores called areolae that facilitate selective exchange and absorption of substances between the diatom and its environment.

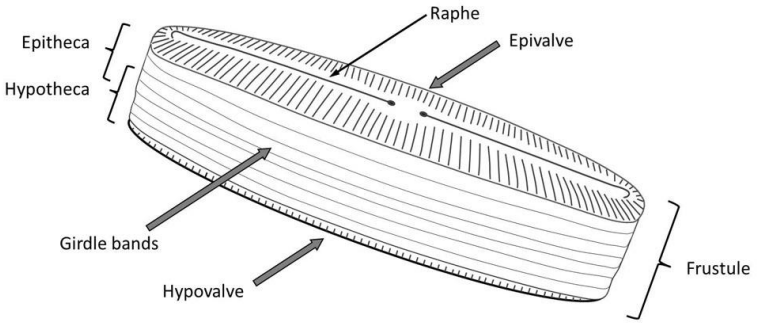

Figure 2 Diagram of a pennate diatom structure showing the basic external parts of the cell wall. Digital illustration from www.diatoms.de.

Frustules are significant components of diatoms, constituting up to 50-60% of the cell's dry biomass (Bayu et al., 2020). They serve as a remarkable manifestation of a diatoms' ability to evolve and acquire new biological traits, allowing them to thrive in different ecological niches and increase chances of survival and reproductive success. For instance, the morphological evolution of diatom silica frustules, characterized by increased mass and enhanced sinking rates, has conferred upon diatoms a competitive advantage in aquatic ecosystems (Smetacek, 1985). Specifically, this evolutionary adaptation facilitates diatoms' vertical migration within the water column that enables access to nutrient-dense strata that remain out of reach for less dense phytoplankton species (Behrenfeld et al., 2021; Du Clos et al., 2021). Frustules are crucial in maintaining the organism’s overall structural integrity, mechanical safeguarding (Hamm et al., 2003), photosynthesis (Goessling et al., 2018), and nutrient exchange (Mitchell et al., 2013). Moreover, diatoms are critical resources in paleoecological studies due to the frustules’ remarkable durability and resistance to decay and deterioration (Harding and Chant, 2000; Philippe et al., 1994).

Diatoms can be broadly divided into two main categories based on overall frustule structure: centric and pennate (Medlin, 2009). This classification is indicative of the variations in their morphology and has implications for their phylogeny. Centric diatoms are radial or circular in symmetry and are typically found drifting freely (planktonic) in marine habitats. They are considered to be the more ancient group, with fossil records dating back to the Jurassic period. Pennate diatoms, on the other hand, are bilaterally symmetric and reside on solid substrates (benthic). Pennate diatoms are believed to have emerged through an evolutionary divergence from centric diatoms with the development of the raphe (Figure 2), a slit-like structure that enables pennates to excrete mucilaginous substances and navigate across surfaces. Certain members of the pennate group, however, are immobile as a result of lacking the raphe system (Babenko et al., 2022). Recent genetic and molecular studies have revealed new insights into the phylogeny of diatoms, challenging the traditional distinction between centric and pennate species (Davidovich et al., 2017; Sato et al., 2020). Several scientists argue for a revised classification system in light of new genetic and molecular evidence (Williams and Kociolek, 2011, 2007) while others maintain the use of terms centric and pennate for use in the descriptive or morphological sense despite their paraphyletic nature (Medlin, 2009). This ongoing debate highlights conflicting perspectives

between traditional morphological classifications and the nuanced relationships revealed by contemporary phylogenetic studies.

The diverse and species-specific shapes and pore patterns of diatom cell walls became the fascination and preferred test objects for microscope lenses in the 19th century (Round et al., 1990). Since then, the applications of diatom frustules have undergone substantial expansion. Apart from its utilization as diatomaceous earth, which consists of fossilized diatom biosilica and is commonly employed in the manufacturing of insecticides, toothpastes, and water filtration systems (Ediz et al., 2010; Ghobara et al., 2019; Losic and Korunic, 2017; Marchan et al., 2023), the distinctive physical properties of frustules have been harnessed in diverse fields such as microtechnology, nanotechnology, and biotechnology and have been comprehensively reviewed and synthesized by several authors (De Tommasi and De Luca, 2022; Ghobara et al., 2019; Korsunsky et al., 2020; Rabiee et al., 2021; Sharma et al., 2021). For example, the silica shells of centric diatoms have been successfully used as microlenses to focus light beyond diffraction limits, as shown in research by De Tommasi et al. in 2010. The photoluminescent properties of these shells have been utilized in the creation of optical sensors, biosensors, and random lasers (De Angelis et al., 2016). Moreover, when coated with metals, these diatom shells have been proven to be effective nanostructured surfaces for plasmonic applications (De Tommasi and De Luca, 2022). Functionalized diatomite nanoparticles have also been considered as highly suitable carriers in drug delivery systems due to their high surface area, biocompatibility, and enhanced capacity for drug loading (Delalat et al., 2015). There are also exciting possibilities in modifying these frustules, such as the metabolic insertion of germanium or titanium oxides to create efficient nanostructured semiconducting devices suitable for optoelectronics (Ragni et al., 2017).

Reproduction and life cycle

A diatom exhibits captivating and complex developmental changes as the cell passes from its initial state to the next generation. It has a life cycle that features the duality of both asexual (mitotic) and sexual (meiotic) reproduction methods (Figure 3) (Fusco and Minelli, 2019; Kaczmarska et al., 2013). Unlike many algal groups, diatoms are predominantly diploid in all stages of their life, where each cell

contains two sets of chromosomes. This reproductive strategy significantly contributes to their genetic variability and ecological success across diverse habitats over the past millions of years.

Asexual binary fission is the most prevalent method of reproduction in diatoms. This process begins when a diatom cell divides and generates two daughter cells. During cell division, each of the two daughter cells inherits one valve of the parent cell's frustule, functioning as an epitheca. The daughter cells subsequently synthesize their own respective hypotheca from scratch to complete the frustule. Due to the rigid nature of silica, new hypotheca elements (e.g., valves and girdle bands) and the hypotheca *per se* are smaller than the parent's. A series of unbroken mitotic divisions can continue for months or years, inevitably resulting in a progressive reduction in cell size. Once a diatom cell reaches a critically minimal size, diminution is reversed by either vegetative cell enlargement or auxosporulation to uphold genetic diversity within the population (Kaczmarska et al., 2013).

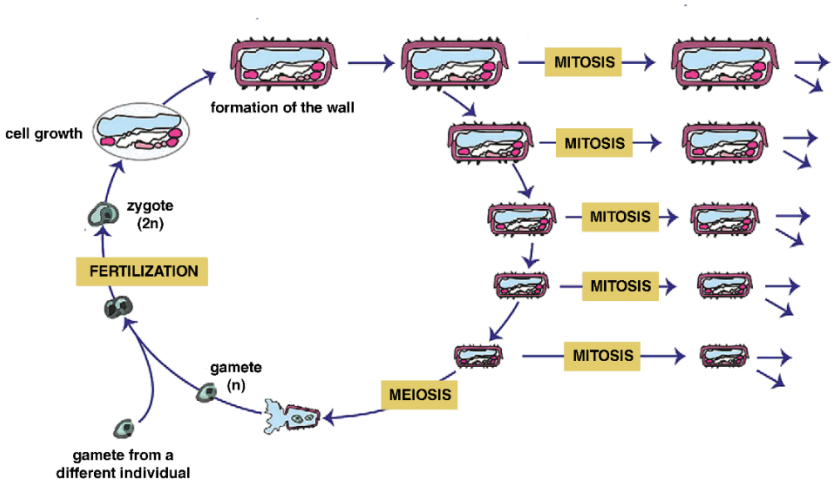

Figure 3 Life cycle of a diatom showing both asexual and sexual life stages. The process initiates with a vegetative cell undergoing consecutive rounds of mitotic divisions, resulting in a series of smaller cells. As the diatom's cell size decreases to a critical minimum level, the diatom transitions to the sexual reproduction phase. This phase is characterized by meiosis that produces gametes, followed by fertilization, resulting in the formation of a zygote. The zygote then grows into a new vegetative cell of maximum size, completing the cycle. Diagram adapted from Fusco and Minelli (2019).

Sexual reproduction in diatoms is an infrequent yet essential process that is triggered by specific environmental or population cues. The nature of these factors are not thoroughly understood, but in

general, it involves the occurrence of cells below the critical size threshold and/or the presence of sexually differentiated cells within the population (Poulíčková and Mann, 2019). Sexual reproduction was shown to be induced by environmental triggers such as light conditions, temperature and nutrient levels (Davidovich et al., 2018; Moore et al., 2017; Mouget et al., 2009). A fundamental difference in sexual reproduction occurs between centric and pennate diatoms: centrics typically exhibit oogamous/anisogamous auxosporulation while pennates are morphologically isogamous (though sometimes anisogamous) and never produce sperm (Poulíčková and Mann, 2019). This means that centric diatoms have differentiated gametocytes and produce large eggs and biflagellate sperms. Fertilization occurs when a sperm successfully penetrates the egg, resulting in the formation of new zygotes. These zygotes can then either transform into auxospores that grow into maximum-sized diatom cells or into resting/dormant spores during unfavorable conditions. On the other hand, sexual reproduction in pennate diatoms involves direct contact and fusion between gametangial cells. This fusion gives rise to a zygospore that subsequently germinates into a new fully formed diploid diatoms.

The capacity of diatoms to transition between asexual and sexual reproduction is a strong indicator of their resilience in diverse habitats. Their mechanisms enable them to proliferate under favorable conditions, making the most out of the available resources at their disposal. Conversely, sexual reproduction, albeit more energy- and time- demanding, introduces genetic variability within the existing population. This genetic diversity plays a crucial role in the diatoms' ability to respond and survive despite the shifts and fluctuations in their environment (Rynearson et al., 2022). Inducing sexual reproduction in diatoms is paramount in their conservation, genetic diversity, and long-term viability in culture collections.

Photosynthetic pathways: a diatom perspective

In diatoms, photosynthesis assumes utmost importance as it plays a crucial role in the global carbon cycle, substantially aiding in the capture of carbon dioxide and generation of dioxygen. Unlike land plants, diatoms have evolved distinct adaptations to the aquatic environment, which augment their photosynthetic efficacy and exert a profound influence on global biogeochemical cycles. Diatoms are deemed to be one of the most important groups of microalgae, contributing around 40% of the overall

primary production in the modern oceans, and their impact on the global process of photosynthesis is equivalent to the combined impact of all rainforests on land (Benoiston et al., 2017).

Chloroplast

Like any other eukaryotic organism, chemical reactions involved in diatom photosynthesis occur within their chloroplasts, serving as sites for the initial steps of fatty acid production. Nevertheless, a diatom chloroplast possesses distinct characteristics that showcase their evolutionary history, setting them apart from chlorophytes and terrestrial plants.

The number, arrangement, and morphology of chloroplasts vary according to diatom genera and species (Ghobara et al., 2019; Mann and Droop, 1996). The diatom chloroplast is enveloped by four highly-packed membranes within the cell as a consequence of a two-step endosymbiotic event (Figure 4) (Benoiston et al., 2017; Scarsini et al., 2019). At the core of the chloroplast lies a proteinaceous body called a 'pyrenoid' that is usually penetrated by two thylakoid membranes. The multiple layers of thylakoid membranes in the chloroplast house pigment-protein complexes responsible for light capture. The aqueous phase surrounding the thylakoids, called the stroma, contains soluble proteins that generating energy through biochemical reactions and serve as chemical reductants. Additionally, the stroma contains essential components such as DNA, ribosomes, RNA and all the enzymes required for transcription and translation of the chloroplast genome.

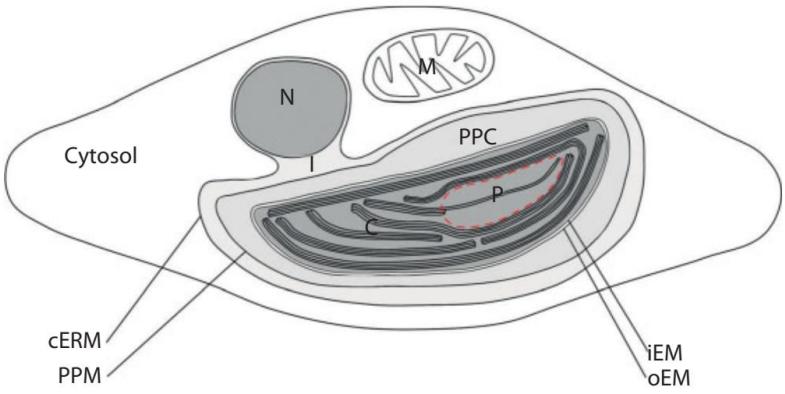

Figure 4 Schematic diagram of the secondary plastid in diatoms. The plastid is enclosed by a total of four membranes: the chloroplast endoplasmic reticulum membrane (cERM), the periplastic membrane

(PPM), the outer envelope membrane (oEM), and the inner envelope membrane (iEM). Within the chloroplast (C), there thylakoids, while the pyrenoid (P) is delimited by dashed lines. I: isthmus, M: mitochondrion, N: nucleus. Illustration from Scarsini et al. (2019).

Upon the uptake of the symbiont, a massive gene transfer to the nucleus occurred and the symbiont became an integral part of the newly generated cell (Benoiston et al., 2017). This interplay between the chloroplast and nuclear genomes is a defining characteristic of the secondary endosymbiotic origin of diatom chloroplasts and is pivotal for their function and regulation.

Pigments

Diatoms consist of two types of pigments within the chloroplast: chlorophylls and carotenoids (Kuczynska et al., 2015). The primary function of these pigments is to absorb and convert light energy into chemical energy via photosynthesis. These pigments serve as basic components that fuel the cells' metabolic processes, as well as impart the diatoms with a characteristic brown or golden-brown hue (Bertrand, 2010).

Diatoms contain chlorophyll *a* (Chl *a*), a universal pigment across all photosynthetic organisms (Figure 5). This pigment principally absorbs light in the blue (~430 nm) and red (~662 nm) bands of the electromagnetic spectrum. Chlorophyll *c* (Chl c_1, c_2, and c_3) participates as an accessory pigment which augments photosynthetic efficiency by absorbing light in the blue-green to yellow-green bands (Kuczynska et al., 2015).

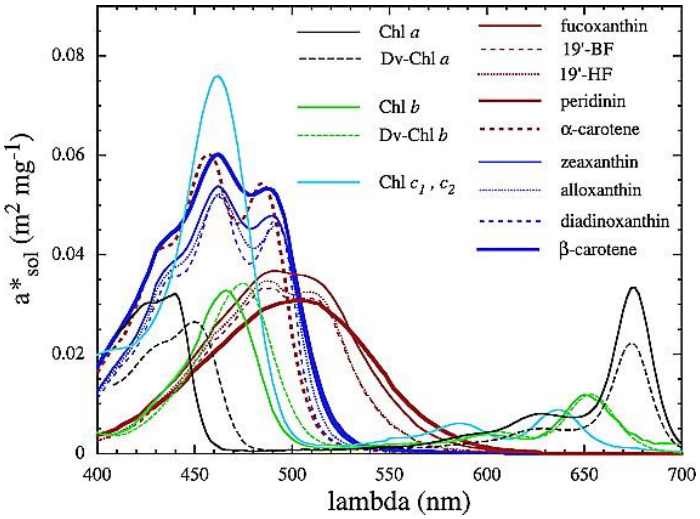

Figure 5 Spectral absorption properties of different microalgal pigments in oceanic waters. The graph presents the specific absorption coefficients of chlorophyll *a* (Chl *a*), chlorophyll *c* (Chl c_1, c_2), and accessory pigments such as fucoxanthin, 19'-hexanoyloxyfucoxanthin (19'-HF), peridinin, diadinoxanthin, and β-carotene across the visible light spectrum (400-700 nm). Each pigment exhibits distinctive absorption peaks, demonstrating their respective roles in capturing light energy for photosynthesis. Data obtained from Lain and Bernard (2018).

Seven kinds of carotenoids are present in diatoms, namely diadinoxanthin (Ddx), diatoxanthin (Dtx), violaxanthin (Vx), antheraxanthin (Ax), zeaxanthin (Zx), β-carotene (β-car), and fucoxanthin (Fx), and amongst them, fucoxanthin being the most dominant (Kuczynska et al., 2015). Carotenoids play a dual role: as an accessory pigment, they absorb light in the green to blue-green spectrum (between 400 and 560 nm), regions poorly absorbed by chlorophylls, and transfer the captured energy to chlorophyll *a* for photosynthesis (Figure 5). Furthermore, carotenoids like diadinoxanthin and diatoxanthin are integral in a photoprotection mechanism known as non-photochemical quenching (NPQ) through the xanthophyll cycle (Bertrand, 2010). These pigments dissipate excess light energy as heat by the de-epoxidation of the diadinoxanthin into diatoxanthin, protecting diatoms from photo-oxidative stress, which can occur when the light energy absorbed exceeds the capacity of the photosynthetic apparatus to utilize it. Conversely, under low light condition, the reversed process occurs: the epoxidation of the diatoxanthin into diadinoxanthin.

The absorption spectra of diatom pigments are a testament to their strategic evolutionary adaptation to prevailing light environments (Croteau et al., 2021; De Tommasi et al., 2021). Diatoms can regulate the quantity and proportions of these pigments in response to changing light scenarios, allowing them to use a wider range of wavelengths than many other photosynthetic species (Nicklisch, 1998). Therefore, the absolute and/or relative ratios of pigments may fluctuate according to the taxon and ecophysiology of the cells.

Diatom pigments also have profound ecological and biogeochemical implications. As one of the most prolific and highly productive group of microalgae, diatoms significantly contribute to the global biological pump (Cavicchioli et al., 2019). The versatility and resilience bestowed by these pigments allow diatoms to flourish in habitats ranging from brightly-illuminated surface waters to low-light polar conditions (Bojko et al., 2019; Nicklisch, 1998; Wulff et al., 2008). When the diatoms die off, they sink to the ocean floor, effectively sequestering carbon into the sediment below.

The electron transport chain (ETC)

Diatoms undergo photosynthesis in two distinct phases: the light-dependent reactions (Figure 6) and the Calvin cycle (Figure 7).

The light-dependent reaction is facilitated by the electron transport chain (ETC) taking place within chloroplasts' thylakoid membranes. The ETC process is triggered when the photosystem II (PSII) absorbs light. The core of PSII contains a reaction center comprising a Chl *a* molecule (P680) that has an absorption peak of 680 nm. As P680 absorbs light, it gets excited and subsequently transfers electrons to the primary electron acceptor. The electrons lost by P680 are replenished by the photolysis at PSII.

Once extracted from water, electrons from PSII moves to the cytochrome b_6f complex (Cyt b_6f) through the mobile electron carrier plastoquinone (PQ). PQ effectively engages in a process of redox cycling, shuttling electrons back and forth between PSII and the Cyt b_6f. Simultaneously, PQ transports protons into the thylakoid lumen which contributes to the establishment of a proton gradient across the thylakoid membrane. These protons are subsequently utilized by ATP synthase to produce ATP through phosphorylation.

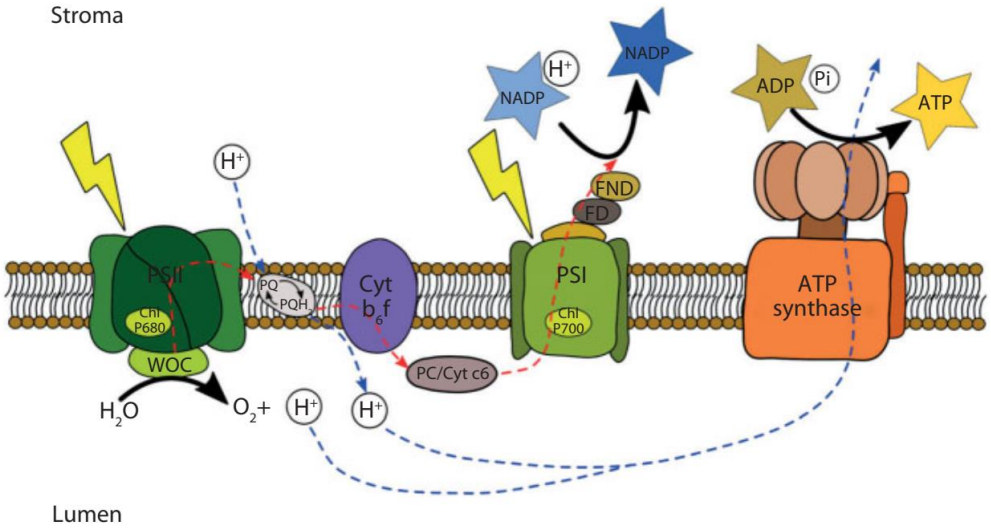

Figure 6 The diagram illustrates the thylakoid membrane, which consists of various components involved in the electron transport chain (ETC). The dashed red lines indicate the linear pathway of electron transport, commencing from water and concluding at NADPH. The dashed blue lines represent the transfer of protons, with the proton gradient between the stroma and lumen being produced by the electron transport chain. Illustration from Scarsini et al. (2019).

The transfer of electrons from the Cyt b_6f to photosystem I (PSI) occurs through the involvement of plastocyanin (Cyt c6). This copper-containing protein acts as a mediator for electron transport across the thylakoid lumen. PSI, which harbors the reaction center Chl *a* molecule P700, absorbs light and harnesses its energy to further stimulate the electrons transferred by Cyt c6. These highly energized electrons are then utilized to convert $NADP^+$ to NADPH. This conversion process is facilitated by the enzyme ferredoxin-$NADP^+$ reductase located on the stromal side of the thylakoid membrane.

The Calvin cycle

The Calvin cycle, also referred to as the C3 pathway, is distinguished by its methodical mechanism which effectively utilizes the chemical energy stored in ATP and NADPH produced in the light-dependent reactions of photosynthesis. The cycle progresses through three clearly defined stages: carbon fixation, reduction, and the restoration of the CO_2 acceptor, ribulose-1,5-bisphosphate (RuBP) (Figure **7**).

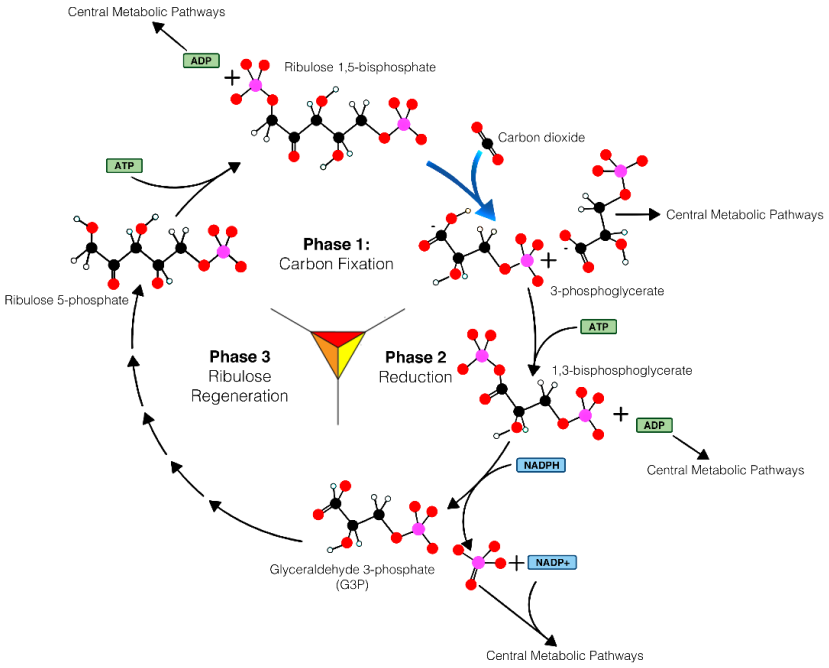

Figure 7 Simplified illustration of the Calvin cycle representing the biochemical pathway by which atmospheric CO_2 is fixed to form organic molecules. Diagram adapted from Jones (2005).

After carbon fixation, the cycle proceeds to the reduction phase, where the 3-PGA molecules undergo a series of enzymatic transformations. Initially, ATP is utilized to phosphorylate 3-PGA, resulting in its conversion to 1,3-bisphosphoglycerate (1,3-BPG). Subsequently, NADPH supplies electrons to 1,3-BPG, leading to the generation of glyceraldehyde-3-phosphate (G3P), a sugar containing three carbon atoms. This step is crucial as it represents the first instance in which the fixed carbon is reduced to a higher energy level and lower oxidation state, enabling the synthesis of glucose and other carbohydrates. For every three molecules of CO_2 fixed, six molecules of G3P are produced. However, only one molecule of G3P can be considered a net gain, as the remaining molecules are needed for the regeneration of RuBP, ensuring the continuity of the cycle.

The last stage of the Calvin cycle is characterized by the restoration of RuBP, which allows for the continuous functioning of the cycle. This intricate procedure involves a sequence of enzymatic reactions that restructure the carbon frameworks of five G3P molecules in order to generate three RuBP molecules, utilizing ATP in the procedure.

The Calvin cycle is not a self-contained process but is rather closely interconnected with various metabolic pathways in the cell. The resulting G3P molecule can be utilized in various biosynthetic pathways, such as the production of lipids.

The dynamics of lipid production in diatoms

Diatoms contain a complex and diverse set of hydrophobic or amphiphilic molecules that play vital functions in the cellular structure and metabolism. They are critical components of the cell membranes as they affect the organism's fluidity and permeability against environmental contributors. The presence of lipids in diatoms can impact buoyancy, consequently affecting their vertical distribution in the water column and accessibility to available light and nutrients. They are pivotal in the biosynthesis of pigments for photosynthesis. Lipids also contribute to diatom defense mechanisms, such as the synthesis of oxylipins, which can serve as deterrents to predators and exert influence on the dynamics of marine food webs (Fontana et al., 2007; Russo et al., 2019). Additionally, specific lipids act as signaling molecules that help regulate growth, reproduction, and responses to environmental conditions.

Diatoms are characterized by their ability to produce highly elongated polyunsaturated fatty acids (PUFAs) such as eicosapentaenoic acid (EPA, 20:5ω3) and docosahexaenoic acid (DHA, 22:6ω3) (Tanaka et al., 2022). The presence of PUFAs in the cell membrane and lipid droplets is crucial for signalling, membrane fluidity and photosynthetic electron transport (Büchel et al., 2022; Fontana et al., 2007; Orefice et al., 2022; Wiktorowska-Owczarek et al., 2015). Their accumulation serves as energy storage and may play a fascinating role in buoyancy and defense mechanisms (Tanaka et al., 2022).

Lipids found in diatoms can be generally classified into neutral lipids, glycolipids, and phospholipids (Figure 8). Their precise subcellular localizations remain ambiguous owing to the intricate membrane structure of chloroplasts arising from secondary symbiosis (Tanaka et al., 2022).

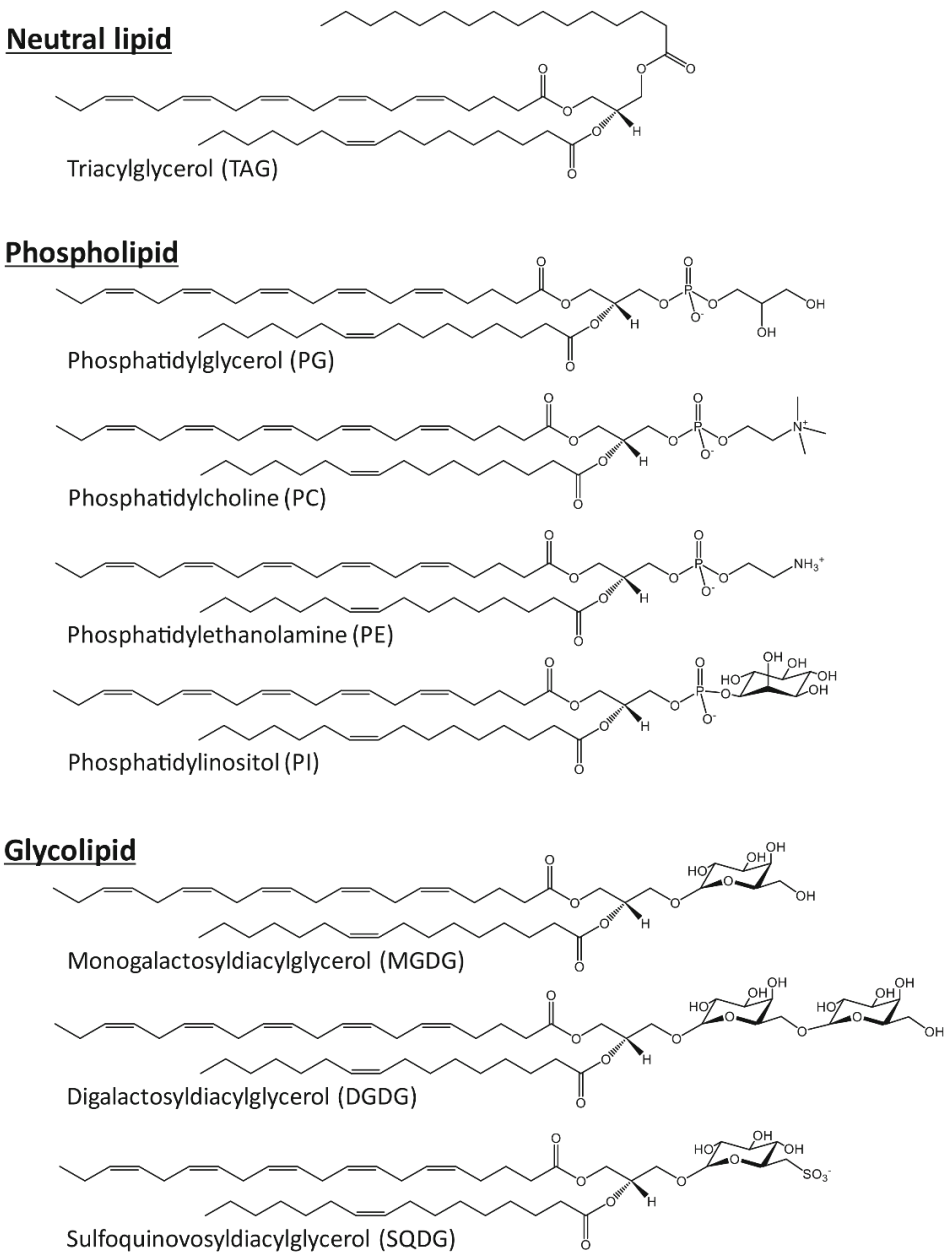

Figure 8 Molecular compositions of lipids commonly present in diatoms. Diagram from Tanaka et al. (2022).

Neutral lipids, mainly in the form of triacylglycerols (TAGs), are the primary source of energy storage and are significantly accumulated during periods of nutrient stress. TAG synthesis is typically thought to occur in the ER. However, several studies suggest another pathway exists in diatom chloroplasts (Balamurugan et al., 2017; Fan et al., 2011; Niu et al., 2013).

Glycolipids such as sulfoquinovosyldiacylglycerol (SQDG), monogalactosyldiacylglycerol (MGDG), and digalactosyldiacylglycerol (DGDG) are found in the thylakoid membranes of chloroplasts. They play essential roles in cellular structure, energy storage, and stress responses. These molecules consist of a lipid moiety linked to a carbohydrate group, which can serve as recognition sites for intercellular interactions and signalling. This can be important in the formation of biofilms with other microorganisms in the benthos and in the response to environmental cues (Laviale et al., 2019).

Phospholipids are generally characterized by a glycerol backbone, two fatty acid chains, and a phosphate group linked to a polar head group, which imparts them with both hydrophobic and hydrophilic properties. Their amphiphilic nature allows the formation of lipid bilayers that are vital for the transport and delivery of molecules between different cellular compartments. As such, they can be found throughout the cell in the plasma membrane and the membranes of various organelles, including the endoplasmic reticulum where they are produced and distributed from.

The manipulation of metabolic pathways involved in diatom lipid synthesis is a prominent area of research in the biotechnology industry due to its ability to increase the production of TAGs for use as biofuel feedstock, as well as long-chain and very long-chain polyunsaturated fatty acids (LC- and VLC-PUFAs) like eicosapentaenoic acid (EPA) and docosahexaenoic acid (DHA). These fatty acids are commonly found in human dietary supplements and are essential components of aquaculture feeds.

Metabolic pathways

Fatty acids serve as fundamental constituents of neutral lipids, phospholipids, glycolipids, and act as progenitors for fatty acid-derived compounds. These acids are biosynthesized *de novo* within the chloroplasts of diatoms (Figure 9). Fatty acid synthesis (FAS) initiates with the transformation of acetyl-CoA into malonyl-coenzyme A (CoA) through the action of acetyl-CoA carboxylase (ACC). Malonyl-CoA is then converted to malonyl-acyl carrier protein (malonyl-ACP) by malonyl-CoA-ACP transacylase (MAT). The acyl chain elongation cycle begins with β-ketoacyl-ACP synthase (KAS) combining malonyl-ACP and acetyl-CoA to form keto-acyl-ACP. This compound is reduced to hydroxy-acyl-ACP by β-ketoacyl-ACP reductase (KAR). The hydroxy-acyl-ACP undergoes dehydration via β-hydroxyacyl-ACP dehydrase (HAD) to produce trans-enoyl-ACP. Enoyl-ACP reductase (EAR) then

reduces the double bond in trans-enoyl-ACP, resulting in acyl-ACP. This acyl-ACP is further elongated by KAS using malonyl-ACP. The cycle concludes with acyl-ACP thioesterase (TE) hydrolyzing acyl-ACP thioester bonds, releasing free fatty acids. Newly synthesized fatty acids can be incorporated into TAGs or other lipid classes within the endoplasmic reticulum (ER) of the cell (Tanaka et al., 2022).

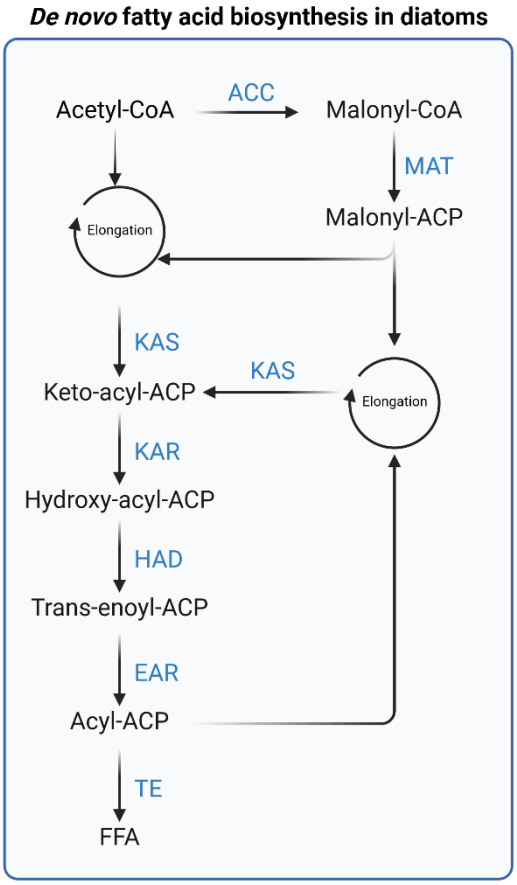

Figure 9 Schematic representation of the fatty acid biosynthesis pathway. This figure illustrates the enzymatic conversion of acetyl-CoA into free fatty acids (FFA) through a series of reactions involving the enzymes acetyl-CoA carboxylase (ACC), malonyl-CoA-ACP transacylase (MAT), β-ketoacyl-ACP synthase (KAS), β-ketoacyl-ACP reductase (KAR), hydroxyacyl-ACP dehydrase (HAD), enoyl-ACP reductase (EAR), and acyl-ACP thioesterase (TE).

The synthesis of neutral lipids in diatoms, mainly in the form of triacylglycerols (TAGs), can be categorized into two main pathways: the acyl-CoA-dependent or Kennedy pathway, and the acyl-CoA-independent or de novo synthesis pathway (Figure 10). In both pathways, glycerol-3-phosphate (G3P)

from the previous Calvin cycle gets modified to create lysophosphatidic acid (LPA), which then gets further modified to produce phosphatidic acid (PA). These reactions are facilitated by the enzymes glycerol-3-phosphate acyltransferase (GPAT) and lysophosphatidic acid acyltransferase (LPAAT), respectively. PA is then dephosphorylated by phosphatidic acid phosphatase (PAP), resulting in the formation of diacylglycerol (DAG). In the Kennedy pathway, DAG is acylated by diacylglycerol acyltransferase (DGAT) to form TAG. On the other hand, the enzyme known as phospholipid:diacylglycerol acyltransferase (PDAT) plays a role in the synthesis of TAGs in diatoms by transferring an acyl group from phospholipids or glycolipids to DAG, resulting in the formation of TAG. This process is recognized as an alternative pathway that is of significant relevance in situations of stress, such as when there is a scarcity of nutrients, as it enables the conversion of membrane lipids into TAGs. Within the diatom cell, TAGs are stored within lipid droplets, serving as reservoirs of energy that can be utilized during periods of stress or scarcity of nutrients (Lupette et al., 2019).

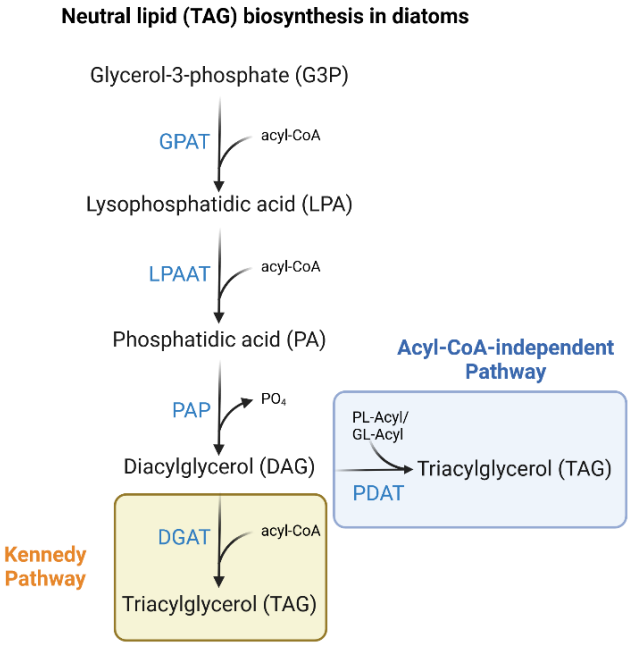

Figure 10 Biosynthetic pathways for triacylglycerol (TAG) formation in diatoms, illustrating the two primary pathways for the TAG synthesis: the Kennedy pathway and the acyl-CoA-independent pathway. The Kennedy pathway begins with glycerol-3-phosphate (G3P), which is sequentially acylated by glycerol-3-phosphate acyltransferase (GPAT) and lysophosphatidic acid acyltransferase (LPAAT) to form lysophosphatidic acid (LPA) and then phosphatidic acid (PA). PA is then dephosphorylated by

phosphatidic acid phosphatase (PAP) to yield diacylglycerol (DAG). Finally, DAG is converted into TAG by the acyl-CoA-dependent enzyme, diacylglycerol acyltransferase (DGAT). The acyl-CoA-independent pathway, alternatively, utilizes the enzyme phospholipid:diacylglycerol acyltransferase (PDAT) to transfer an acyl group from a phospholipid (PL) or glycolipid (GL) to DAG, leading to TAG formation. This pathway bypasses the need for acyl-CoA as an acyl donor.

Phospholipids in diatoms are synthesized through several well-defined pathways, of which the glycerol-3-phosphate (G3P) pathway is central. G3P acts as the backbone to which fatty acid chains are linked by acyltransferase enzymes, leading to the formation of lysophosphatidic acid (LPA) and subsequently phosphatidic acid (PA). PA is a key intermediate in phospholipid biosynthesis, serving as a precursor for the generation of various phospholipids, including phosphatidylcholine (PC), phosphatidylethanolamine (PE), and phosphatidylinositol (PI). The conversion of PA to CDP-diacylglycerol (CDP-DAG) is a critical step, catalyzed by CDP-DAG synthase, which then branches into different pathways for the synthesis of specific phospholipids.

The process of glycolipid synthesis primarily focuses on the production of galactolipids and sulfolipids. These lipids are important components of the thylakoid membranes, which are associated with the photosynthetic apparatus. The synthesis of monogalactosyldiacylglycerol (MGDG) and digalactosyldiacylglycerol (DGDG) begins with the formation of diacylglycerol (DAG) from phosphatidic acid (PA). The subsequent galactosylation of DAG, facilitated by galactosyltransferases, leads to the formation of MGDG which can then undergo further galactosylation to produce DGDG. The synthesis of sulfoquinovosyldiacylglycerol (SQDG) involves the addition of a sulfoquinovose group to DAG, thereby contributing to the formation of another crucial component of the thylakoid membrane.

The regulation of lipid metabolism in diatoms is intricate and strongly influenced by environmental factors such as the intensity of light, temperature, and availability of nutrients (especially silicate, nitrogen, and phosphorus). These parameters can have a significant impact on the activity of enzymes involved in the synthesis and breakdown of lipids, resulting in modifications to lipid composition and buildup. For example, when faced with limited nutrients like nitrogen or phosphorus, diatoms can

prioritize the accumulation of triacylglycerols (TAGs) as a means of survival (Brembu et al., 2017; Huang et al., 2019). This adaptation involves not only the increased activity of enzymes involved in TAG synthesis but also alterations in the expression of genes responsible for fatty acid desaturation and the restructuring of membrane lipids.

Additionally, lipid degradation pathways, such as β-oxidation, play pivotal roles in the turnover of lipids and the liberation of stored energy. β-oxidation entails the successive elimination of two-carbon segments from fatty acids, resulting in the release of acetyl-CoA. Subsequently, acetyl-CoA can be utilized in the citric acid cycle to generate energy. This mechanism enables diatoms to effectively utilize their lipid reserves in situations where external nutrients or energy sources are scarce.

The metabolic processes of lipids in diatoms are intricate and are carefully controlled by environmental factors and cellular requirements. Enzymes, such as acetyl-CoA carboxylase (ACC) and diacylglycerol acyltransferase (DGAT), play a significant role in lipid synthesis and can be manipulated to increase lipid production. Understanding the regulatory mechanisms of lipid metabolism at the molecular level is crucial for optimizing lipid yields in diatoms. This optimization is particularly relevant when considering the effects of environmental variables, such as light and nutrient availability, on lipid composition and accumulation. Light quality and quantity have been hypothesized to directly influence the lipid profile in diatoms, suggesting that different light conditions could induce the production of specific lipid types (Cointet et al., 2019a). For example, increased light intensity may promote the synthesis of storage lipids for energy sequestration, whereas specific light wavelengths might modulate the production of long chain polyunsaturated fatty acids (LC-PUFA) (Duarte et al., 2021). Similarly, nutrient availability plays a critical role in lipid metabolism. Under nutrient limitation, diatoms may shift towards increased storage lipid accumulation as an adaptive strategy, whereas nutrient-rich conditions could enhance the synthesis of structural and functional lipids (Cointet et al., 2019a; Huang et al., 2019).

Diatom-derived lipids are direct source of essential fatty acids for aquatic organisms, both in the natural environment and in aquaculture (Lebeau and Robert, 2003a). PUFAs like EPA and DHA hold significant commercial value due to their importance in human health, including cardiovascular health, brain function, and inflammation reduction (Sapieha et al., 2011). With the growing demand for sustainable PUFA sources, diatoms are being considered as an appealing alternative to fish oil, the

current primary source of these essential fatty acids. In addition to dietary supplements, diatom-derived lipids are being investigated for their potential in biofuel production (Vinayak et al., 2019).

Diatom cultivation: general techniques and applications

Autotrophic cultivation of diatoms relies on light as the main source of energy for growth. Batch cultivation is a primary method employed in the cultivation of diatom cells, wherein these cells are cultivated within enclosed vessels (e.g., flasks, carboys, or bioreactors) and are harvested after a fixed culture period (Lebeau and Robert, 2003b). Continuous cultivation, on the other hand, involves the introduction of a continuous supply of fresh growth medium into the culture while simultaneously removing an equal volume of the old culture. By keeping the algae in a steady-state diatom biomass production is maintained over extended periods. Continuous cultivation is particularly advantageous in large-scale biotechnological applications of diatom cultivation where a reliable and substantial yield of biomass is imperative (Wang and Seibert, 2017).

Photobioreactors are cultivation systems specifically designed to enhance the growth conditions of diatoms. These reactors provide meticulous regulation of crucial factors, including light intensity, temperature, and nutrient availability. By replicating the natural habitat of diatoms, photobioreactors facilitate researchers and industrial operators in attaining optimal productivity and exerting greater command over diatom growth. Their utility is particularly pronounced in extensive production contexts, where the precise management of environmental conditions is imperative for achieving substantial yields.

The cultivation of diatoms in biofilms is a novel method that enables the growth and examination of diatom species within complex and natural-like communities. In contrast to conventional cultivation techniques where diatoms grow freely in liquid media, biofilm cultivation aims to replicate their natural environment, where diatoms commonly adhere to surfaces and establish organized communities (Eich et al., 2015). Furthermore, it is an active and emerging area of research in phycology to address the challenges linked with conventional suspension culture methods such as the high energy requirements for pumping and mixing these vast quantities of water, as well as the voluminous water requirements (Lee et al., 2014; Osorio et al., 2021; Wang et al., 2017). Solutions to these problems include the use of

flocculants or centrifugation, as well as development and investigation of innovative harvesting techniques such as microstrainers, dissolved air flotation, and electrocoagulation (Sharma et al., 2013). Contrary to cultures in suspension, microalgae grown in biofilm are attached on a solid substrate where they are supplied with nutrients and encouraged to proliferate and embed in a complex, self-produced three-dimensional matrix under controlled environmental conditions. The density of the biofilm renders several advantages to the microalgal colony, such as increased resistance to stressors and enhanced nutrient availability. The higher biomass density resulting from biofilm cultivation significantly reduces the need for dewatering during harvest, rendering biofilm system a more productive and cost-efficient alternative to their suspension counterparts.

Genetic engineering and selective breeding have gained significant significance in the realm of diatom cultivation to grow strains with enhanced attributes. Scholars are exploring approaches to modify the genetic composition of diatoms to augment their growth rates, lipid production, and other favorable characteristics (Daboussi et al., 2014; Li et al., 2014).

Context and objectives of the thesis

Despite the abundance, diversity, and demonstrated potential of diatoms, they remain perplexingly underutilized in biotechnology (Hildebrand et al., 2012; Sharma et al., 2021). Diatoms have not been a focus of research to the same extent as bacteria, yeast, and other groups of algae, as evidenced by the substantially lower and stagnant number of publication over the years (Sharma et al., 2021). This is attributed to several factors, including the challenges in optimizing their growth and culture conditions. Perhaps, it is also due to a historical bias towards species with well-established research foundations. Nevertheless, ongoing scientific investigations and technological advancements hold promise for enhancing the viability of diatom-based biotechnological applications.

A high-throughput screening method for marine benthic diatoms had been set up as part of the Atlantic MicroAlgae (AMI) program, a collective dynamics initiative funded by the Pays de la Loire region (2015-2020). It explored the potential of the marine benthic diatoms hosted in the Nantes Culture Collection (NCC) of Nantes Université as a valuable reservoir of strains capable of producing interesting fatty acids. The integrated screening approach is based on the use of high-performance analytical

instruments such as gas chromatography combined with mass spectrometry, vibrational spectroscopy and chlorophyll fluorescence measurement (PAM fluorometry or Pulse-Amplitude Modulation fluorometry). PAM fluorometry and spectroradiometry were used as alternative methods to replace traditional cell counting techniques using the hemocytometer, while high throughput screening using FTIR spectroscopy (HTSXT-FTIR) was used for rapid biochemical profiling (Cointet et al., 2019b). Using this new screening procedure, five benthic diatom strains out of 33 (*Amphora* sp. NCC169, *Nitzschia alexandrina*, *Nitzschia* sp. 5 NCC109, *Staurosira* sp. NCC182, and *Opephora* sp. 1 NCC366) were selected for their high lipid productivity, which reached a maximum of 30% of their dry biomass weight under experimental conditions. Moreover, these species have the potential to produce high-quality lipids such as eicosapentaenoic acid (EPA) and docosahexaenoic acid (DHA) under optimized conditions (i.e., without nutrient limitation and under low light intensity). This research finding further cements the reputation and potential of benthic diatoms as remarkable reservoirs of lipids for aquaculture, biofuel production, pharmaceutics, nutraceutics, and research in biotechnology in general, and also paves the groundwork for the present thesis. The primary aim of this study was to evaluate whether a biofilm-based culturing strategy—simulating and mimicking the natural way of growth of benthic diatoms in terms of light and nutrient availability—improves their lipid productivity and quality, specifically in terms of polyunsaturated fatty acids (PUFAs). To address this main question, this manuscript is divided into four chapters:

The first chapter of this thesis is on “Diatom Biofilm: Ecology and Cultivation from Laboratory to Industrial Level”. It aims to underscore the importance of diatoms, especially benthic diatoms and their corresponding biofilms, from various ecological and biotechnological perspectives across different levels of production. Benthic diatoms play essential roles in ecosystem processes, husbandry, nanotechnology, and production of valuable bioactive compounds. These siliceous microorganisms are vital to nutrient recycling in numerous coastal and intertidal zones. They serve as nutrient source for larval organisms and invertebrates in aquaculture and as feed supplements for poultry and dairy farm industries. Their intricately unique biosilica structures are invaluable in nanotechnology due to their exceptional physicochemical properties and characteristics. Furthermore, the potential of biofilm-based

culture systems in the advancement of research and biopharmaceutical applications in the field of microalgal biotechnology is discussed.

The second chapter, “Development of the porous substrate photobioreactor (PSBR) for biofilm cultivation”, describes the historical development and current state of biofilm-based systems for microalgal cultivation. It unfolds the process of constructing the lab-scale PSBR used in the research study—from inception into development until optimization. This involves comparison of existing technologies, and conversion of an existing laboratory-scale suspension photobioreactor from Synoxis Algae to a simple functioning PSBR prototype. Preliminary experiments were conducted using *Nitzschia laevis*, a robust and fast-growing species of benthic diatom. Two trials were conducted using the biofilm PSBR. These trials were conducted at the premises of Synoxis Algae in the midst of consequential COVID-19 restrictions; hence, research could only be performed as officially permitted. The conclusion of our research in this chapter has led to the utilization of the engineered PSBR in future diatom cultivation studies in Chapter III.

The third chapter focuses on experimenting with the use of the improved PSBR for culturing the benthic diatom *Amphora* sp. NCC169 and its potential on the species' biomass and lipid productivity. This genus has been identified as potentially interesting for biofuel production. Its lipid content normally ranges from 21-28% but can reach up to 40% under the right culture conditions. *Amphora* sp. NCC 169 was previously shown to produce high quality lipids (PUFA = 16.4%; EPA = 8%) (Cointet, 2019). However, valorization of *Amphora* sp. NCC169 was impeded by existing mass-production technologies. Attempts have been made to grow *Amphora* sp. NCC169 in an airlift photobioreactor, but investigations have demonstrated the inability of the species to grow in suspension or agitated conditions (Cointet, 2019). There is great potential in valorizing the growth and lipid production of *Amphora* sp. NCC169 using a biofilm photobioreactor which taps into the species’ innate but overlooked ability to form stable biofilms in benthic environments.

The first part of this chapter compares the utilization of the constructed PSBR versus Fernbach flasks towards the valorization of *Amphora* sp. NCC169 for lipid production. We hypothesize that cultivating *Amphora* sp. NCC169 in a PSBR will lead to higher biomass and lipid productivity than when the cells are cultivated in suspension in a Fernbach flask. This hypothesis was based upon previous research that

highlighted the role of turbulence in the diminished growth of *Amphora* sp. NCC169 biofilms and provided a basis for testing the efficiency of the PSBR in comparison to traditional laboratory cultivation techniques. Following comparative analyses, this hypothesis has been confirmed. It was found that the PSBR significantly supports the growth and development of *Amphora* sp. NCC169 biofilms better than conventional cultivation methods, effectively mitigating the adverse effects of turbulence observed with traditional setups. This confirmation not only validates the enhanced cultivation capabilities of the PSBR but also underscores the importance of environmental conditions in optimizing the growth of benthic diatoms.

The second part of Chapter III assesses the effect of light quality on the biomass and total lipid rate of *Amphora* sp. NCC169 cultivated in a porous substrate photobioreactor. It makes use of the PSBR's highly controlled LED panels to compare the effect of RGB (red, green, blue) light and RB (red, blue) light on the biomass and lipid productivity of *Amphora* sp. NCC169 cells. Traditional laboratory set-up utilizes RGB light for benthic diatom cultivation. However, benthic diatoms have typical preference for RB light that corresponds to the peaks of light absorption by chlorophyll a and chlorophyll c, which are the main photosynthetic pigments in diatoms. Our hypothesis, which posited that cells exposed to RB light would exhibit distinctive growth patterns and photosynthetic characteristics compared to those subjected to a combination of RGB lights, was subjected to thorough examination. It was determined that the differences observed in growth patterns and photosynthetic characteristics under RB light exposure, when compared to RGB light exposure, were not statistically significant. Furthermore, contrary to expectations set by existing literature, an enhancement in diatom biomass due to blue light was not observed. These findings suggest that the impact of light spectrum on diatom growth and photosynthesis may not be as pronounced as previously thought, indicating a need for further research to elucidate the specific conditions under which light quality influences diatom biomass.

Chapter I

Diatom Biofilm: Ecology and Cultivation from Laboratory to Industrial Level

Abstract

Having previously established a comprehensive understanding of the biological significance and potential biotechnological applications of diatoms in the preceding introduction, this chapter shines the spotlight on diatom biofilms and benthic diatoms. This chapter thoroughly investigates the importance, variety, and flexibility of diatoms in the formation of biofilms, highlighting their ecological functions and potential for use in biotechnology. It includes a comprehensive analysis of the processes by which diatom biofilms are created, as well as the different methods of cultivating biofilms, including both small-scale laboratory experiments and large-scale production systems. Furthermore, the exploration of biofilm technology's application across several establishes revealed the need for ongoing research and development to optimize diatom biomass and lipid productivity for biotechnology in the succeeding chapters.

Diatom Biofilm: Ecology and Cultivation from Laboratory to Industrial Level

Mary Dianne Grace Arnaldo[1], Aurélie Mossion[1], Thierry Beignon[2], Hugo Vuillemin[2], Freddy Guihéneuf[3], Gaëtane Wielgosz-Collin[1], Vona Méléder[1]

[1] Nantes Université, Institut des Substances et Organismes de la Mer, ISOMer, UR 2160, F-44000 Nantes, France

[2] Synoxis Algae, Z.I, Les Relandières, 44850 Le Cellier, France

[3] SAS inalve, 181 Chemin du Lazaret, 06300 Villefranche-sur-Mer, France

Abstract

Several species of diatoms are benthic and thus capable of forming highly productive biofilms in coastal and estuarine environments. These biofilms have numerous ecological benefits and hold promising potential in biotechnology.

In this chapter, we start by presenting the importance of diatoms in biofilm formation. We highlight the influence of biofilms in the ecosystem, in terms of primary and secondary productivity. We summarize the different techniques available for biofilm cultivation at various scales, and enumerate the associated strategies, advantages, and issues. We explore the products generated from biofilm culture. Finally, we examine the potential of biofilm culture in the context of microalgal biotechnology.

1. Introduction

Diatoms belong to one of the most common groups of eukaryotic and photosynthetic microorganisms on Earth. They are unicellular, carotenoid-rich microalgae under the phylum Bacillariophyta and they possess a siliceous cell wall (frustule) composed of two overlapping halves (thecae). There are an estimated 250 extend genera and 200,000 species of diatoms[1], which exist ubiquitously in the world's water bodies (Gordon et al., 2008). Each of these species display unique and exquisite biosilica

[1] Editorial note: The estimated number of diatom species can vary in the literature depending on the methodology used for estimation. However, regardless of the specific number, diatoms are widely recognized as one of the most diverse groups of algae species.

nanostructures, along with a plethora of functional molecules and compounds, making diatoms highly attractive for a wide variety of biotechnological applications (Singh et al., in press).

In coastal and tidal zones, diatoms are the dominant eukaryotic portion of the microphytobenthos (MPB) (Bolhuis et al., 2013). The majority of diatoms are benthic, exhibiting the ability to adhere to and colonize any surfaces that offer sufficient moisture, adequate illumination, abundant nutrients, and a favorable environmental condition (Borowitzka, 2018). Benthic diatoms can be categorized into different life forms based on the substrate they inhabit, such as rocks (epilithic), sand (episammic), plants (epiphytic), or wood (epidendric) (Baker et al., 2022). Additionally, some diatoms are considered epipelic if they live freely between sediment particles, or epipsammic if they are closely attached to individual sediment particles (Blommaert et al., 2018). Certain species of benthic diatoms exhibit multimodal morphology and possess an inducible planktonic phase (Sabir et al., 2018).

Both planktonic and benthic forms of diatoms secrete extracellular polymeric substances (EPS) through the apical pores or the longitudinal raphe, respectively (Hoagland et al., 1993; Molino and Wetherbee, 2008) (Underwood, n.d.). These mucilaginous secretions exist in various forms, such as stalks, tubes, apical pads, biofilms, and fibrils. They generally consist of high molecular weight compounds, including polysaccharides, lipids, proteins, and DNA. Planktonic diatoms employ EPS to aggregate in the water column, while benthic species use them for motility and the formation of phototrophic assemblages with other microorganisms (*e.g.*, microalgae, bacteria, fungi, protozoa) on the benthos (Kim et al., 2021).

Benthic diatoms encounter challenging environmental conditions within their ecological niches. Their high capacity to adapt and thrive in such settings has enabled them to evolve and showcase exceptional genetic, morphological, and biochemical diversity. Benthic diatom species have found application various fields, including food production, wastewater treatment, carbon dioxide sequestration, and the production of macro- and micro-molecules with bioactive properties (Sansone et al., n.d.).

There is a high demand for benthic diatoms in aquaculture, particularly for rearing marine invertebrates such as abalones, sea cucumbers, and sea urchins. Benthic diatoms play a crucial role in directly nourishing all life stages of grazers and filter-feeders, as well as larval and early juvenile stages

of some fish species. The bioavailable macromolecules found in EPS and benthic diatoms *per se* provide adequate nutrition and also serve as chemical cues for the recruitment and survival of early and post-larval species (Castilla-Gavilán et al., 2020; Dobretsov and Rittschof, 2020; Harder et al., 2002; Kuehl, 2020; Moxley and Coyne, 2020).

Some species of benthic diatoms are utilized as feed supplements for the poultry and dairy industry. Defatted biomass of *Staurosira* sp. has been effectively used to substitute up to 7.5% of corn and soybean meal in broiler diets, potentially reducing soybean usage by 2.4 million tons every year (Austic et al., 2013; Leng et al., 2014).

The diversity, intricacy, and integrity of diatom frustules makes them exceptional materials for nanotechnology, with the potential to surpass the performance of modern engineering (Ghobara et al., in press). Chain clusters of *Nitzschia palea* frustules, when integrated into microfluidic systems, exhibit specific elastic properties that are ideal for rapid detection of viruses, drugs, or explosives in drug delivery, and virus detection application (Wang et al., 2012). These elastic biosilica structures possess unique structures and optical properties, making them excellent sensors, biocarriers, and micro-devices that are of industrial importance.

Benthic diatoms are prolific producers of lipids as metabolites. Typical lipid fractions from diatoms have been found to range from 15 to 25% of their dry weight, although certain strains can reach remarkable lipid levels of up to 70 to 85% by regulating the culture conditions (Cointet et al., 2019a; Kuczynska et al., 2015; Rodolfi et al., 2009; Wang and Seibert, 2017). Through a novel screening procedure, five benthic diatom species (*i.e.*, *Amphora* sp., *Nitzschia* sp., *Nitzschia alexandrina*, *Opephora* sp., and *Staurosira* sp.) were identified as impressive lipid reservoirs with potential for various biotechnological applications (Cointet et al., 2019b). These diatoms exhibit high levels of compositional diversity, including membrane-bound polar lipids, triglycerides, and lipid-derived free fatty acids (Dunstan et al., 1993; Lee et al., 1971; Wang and Seibert, 2017). Additionally, they contain lipids such as EPA and phytosterols that have promising nutritional value and bioactivity.

Benthic diatoms are remarkable repositories of pigments, polysaccharides, phenolic compounds, sterols, enzymes, and an array of metabolites with high bioactivity that hold immense value in the nutraceutical, pharmaceutical, and cosmeceutical industries. Diatoms contain fucoxanthin, a potent

bioactive pigment, with significantly higher levels compared to its primary commercial source, brown algae (Phaeophytes). In fact, diatoms can contain up to 100 times more fucoxanthin per dry weight (Marella et al., 2020). Benthic diatoms, in particular, exhibit enhanced fucoxanthin: chl *a* ratios as an adaptive mechanism in extremely low light conditions (McGee et al., 2008). Aqueous extracts from diatoms such as *Melosira* sp., *Amphora* spp., *P. tricornutum*, and *Nitzschia cf. pusilla* have demonstrated antithrombogenic and antileukemic activities (Prestegard et al., 2009). Lipid fractions obtained from *Staurosira* sp., have exhibited antibacterial activity against *Bacillus subtilus* and antiproliferative activity against breast cancer cell line MCF-7. Additionally, lipid fractions from *Nitzschia alexandrina* and *Entomoneis paludosa* have shown effectiveness against proliferation of MCF-7 breast cancer and NSCLC-N6 lung cancer cell lines (Cointet, 2019).

Biofilm adhesion is a strategy that microorganisms have employed for over three billion years to thrive and withstand temporal variabilities (Westall et al., 2001). Biofilm communities exhibit structural and ecophysiological differences compared to their planktonic counterparts. Within a biofilm matrix, highly dense cell aggregates are embedded while allowing continuous flow and assimilation of water, nutrients, and gases, exhibiting a retentostatic behavior. A retentostat is a chemostat that retains the biomass completely while diluting or removing effluents through a filter (Liu et al., 2019). The self-produced structure of a biofilm confers physical, chemical, and biological stability, resulting in increased resistance and tolerance towards antimicrobial substances, heavy metals, and toxins(Harrison et al., 2007).

As one of the most successful life forms on Earth, biofilms serve as a nexus bridging various biological fields. The groundwork for biofilm research was laid in the mid-1920s to early 1930s when scientists observed the growth of certain microbes exclusively in attached films (Winogradsky, 1928; Zobell and Allen, 1933). Since then, the investigation of biofilms has expanded across a wide range of scientific and biotechnological disciplines, including evolution, microbiology, ecology, biogeochemistry, medicine, and public health.

Biofilm cultivation, also referred to as attached or immobilized cultivation, has emerged as an active area of research and development in the field of microalgae. In the early years of the 21st century, significant scientific attention was directed towards biofilm research as a means to address various

challenges associated with traditional suspension culture methods. Conventional microalgal cultivation involves growing cells either in open systems such as carboys, tanks, and ponds, or in closed cultivation systems using photobioreactors. However, the industry continues to face significant hurdles due to the exorbitant costs associated with low biomass productivity, high water consumption, and substantial energy requirements. Harvesting and dewatering equipment costs can account for as much as 90% of the total production cost (Amer et al., 2011), and the energy required for dewatering during harvest adds an additional 5-20% to the overall expenses (Singh and Patidar, 2018). Scientific efforts are currently focused on improving culture designs and biomass-recovery technologies. Simultaneously, researchers are exploring the potential of biofilm cultivation as an alternative to conventional suspension culture systems. The key advantage of biofilm systems lies in their ability to significantly reduce the cultivation volume. Harvesting can be easily accomplished through methods such as sloughing or scraping, minimizing or even eliminating the need for further steps to dewater and concentrate the biomass (*e.g.*, centrifugation, flocculation) (Gross et al., 2013).

Benthic diatom research is gaining momentum in recent years. However, the prevailing cultivation methods for benthic diatoms primarily rely on suspension or planktonic culture technologies. Studies have shown that while some certain species of benthic diatoms can grow under agitated conditions, others exhibit higher biomass productivity and lipid rates when cultivated in undisturbed conditions (Cointet et al., 2021; Lebeau and Robert, 2003b). It is understandable that growth is more favorable when diatoms are provided with conditions that closely mimic their natural adaptation strategies.

Biofilm-based culture systems have the potential to advance benthic diatom research. The inability of certain species to grow in suspension culture necessitates a reassessment of their eco-physiology and lipid production capacity under more suitable culture conditions using biofilm systems. Research studies have demonstrated the promising application of biofilm-based photobioreactors for cultivating microalgae, but their utilization in benthic diatom studies remains limited to date (Benstein et al., 2014; Berner et al., 2015; Gao et al., 2015; Naumann et al., 2013). The development and implementation of a highly controlled biofilm system could enhance the growth of benthic diatoms, improve their lipid production, and unlock their bioactivities for biopharmaceutical application.

This book chapter seeks to underscore the significance of diatoms and their biofilms from both ecological and biotechnological perspectives. It delves into the mechanisms of biofilm formation, emphasizing their impact on the surrounding ecosystem. The chapter also explores various techniques for cultivating biofilms at different scales, discussing their respective advantages and challenges. Finally, it examines the potential of biofilm culture in the context of microalgal biotechnology.

2. Natural biofilms

2.1 Ecosystem functions

Biofilms shape the basic chemistry of the Earth's surface and play major roles in the formation and recycling of elements vital to life. They essentially exist as a highly structured conglomerate of different photoautotrophic and heterotrophic microbial species. Their community structure, composition, and distribution are remarkably variable due to species-specific tolerance to environments with vast physicochemical fluctuations. In nature, coastal and intertidal areas like mudflats, rocky coasts, and sandy beaches are important niche spaces for diverse biofilm communities (Figure 11).

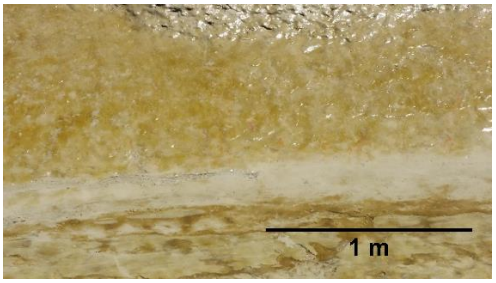

Figure 11 Golden biofilm on the intertidal sediments in western France (© Vona Méléder)

Microalgal biofilms are regarded to be the most productive photoautotrophic system in the biosphere. In the world's estuarine and intertidal zones, benthic diatoms are frequently one of the dominant groups in the microphytobenthos (Marshall et al., 1971; Osuna-Cruz et al., 2020; Virta et al., 2019). They are considered the richest and most abundant group of benthic algae, playing a pivotal role in ecosystem functioning and services. In these niches, phototrophic benthic diatom biofilms significantly contribute to primary production, zooplankton settlement, and numerous biogeochemical processes (Johnson et al.,

2015). These assemblages also help stabilizing sediments of coastal environments while serving as primary sources of fixing carbon provided to marine food webs(Johnson et al., 2015).

Field studies conducted in heterogeneous marine coastal environments have demonstrated that a positive correlation between benthic diatom diversity and ecosystem productivity (Virta et al., 2019). Biofilms play a crucial role in regulating nutrient fluxes, and its estimated that MPB communities significantly contribute to intertidal carbon retention (Oakes and Eyre, 2014). Additionally, benthic diatoms have special light-harvesting acclimation mechanism that facilitates their migration and survival in changing light conditions. Live and cultivable benthic diatoms have been observed in depths as low as 191 m, thereby extending primary productivity in these areas (McGee et al., 2008).

Benthic diatoms play a crucial role as the primary food sources for many organisms within the intertidal zone. Mollusks, bivalves, crustaceans, and juvenile fishes directly depend on them for nourishment. Benthic diatoms have small size, making them easily ingestible, while providing sufficient nutrients. Their significance as primary producers is largely attributed to their high total lipid content, which can reach as high as 81.5% (de la Peña, 2007; de Viçose et al., 2012; Viana et al., 2007). Furthermore, the adherence of benthic diatom biofilms to the substrates provides stability and accessibility to grazers with limited motility. Diatom biofilms also release potent chemical cues that support the settlement and survival of faunal communities, such as polychaetes, nematodes, and crustaceans (Hendrarto and Nitisuparjo, 2011).

In estuarine environments, sediments are prone to erosion due to the constant movement of water and the highly variable physicochemical parameters. The secretion of EPS by pennate benthic diatom biofilms plays a crucial role in binding the cells and sediment particles together, forming a cohesive network of matrices that reduces resuspension and increases the stability of the sediment (Holland et al., 1974; Paterson, 1995). Epipelic benthic diatoms have the ability to migrate and stratify vertically between sediment layers or within the biofilm itself, depending in the environmental conditions (Underwood et al., 2005). This vertical migration provides increased stability to the deeper layers of the sediment. Benthic diatom biofilms facilitate habitation of intertidal areas by grazers and filter feeders (Holland et al., 1974). For example, in the Bot River estuary (Western Cape of South Africa), the colonization of inundated areas by benthic diatoms is followed by the settlement of macrophytes (Bally

et al., 1985). The presence of macrophytes in the substrate enhances the retention of sediment particles which directly affect the structure and quality of the benthic zone.

Benthic diatom communities also play a crucial role as bioindicators of ecological health and status. They have been listed as Biological Quality Elements (BQE) under the European Water Framework Directive due to their widespread distribution, rapid response to ecological changes, and their durable siliceous frustules to provide insights into temporal environmental influences (Almeida and Feio, n.d.; Wang et al., 2019). The abundance and diversity of benthic diatoms are particularly important in characterizing various environmental features, including temperature, salinity, pH, hydrodynamics, pollution, and eutrophication (Hajnal et al., 2009; Lecointe et al., 1993). Diatom communities are useful proxies in tracking river inputs and marine interflow when environmental data is lacking (Kirsten et al., 2018).

Benthic habitats are often characterized by highly dynamic and steep gradients of temperature, light, pH, oxygen, and nutrient availability. Physical disturbances have a significant influence on the processes that govern the cycle of nutrients in coastal ecosystems. The microphytobenthos and sediment feeders engage in complex feedback and reciprocal interactions that contribute to nutrient recycling in benthic habitats. Water trapped between sediment particles contains elevated levels of nutrients, particularly nitrogen and silica (Forehead et al., 2012). Benthic diatoms have the ability to access nutrients from both the water column and sediment porewaters through planktonic and vertical migration strategies.

The colonization of benthic diatom biofilms on the sediment paves the way for the migration of organisms at higher trophic levels. The presence of key functional species in benthic habitats is directly related to the availability and abundance of microphytobenthos in the area. Faunal activity and subsequent bioturbation of the sediments enhance the diffusion and release of nutrients from porewaters. providing sufficient quantities to support microalgal growth. Bioturbation also influences factors such as oxidation demand, sediment permeability, water content, organic matter availability, remineralization and nutrient efflux (Lohrer et al., 2004). In a reciprocal relationship, benthic diatoms utilize the dissolved organic and inorganic compounds generated by higher organisms for their own growth. Moreover, benthic diatom species have been found to actively mitigate the levels of toxic phthalate acid esters (PAEs), polyaromatic hydrocarbons (PAHs), and polychlorinated biphenyls (PCBs) in the sediment

layers through oxygenation (Jeremiason et al., 1998; Li et al., 2015). Benthic sediments are host to intricate biogeochemical interactions that provide a substantial portion of the nutrients required for ecosystem production.

On the other hand, natural biofilms pose a persistent and challenging problem in the environment. Among all diatom species in the ocean, approximately 8-10 benthic diatom genera have been identified as highly prolific micro-fouling agents (Molino and Wetherbee, 2008). They consequently facilitate the settlement and colonization of other fouling species, such as barnacles, bryozoans, and polychaetes. Over time, the accumulation of these organisms can cause significant economic and structural damage to aquatic surfaces, including water pipes and vessel hulls. They also contaminate devices and contribute to a significant proportion of human infections in clinical environments. To effectively prevent, detect, and treat fouling organisms, it is imperative to understand the biochemistry and ecophysiology of biofilms.

2.2 Structure and formation

Biofilm communities consist primarily of water, with the dry mass of microorganisms being held together by a matrix composed of organic or inorganic substrates and extracellular EPS (Cheng et al., 2010). The structure of biofilms is not uniform and is influenced by a variety of intrinsic and extrinsic physical and biological factors that can vary in intensity, including nutrient availability, temperature, pH, and cellular growth. Within the biofilm matrix, different microorganisms with unique morphological and ecophysiological characteristics coexist, forming a highly interconnected network. Despite their individuality, these microorganisms engage in extensive metabolic cooperation and structural organization in coordination with neighboring cells.

In general, the process of biofilm formation involves a dynamic turnover that comprises three fundamental steps: (1) attachment, (2) colonization/development (3) and maturation/detachment (Figure 12). A functional biofilm community progresses through these phases in a pseudo-steady state, maintaining a continuous and balanced cycle of growth and detachment.

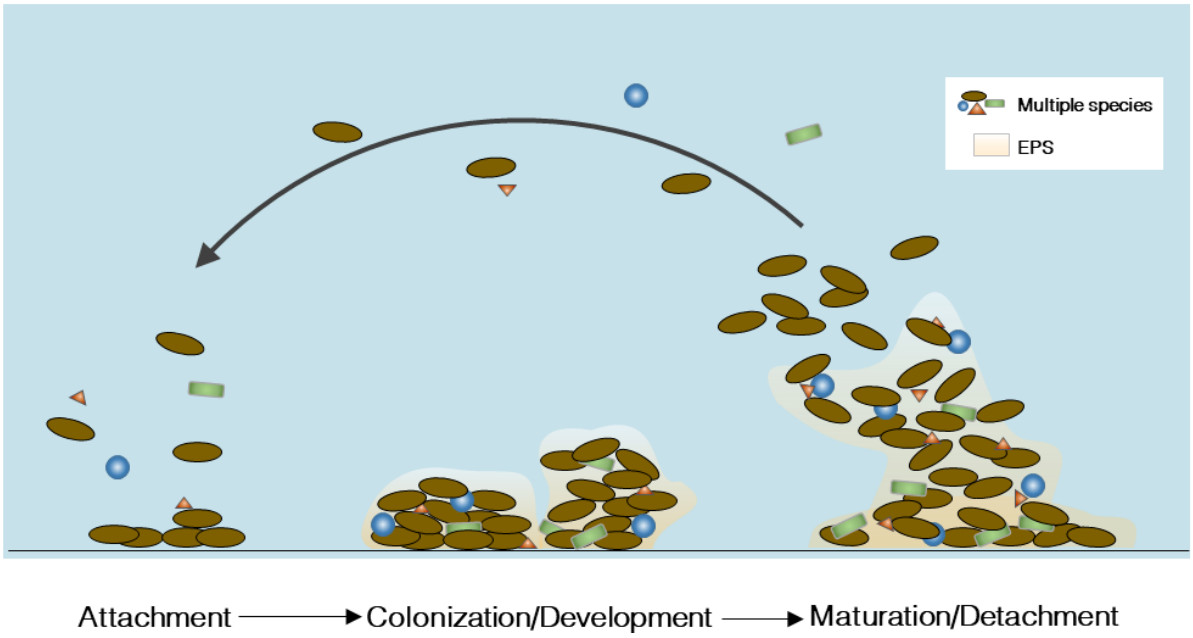

Figure 12 Schematic representation of a biofilm formation. Free-floating diatoms cells are initially transported by fluid flow until they adhere on substrates. They transition into an assembly of immobilized cells on a firm surface. The colonization stage starts as soon as the cells have irreversibly attached to the substrate. During this stage, the biofilm produces an increased amount of EPS. As the biofilm develops, it forms dense, heterogeneous, three-dimensional matrices with strong surface interactions. Physical space and nutrients become restricted, which activates the cells' survival mechanisms. Starving cells release enzymes that break the EPS polymers, actively detaching from the mature biofilm network.

During the initial stage of formation, cells are transported and adhere themselves to solid substrates. They transition from free-floating units into an assembly of immobilized cells on a firm surface. Microorganisms can be passively transported into the substrate by fluid flow, aided by gravity, advection, and/or by active motile processes (Ozkan et al., 2012).

The success and extent of initial attachment are strongly influenced by various factors, including the microbial cell surface (*e.g.*, hydrophobicity, presence of appendages), physico-chemical properties of the fluid medium (*e.g.*, pH, temperature, nutrient, ionic strength, and flow velocity), the rate of cell movement, and the characteristics of the substrate (*e.g.*, ionic charge, texture, porosity, hydrophobicity). The classical Derjaguin, Landau, Verwey, and Overbeek (DLVO) theory, as well as the Extended DLVO

(XDLVO) theory, explain the physical forces that influence cell adhesion (Cheah and Chan, 2021; Tong et al., 2021). These models describe the overall interaction between cells and the substrate as a result of attractive van der Waals forces, and repulsive electrostatic double-layer interactions. While the classical DLVO theory assumes that cells and substrates are chemically inert, the "X" in XDLVO accounts for additional forces such as steric effects, hydration forces, and specific ion effects in aqueous media (Van Oss, 1993). As such, higher attachment rates can be obtained from increasing nutrient concentrations in the medium (Berhe et al., 2017). A wide range of solid materials can serve as substrate for biofilm formation, with higher average surface roughness (R_a) generally promoting biofilm formation (Teughels et al., 2006; Tong et al., 2021). R_a is calculated as follows:

$$R_a = \frac{1}{l}\int_0^l |y(x)|dx \qquad \text{(Eq. 1)}$$

Where:

R_a: average roughness (in length unit)

l: length of the sampling profile over which the roughness is measured (in length unit)

$y(x)$: height deviation of the surface profile from the mean line at a given x position along the length of the sampling profile.

The equation represents the integral of the absolute difference between the vertical departures and the mean line, divided by the length of the sampling profile (Figure 13). The resulting R_a value provides a quantitative measure of surface roughness, which influences the attachment and colonization of microorganisms in biofilms (Gadelmawla et al., 2002; Lu et al., 2003).

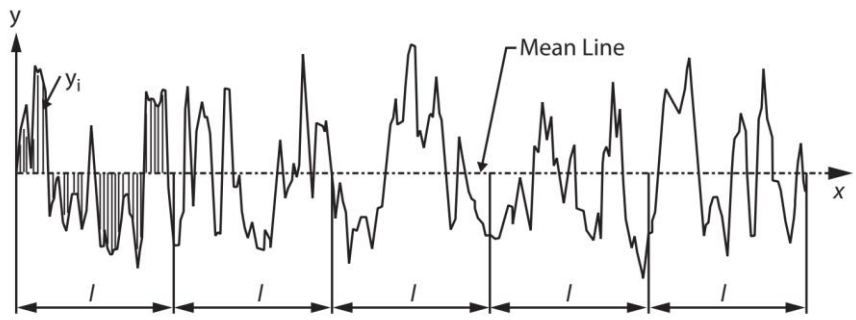

Figure 13 Variables in determining the arithmetic average roughness (R_a)

In dynamic flowing systems, the presence of rough surface textures helps to reduce the shear force experienced by the cells, and facilitates a larger surface area for attachment (Gross et al., 2016). This interaction between surface roughness and flow dynamics is further influenced by the cell size. For example, studies have shown that *Cylindrotheca fusiformis* (length = 20 – 60 µm; width = 2 – 6 µm), which are larger in size, have a higher rate of cell adhesion on rough substrata compared *Navicula incerta* (length = 10 – 15 µm; width = 2 – 7 µm). The larger size of *C. fusiformis* allows for more attachment points and enhances their ability to adhere to roughened surfaces (Tong and Derek, 2022). In dynamic flowing systems, rough surface textures play a role in reducing the shear force experienced by cells and facilitate greater surface area for attachment. This allows cells to initially settle on the surface in a reversible preliminary attachment state. After the initial settlement, cells secrete adhesive EPS to establish stronger links between algal cells and the interacting surface, subsequently facilitating irreversible secondary cellular attachment.

After the cells have irreversibly attached to the substrate, the colonization stage begins. During this stage, the biofilm produces an increased amount of EPS, a mechanism that serves multiple functions. Primarily, it supports an intracellular network connecting the cells. Additionally, it shapes and maintains the micro-habitat conditions, ecophysiological status, development, and stability of the biofilm (Toyofuku et al., 2016). The EPS acts as a protective barrier that effectively filters out toxic compounds, harmful phagocytes and bactericides away from the cell community (Qureshi et al., 2005). However, EPS within the biofilm also sequesters nutrients, vitamins, and other molecules away from it. As the biofilm growth thicker and older, there is restricted space for cell division and limited nutrient availability. During the stationary phase, cells activate survival mechanisms to adapt to stress of nutrient limitation. Consequently, there is an increase in the production of metabolites such as lipids, antibiotics, and pigments. These metabolites create chemical concentration gradients that signal other planktonic cells to be attracted to the biofilm surface (Roeselers et al., 2008).

During its development, the biofilm undergoes the formation of dense, heterogeneous, three-dimensional matrices consisting of compact cellular micro-colonies with strong surface interactions. The structure and distribution of the biofilm are irregular, forming randomly different shapes and textures according to prevailing environmental forces. In high-sheer scenarios, they can take on flat,

long-stranded configurations, while in low-shear conditions, they may mold into thick, mushroom-like aggregates (Costerton et al., 1995). This process is highly dependent on nutrient concentration and availability rather than cellular substrate affinity (Cheng et al., 2010). In mature biofilms, cells primarily allocate their resources to uptake nutrients and expend energy for EPS secretions rather than for growth. As nutrients become limited, starving cells release enzymes that cleave the EPS polymers, actively detaching from the mature biofilm network (Qureshi et al., 2005).

Two physical phenomena can be observed in the natural detachment of biofilms: Sloughing and erosion. Sloughing is the result of fluid shear stress, weak cohesion, and depletion of nutrient supply. Biofilm cells undergo continuous slough-off cycles when subjected to low shear rates. On the other hand, under high shear stress conditions, the primary detachment mechanism is continuous erosion, leading to a smoother biofilm structure (Van Loosdrecht et al., 2002). In addition to natural detachment, biofilms can also undergo detachment due to external factors such as predatory grazing, or anthropogenic interventions, including the use of biocides, or physical scraping.

A “true” biofilm cell retains the phenotypical and genotypical characteristics of the parent biofilm community as it detaches from the biofilm network (Donlan and Costerton, 2002). This distinguishing feature sets them apart from planktonic cells that may simply become “stranded” during detachment but do not retain the specific characteristics of the biofilm community.

3. Artificial algal biofilm systems

Biofilm culture systems offer a promising and advantageous alternative to suspension-based cultures. Unlike suspension cultures, biofilm cultivation involves using a solid substrate on which the cells adhere and proliferate. At harvest, the majority of the biomass can be easily removed by manual or mechanical sloughing, significantly reducing the cost and energy required for concentrating and dewatering the final suspension.

The use of artificial biofilm systems in research dates back to the 1970s, particularly in the field of wastewater research (Hassard et al., 2015). Initially, algal biofilm devices were employed to assess the effects of biofilm formation on water transport and bioremediation. The biofilms developed for water treatment comprise various autotrophic and heterotrophic microorganisms, including microalgae,

bacteria, fungi, which play a vital role in utilizing nutrients present in wastewater (Katarzyna et al., 2015; Kesaano and Sims, 2014). Presently, biofilm systems are still predominantly used for heterotrophic wastewater remediation. However, over the past few decades, these culture systems have expanded to monospecific microalgal cultivation, thereby broadening their application (Liu et al., 2013; Naumann et al., 2013).

Indeed, there has been a significant amount of research focused on biofilm-based microalgae culture systems, driven by the need to overcome challenges associated with large-scale industrial production. In these systems, the biofilm comprises a single species of microalgae, densely inoculated onto the surface of an attachment material. However, in open and/or large-scale biofilm cultivation systems, it is inevitable to encounter biological contaminants such as algae, bacteria, fungi, or protozoa, leading to the formation of a mixed biofilm community (Naumann et al., 2013). In these systems, cell aggregates are supplied with nutrients and encouraged to form a photosynthetically active biofilm. Throughout the entire culture cycle, the species composition of the biofilm remains stable, despite the presence of biological contaminants. The growth of microalgae in biofilm systems is denser than that in dilute microalgal suspension systems, so primary (flocculation) and secondary (centrifugation) concentration procedures for harvesting is no longer required (Miranda et al., 2017; Palma et al., 2017). The high yield resulting from biofilm-based culture systems is useful for bioenergy production or novel applications that require dense biomass, such as pigment or lipid extractions.

Since biofilm growth and development are influenced by several factors, various designs have been created for biofilm culture depending on the scale, target species, and intended application. The efficiency of the system is highly influenced by the attachment material, surface area, and overall design.

Small-scale biofilm systems have been developed to investigate biofouling mechanisms, aquaculture feeding behavior, algal ecophysiology, and geographical substrate topography on the laboratory scale (Mannix-Fisher, 2021; Milagros et al., 2010; Murdock and Dodds, 2007). On the other hand, large-scale biofilm systems are primarily utilized in wastewater treatment facilities and, more recently, in microalgae cultivation.

3.1 Bioassay devices

A variety of lab-scale devices have been designed to evaluate the formation of photoautotrophic biofilms on artificial surfaces. This includes several common microtiter plate models, such as the classic 96-well microtiter plate assay and the Minimum Biofilm Eradication Concentration (MBEC) device, which are most commonly used to test antimicrobial susceptibility against biofilm colonies (Antunes et al., 2019). In this method, polystyrene microtiter plates are inoculated with microbial cells. After a specific time period, the planktonic cells are removed, and the biomass of the remaining biofilm is stained and quantified using plating or spectrophotometry. The MBEC device, also known as the Calgary Biofilm Device (CBD), utilizes specialized pegged coverlids that fit into the microtiter cell wells (Gilmore, 2011) (Figure 14A). Sessile biofilms that develop on the surface of the pegs are considered a true result of the biofilm forming process, as opposed to the biomass found in the wells, which could also be a product of sedimentation (Figure 14B). The biofilm cells from the pegs are harvested through sonication, but the efficiency of this process may vary.

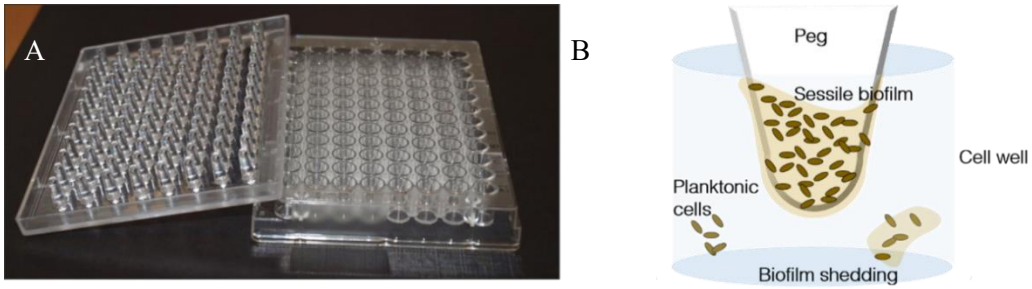

Figure 14 A) Commercially available MBEC microtiter plate used to evaluate biofilm formation (© Brendan Gilmore). B) True biofilms are distinguished by quantifying the cells that adhered on the microtiter pegs.

Furthermore, the BioFilm Ring Test® (BRT®) adapts the microtiter plate assay to study the initial formation of biofilms (Badel et al., 2011; Chavant et al., 2007). In this method, a solution of cells mixed with magnetic microbeads is loaded into the wells (Figure 15). After a defined incubation period, the non-immobilized beads are collected using a magnet, while the immobilized beads remain in place. Images are captured before and after magnetization to estimate the biofilm index (BFI), which ranges from 0 to 30, with low values (<2) indicating a high level of biofilm immobilization of the magnetic beads.

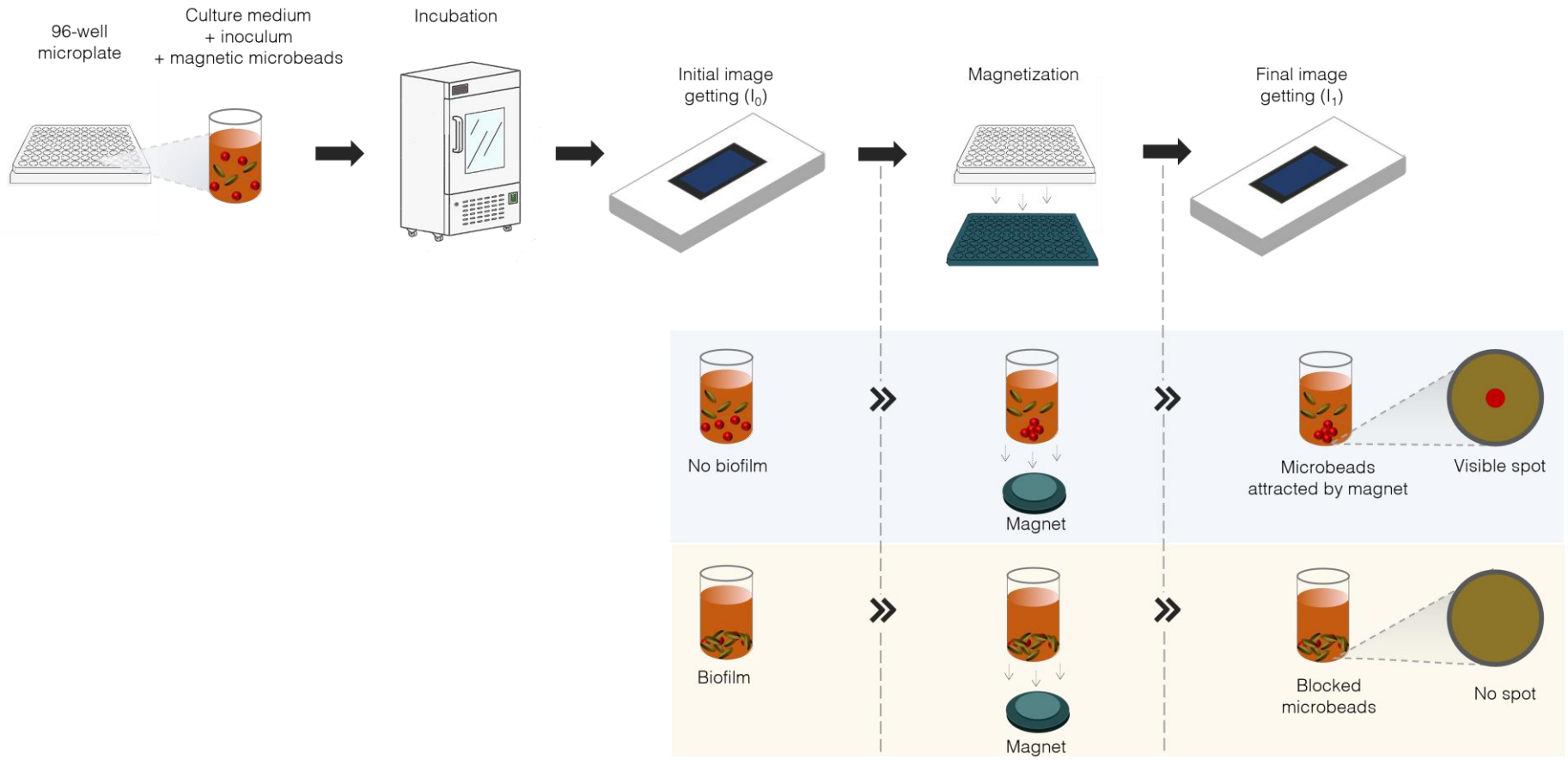

Figure 15 Schematic representation of the development and quantification of biofilms using the BioFilm Ring Test®. Initial cell suspension is inoculated in a 96-well microplate and mixed with magnetic microbead solution. After incubation, the plate is read using a dedicated scanner to get the initial image (I_0). Magnetization is done for 1 minute using a block of magnets positioned at the bottom of each well. During magnetization, free unblocked magnetic microbeads are attracted by the magnetic field toward the center of the wells, forming a visible spot. On the other hand, magnetic microbeads that are embedded in a biofilm are blocked and remain undetectable. The plates are scanned to get the final image (I_1). The software BioFilm Control Elements compares the I_0 and I_1 images and calculates the corresponding biofilm index (BFI) ranging from 0 to 30. A high BFI value indicates high bead magnetism corresponding to low biofilm formation capacity. A low BFI value suggests immobilization of beads due to biofilm formation.

The Robbins device and Modified Robins Device (MRD) are parallel-plate flow chamber systems that find widespread use in the analysis of biofilm development, both *in*- and *ex situ* (McCoy et al., 1981). The system consists of a closed tubing setup with evenly spaced threaded holes placed along a liquid stream (Figure 16A). To initiate biofilm formation, the sanitized device is filled with a growth medium. A batch of microorganisms is then inoculated by flushing the device with a stock culture solution, followed by a continuous pump of the sterile growth medium. Due to its multiple ports, the system allows for screening of various types of biofilm substrates using the same experimental parameters.

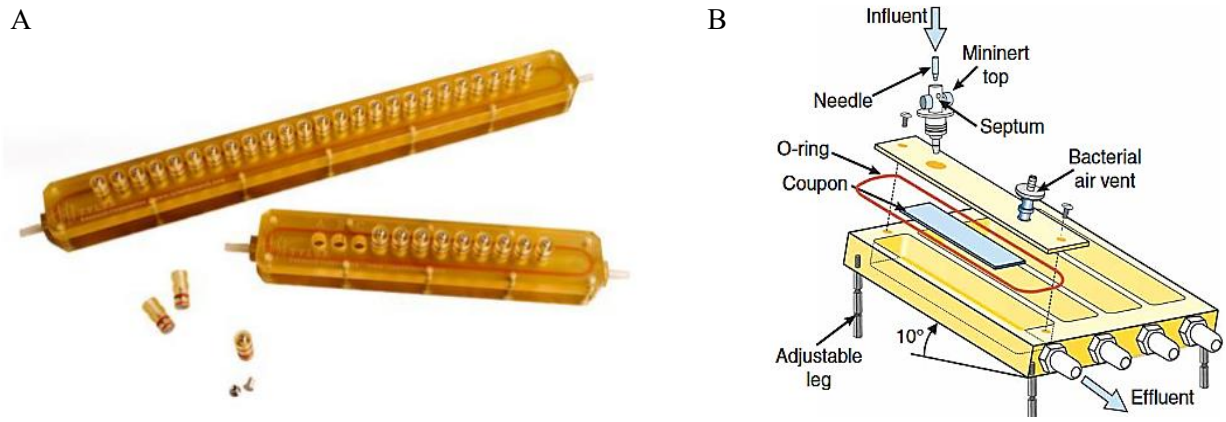

Figure 16 Flow chamber systems used to investigate biofilm development. A) Multiple ports in a closed Low Pressure Modified Robbins Device (LPMR) setup allow for simultaneous biofilm screenings (© Tyler Research Corporation). B) The Drip Flow Biofilm Reactor (DFR) has a tilt angle of 10° and a designated outflow port to drain planktonic cells, allowing true biofilm cells to be retained on the coupon (Mannix-Fisher, 2021).

The Drip Flow Biofilm Reactor (DFR) is a model specifically designed to study biofilm formation at the air-liquid interface under mild shear stress conditions (Goeres et al., 2009). It consists of an airtight, multi-channelled block with effluent inflow and outflow ports on each end of the channel (Figure 16B) (Goeres et al., 2009). Within the channels, there are coupons with known surface area, such as glass microscope slide, where biofilms can grow. The cell inoculum is introduced through a needle port on the lid. After incubation, the DFR is tilted at a downward angle of 10° to drain the

channels of the inoculum. Subsequently, nutrient medium is continuously dripped onto the coupons, allowing the formation and establishment of mature biofilms over time. To conclude a run, the coupons are rinsed to remove planktonic cells, and the biofilm aggregates are then resuspended for viable cell enumeration.

The DFR has found extensive use in biofilm control in clinical environments and food processing. Due to its versatility, researchers have made several modifications to adapt it to their specific needs. In the context of microalgae, the DFR has been used in various investigations, including studying CO_2-mediated development and metal excretion and sorption in phototrophic biofilms (Coutaud et al., 2019; Vázquez-Nion et al., 2020).

Laboratory-scale closed rotary biofilm reactors were initially developed in the late 1960s and have since been widely used to mimic different hydrodynamic conditions for studying biofilm growth and development. These reactors are designed to replicate the biofilm environment found in both natural and artificial water systems, such as rivers, potable water supplies, and ship hulls. Closed rotary systems are also used for investigating the effects of different biotic and abiotic factors in biofilm control, gene expression, and enzymatic activity (Pavarina et al., 2011). These reactors come in different types, but they are typically composed of a revolving inner cylinder contained within a bigger culture chamber. The inner barrel is equipped with multiple removable coupon substrates, which can be made from a variety of materials. Inoculum is directly added into the culture chamber, which is filled with sufficient culture medium, and the biofilm is allowed to grow under batch phase conditions for a period. After this initial phase, the continuous flow of nutrients is initiated to support growth and development of the biofilm. The rotation speed and the frequency of the cylinder can vary significantly depending on the specific reactor design and the environment it aims to mimic. To assess biofilm development, researchers can detach the coupons and conduct viability assays on the re-suspended cells at any time. A significant advantage of rotary biofilm reactors is the ability to test multiple coupon materials simultaneously. However, the number of strains that can be tested in a single run is limited, and there is a higher risk of introducing contamination during interval sampling.

3.2 Mass production devices

Routine hatchery procedures in the aquaculture of several invertebrates (*e.g.*, abalone, sea cucumber, and sea urchin) require critical provision of healthy and stable supply with benthic diatoms throughout the culturing period (Chang and Chen, 2008; de la Peña, 2007). Laboratory-scale benthic diatom stock cultures are typically cultivated in Erlenmeyer flasks, where they are given the opportunity to form a thin biofilm layer before being scaled up for biomass production. The transition to pilot-scale operations does not require specialized equipment or extensive training. Solid surfaces made of corrugated polyvinyl roofing sheets are intentionally prepared and left to be naturally or artificially colonized by benthic diatom biofilms at least two to three weeks before use (Body, 1987; Kawamura, 1996; Milagros et al., 2010). Additionally, these sheets can be grown together with supplementary crustose coralline red algae to create an even more realistic simulation of natural settlement conditions. Once fully prepared, the sheets are fully immersed and evenly arranged within the culture tanks just before larval stocking takes place (Figure 17).

Figure 17 Biofilm-coated settling plates in abalone culture (© Milagros de la Peña)

These biofilm-coated corrugated sheets play a crucial role in providing essential nourishment and serving as settlement and metamorphosis cues for the larvae and early juveniles (Figure 18). The water flow within the culture tanks is carefully regulated, tailored to the specific life stage of the organisms being cultivated. Additionally, nutrients are regularly added to stimulate adequate and continuous growth of the algal biofilm on the sheets.

Figure 18 Settlement of juvenile *Haliotis asinina* on biofilm-coated corrugated sheets (© Milagros de la Peña)

In recent years, researchers have been actively investigating the potential of biofilm photobioreactor designs for various microalgae-based applications. These innovative designs have primarily focused on effectively removing nutrients and heavy metals from wastewater effluents, employing either single or mixed species of microalgae (Boelee et al., 2014; De Godos et al., 2009; He and Xue, 2010; Posadas et al., 2013; Schultze et al., 2015; Shi et al., 2014; Zamalloa et al., 2013). However, biofilm technology is emerging as a promising alternative to suspension culture systems and is being used to improve biomass production (Blanken et al., 2014; Morales et al., 2020; Zhuang et al., 2014). Multiple studies using biofilm photobioreactors investigate lipid accumulation in microalgae for the production of microalgae-derived products, such as lipids and pigments (Cheng et al., 2014; Genin et al., 2014; Johnson and Wen, 2010; Schnurr et al., 2013; Wood et al., 2022). Interdisciplinary studies have also been conducted, combining wastewater treatments and by-product valorization using microalgal biofilms (Bernstein et al., 2014; Christenson and Sims, 2012; Wood et al., 2022). This integration enhances the feasibility of algal biorefinery and facilitates circular economy.

Several research papers have provided summaries of different biofilm photobioreactors (PBRs) based on their configuration, orientation, or operation (Choudhary et al., 2017; Gross et al., 2015; Hoh et al., 2016). In general, PBRs can be classified according to the relative movement of the substrate to the culture medium, which can be either stationary or rotating (Table 1). Additionally, they can be categorized as either horizontal or vertical based on the orientation of the support substrate.

Table 1 Algal biofilm cultivation systems (modified from Gross et al. 2015). The superscript indicates the phylum/division: (a) Chlorophyta (b) Ochrophyta (c) Cyanobacteria (d) Haptophyta (e) Charophyta.

Biofilm cultivation system	Species	Scale	Reference
Stationary biofilm design			
Algal biofilm membrane photobioreactor	*Chlorella vulgaris*[a]	Lab	(Gao et al., 2015)
Algal disk/vertical plate-attached photobioreactor	*Scenedesmus obliquus*[a]	Pilot	(Liu et al., 2013)
Algal turf scrubber	Polyculture	Pilot	(Mulbry and Wilkie, 2001)
Algal-based immobilization reactor	*Scenedesmus* sp.[a]	Lab	(He and Xue, 2010)
Concrete slab algae biofilm photobioreactor system	*Botryococcus braunii*[a]	Lab	(Ozkan et al., 2012)
Enclosed biofilm tubular reactor	*Chlorella sorokiniana*[a]	Lab	(De Godos et al., 2009)
Flat-plate parallel horizontal photobioreactor	*Nitzschia palea*[b] *Scenedesmus obliquus*[a]	Lab	(Schnurr et al., 2013)
Flow lane biofilm reactor	Polyculture Cyanobacteria[c]	Lab	(Boelee et al., 2014; Di Pippo et al., 2013; Gismondi et al., 2016; Posadas et al., 2013)
Parallel plate air lift reactor	Polyculture	Lab	(Genin et al., 2014)
Polystyrene rocker system	*Chlorella* sp.[a]	Lab	(Johnson and Wen, 2010)
Porous substrate bioreactor/twin-layer biofilm photobioreactor	*Halochlorella rubescens*[a] *Isochrysis* sp.[d] *Tetraselmis* sp.[a] *Phaeodactylum* sp.[b] *Nannochloropsis* sp.[b]	Lab	(Arnaldo, n.d.; Murphy and Berberoglu, 2014; Naumann et al., 2013; Schultze et al., 2015; Shi et al., 2014; Zhang et al., 2015)
	Amphora sp. NCC169[b] *Anabaena variabilis*[c] *Spirulina platensis*[c]		
Roof-installed parallel plate microalgae biofilm reactor	*Scenedesmus obliquus*[a]	Lab	(Zamalloa et al., 2013)
Single-layer-attached photobioreactor	*Botryococcus braunii*[a]	Lab	(Cheng et al., 2014)
Suspended-solid-phase photobioreactor	*Scenedesmus* sp.[a]	Lab	(Zhuang et al., 2014)
Rotating algal biofilm cultivation system			
Algadisk	*Chlorella sorokiniana*[a]	Lab/Pilot	(Blanken et al., 2014; Sebestyén et al., 2016)
Drum biofilm reactor	*Chlorella vulgaris*[a]	Lab	(Shen et al., 2016)
Photorotating biological contactor	*Klebsormidium* sp.[e]	Lab	(Orandi et al., 2012)
Revolving algal biofilm cultivation system	*Chlorella vulgaris*[a]	Lab/Pilot	(Gross et al., 2015, 2013; Gross and Wen, 2014)
Rotating algal biofilm conveyor belt	*Chlorella autotrophica*[a] *Tetraselmis suecica*[a]	Lab/Pilot	(Grenier et al., 2019; Morales et al., 2020)
Rotating algal biofilm (RAB™) reactor	Polyculture	Lab/Pilot	(Bernstein et al., 2014)
Rotating algal biofilm reactor with spool harvester	Polyculture	Lab/Pilot	(Christenson and Sims, 2012)

Stationary biofilm systems require a device (*e.g.*, pump, spray) to deliver the culture medium onto the biofilm surface. In comparison to rotating biofilm systems, stationary designs require very low capital investment because there are few moving parts involved (Gross et al., 2015). However, rotating biofilm systems offer the advantage of mitigating the risk of photo-inhibition due to the alternation of light and dark cycles, resulting in a two-fold increase of biomass productivity compared to stationary types (Grenier et al., 2019; Hoh et al., 2016).

Horizontal biofilm reactors have denser biofilms with more effective photosynthetic light absorption compared to their vertical counterparts (Hoh et al., 2016; Jha et al., 2022). However, they require a larger surface area for cultivation, which may not be feasible in limited spaces. On the other hand, vertical biofilm reactors can overcome this limitation by allowing the installing multiple perpendicular substrate layers at once (Liu et al., 2013). Additionally, vertical reactors have an effective light dilution capacity that leads to high biomass productivity. However, a potential drawback is mutual shading by adjacent layers, particularly if they are too tall, which may result in non-uniform illumination and hinder overall productivity.

Almost all of these systems are constantly or intermittently submerged in the culture medium. In this scenario, the substrates are usually made of impermeable materials. However, a new type of biofilm photobioreactor, known as a porous substrate photobioreactor (PSBR), takes a different approach. It uses a thin microporous substrate that completely separates the bulk of the biofilm from the culture medium (Naumann et al., 2013; Nowack et al., 2005; Shi et al., 2007). The substrate physically confines the cells on one side while allowing the continuous downward flow and diffusion of nutrient-rich medium from the other side.

Although some marine diatom species thrive in a traditional suspension airlift PBR, other benthic species were unsuccessful (Figure 19) (Cointet et al., 2021). The failure of these species to grow in suspension led to a re-evaluation of their cultivation conditions and prompted a collaboration between Synoxis Algae and Nantes University (Nantes, France) to develop a PSBR specifically designed for benthic diatoms (Arnaldo, n.d.). Trial cultivation of *Nitzschia laevis* using the initial design of the PSBR resulted in a total lipid rate of 25% (dry weight) after five culture days (

Figure **20**). Moreover, the cells achieved a specific growth rate (μ) of 0.26 day^{-1}, which was higher than the previously recorded value for *N. laevis* (μ = 0.17 day^{-1}) under photoautotrophic conditions (Wen and Chen, 2000). The design was subsequently improved (Figure 21) and is currently being used to grow *Amphora* sp. NCC169 for ecophysiological investigation and high-value lipid production.

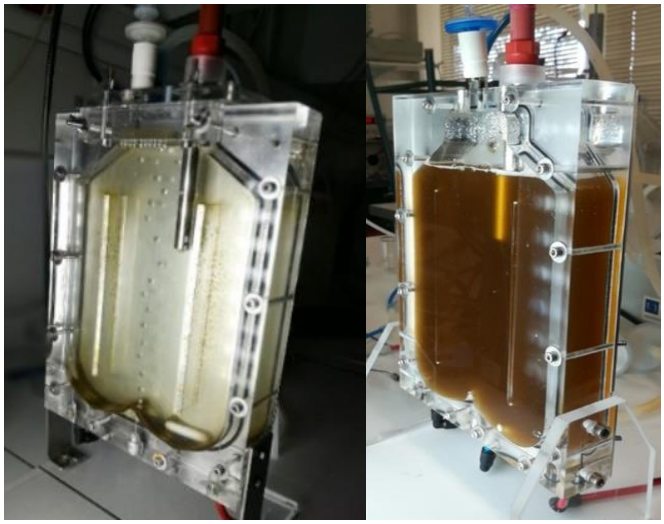

Figure 19 Growth of marine benthic diatom (A) *Amphora* sp. NCC169 and (B) *Entomoneis paludosa* in an airlift photobioreactor (©Eva Cointet)

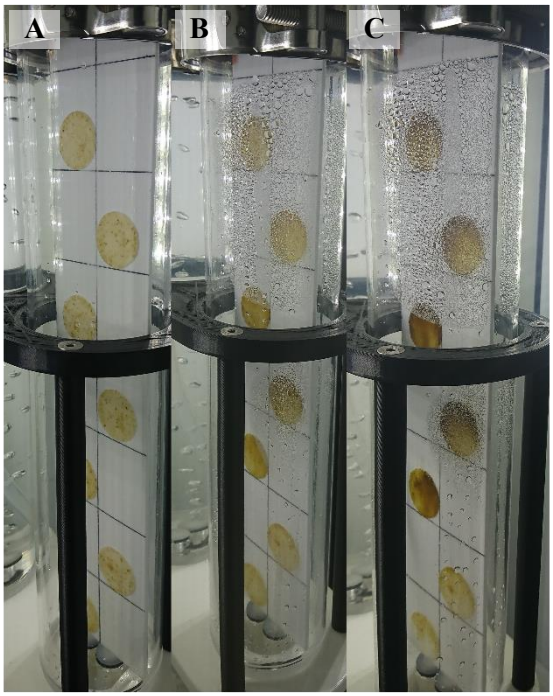

Figure 20 Growth progression of *N. laevis* in PSBR during (A) launch, (B) day 2, and (C) day 5

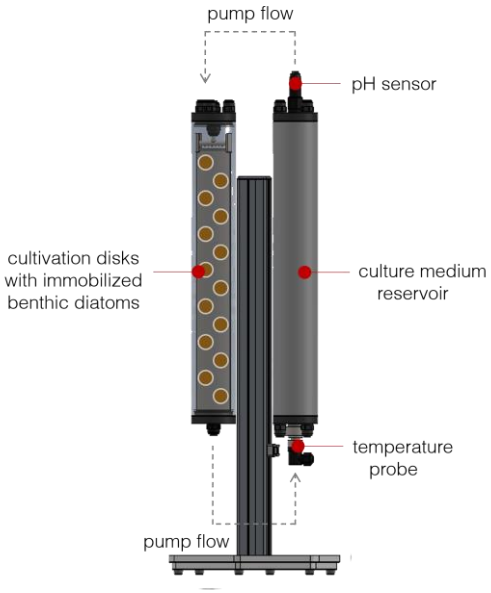

Figure 21 Schematic diagram of improved Synoxis Algae PSBR

The pilot raceway-based rotating algal biofilm system developed by SAS inalve (Nice, France) is effectively used in the mass production of *Tetraselmis suecica* (Morales et al., 2020) (Figure 22). Additionally, algal turf scrubber (ATS) and rotating algal biofilm reactor (RAB™) technologies have been successfully implemented at the commercial scale for various application, including wastewater treatment and biomass and biofuel production (Christenson and Sims, 2012; Gross et al., 2013). Notably, Gross-Wen Technologies' vertically oriented RAB™ conveyor belts have significantly reduced the cost associated with wastewater treatment plants in Iowa (USA), and are set to become the largest algae-based wastewater facility in the country by 2023 (Gross-Wen Technologies, 2022).

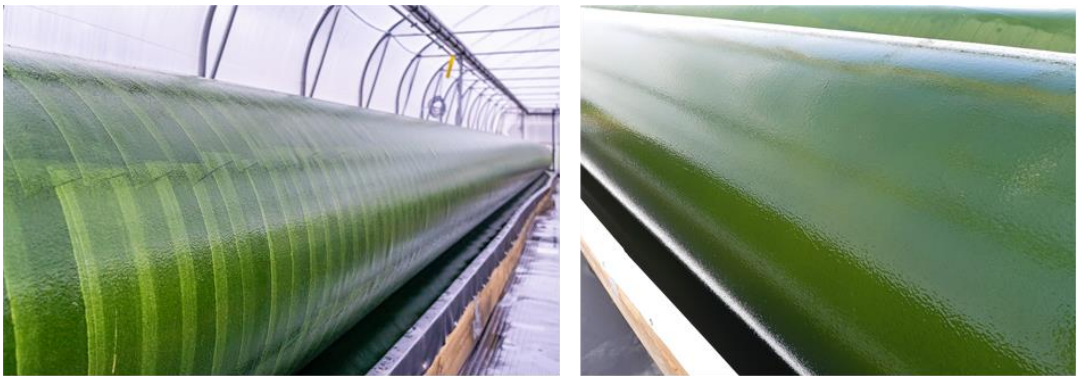

Figure 22 *Tetraselmis suecica* produced on a Rotating Algal Biofilm system developed by inalve (© Freddy Guihéneuf)

The successful large-scale applications of biofilm systems are highly dependent on the ecophysiological behavior of the immobilized cells. Traditionally, potential species for scale-up are screened by evaluating their biochemical properties in laboratory setting (*e.g.,* lipid content, or pigment composition). However, this approach may lead to issues when the selected strains underperform after the scale transfer to the larger-scale system. An alternative strategy is to first grow the species under large-scale conditions, and then conduct an in-depth laboratory-scale ecophysiological investigation (Wang et al., 2017). This approach helps to better understand how the species behave and perform in the actual large-scale environment, improving the success rate of biofilm-based systems in potential applications.

4. Conclusion and perspective

Benthic diatom cultivation is still predominantly carried out using suspension culture methods, which overlooks the evolutionary advantage of their biofilm-forming capacities. The emerging paradigm shift in microalgal culture towards the use of biofilm technology addresses the most pressing challenges in suspension culture and presents opportunities for exploring and valorizing high value benthic diatom products. However, the adaptation of biofilm-based culture systems is still in its early stages, and further fundamental research and development are needed to fully unlock its potential. The lack of validated standard procedures presents a significant bottleneck that hampers comparisons among different biofilm designs and reported studies. Although a handful of biofilm photobioreactors have reached pilot scale, they have primarily been utilized for wastewater systems. The heterogeneity of biofilm growth still requires comprehensive investigation to understand the physicochemical parameters at play within the cultivation system. Additionally, the environmental impact and economic viability of most biofilm designs need to be thoroughly characterized.

Elucidating the characteristics of biofilms and understanding species-specific ecophysiology through biofilm cultivation represents an efficient and promising interdisciplinary approach. This approach has the potential to revolutionize high-biomass and high-value product development, making it a futuristic and valuable avenue for research and industrial application.

Chapter II

Development of the porous substrate photobioreactor (PSBR) for biofilm cultivation

Abstract

Following the examination of the ecological functions and potential biotechnological applications of diatom biofilms, Chapter II subsequently transitions to the inception, construction, and scientific exploration of the PSBR system to optimize the cultivation of benthic diatom. Here, the conceptual framework behind the PSBR is outlined with special emphasis on the design principles. A detailed description of the PSBR's construction, operational parameters, and the rationale behind its design choices is provided. Moreover, Chapter II addresses the technical hurdles encountered in optimizing the PSBR during the development and testing phases, and probes into the preliminary experimental set-ups used to evaluate the PSBR's performance, presenting data on *Nitzschia laevis* biomass yield, lipid content, and productivity comparisons between the PSBR and traditional suspension cultures. The utilization of the PSBR underscores a significant advancement in benthic diatom cultivation towards realizing their full potential in biomass and lipid production for biotechnological applications.

1. Introduction

The use of algal biofilm systems began in 1970s for wastewater treatment purposes (Hassard et al., 2015). The biofilm used for water treatment consists of different autotrophic and heterotrophic microorganisms (e.g., microalgae, bacteria, fungi) that play an important role in utilizing the nutrients in wastewater (Katarzyna et al., 2015; Kesaano and Sims, 2014). Biofilm-based production systems are still predominantly used for wastewater treatment, but it has since then expanded to algal biomass production (Liu et al., 2013; Naumann et al., 2013). For this purpose, the biofilm consists of a single species of microalga that are densely inoculated onto the surface of an attachment material. The cell aggregates are fed with nutrients and allowed to form a photosynthetically active biofilm. The species composition of the biofilm is stable for the entire duration of the culture cycle. The growth of microalgae in biofilm systems is denser than those from dilute microalgal suspension systems, so primary (flocculation) and secondary (centrifugation) concentration procedures for harvesting is no longer required (Miranda et al., 2017; Palma et al., 2017). The high yield resulting from biofilm-based culture systems is useful for novel applications in microalgal biotechnology that require dense biomass, such as pigment or lipid extractions.

Over the past 20 years, there has been an abundance of scientific papers relating to biofilm-based systems, and they are well-reviewed (Berner et al., 2015; Gross et al., 2015; Hassard et al., 2015; Hoh et al., 2016; Katarzyna et al., 2015; Kesaano et al., 2015; Podola et al., 2017). To summarize, a biofilm system can be classified either as (i) stationary biofilm or (ii) rotating biofilm according to the kinetics of the biofilm substrate relative to the culture medium (Gross et al., 2015). The biofilm can be fully submerged in the culture media, partially submerged, or have porous substrates where algal cells are separate from the bulk of the culture media and receives nutrients by diffusion or evaporation (Podola et al., 2017). Most of these algal biofilm systems have been primarily used for planktonic green algae. Several designs have been used for diatom cultivation, such as the flat-plate parallel horizontal photobioreactor and porous substrate photobioreactor (PSBR)/twin-layer biofilm photobioreactor. Biofilm systems using polyculture have also included diatom species like *Nitszchia* sp., *Cymbella* sp., *Melosira* sp., *Gomphonema* sp., *Synedra* sp., *Eunotia* sp., *Diatoma* sp. and *Navicula* sp. mixed in with other groups of microalgae (Boelee et al., 2014; Christenson and Sims, 2012; Genin et al., 2014).

The configurations of biofilm system are highly variable, and each design has its own advantages and limitations. Stationary biofilm designs, in general, have lower energy expenditure because the system has little to no moving parts. However, they can require significant land resources for scaling up, especially when they're oriented horizontally. Net photosynthetic productivities are higher in unsubmerged biofilm-based systems due to the gas exchange that occurs directly between the gas phase and the biofilm (Podola et al., 2017). Rotating biofilm systems on the other hand, have harvesting advantages because the biomass can be scraped off when the biomass is in the air phase or microalgae can be sloughed off straight into the wastewater. A PSBR is reported to have higher biomass yield than other cultivation systems, but demonstrates reduction in productivity over time (Podola et al., 2017). Cotton-based materials show provide better attachment surfaces, but deteriorates rapidly and requires frequent replacement (Gross et al., 2013; Gross and Wen, 2014). These being said, there are considerable variations between experiments (e.g., species composition, productivity measurements) that limit conclusive comparisons between systems.

2. Construction and functionality of the biofilm photobioreactor

Considering all available information, this present work built a low-maintenance system for benthic diatom cultivation adapted from the vertically-oriented PSBR design previously described by University of Cologne (Podola et al., 2017; Shi et al., 2007) (Figure 23).

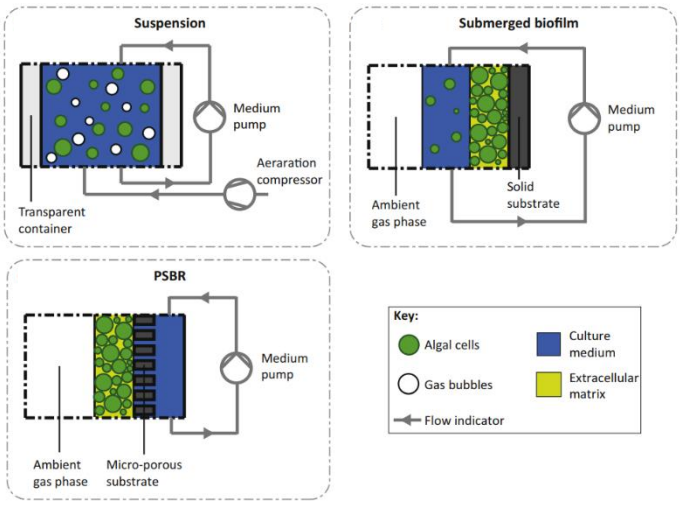

Figure 23 Schematic representation of three different bioreactor configurations for the cultivation of algal cells: a suspension-based system, a submerged biofilm system, and a PSBR (Podola et al., 2017)

The functional structure of this design, also described and known as the Twin-Layer system (Naumann et al., 2013; Shi et al., 2007) or attached cultivation system (Liu et al., 2013), is composed of (i) a source layer that could be made of either textile, plastic, or metal (Liu et al., 2013; Schultze et al., 2015; Shi et al., 2014; Wan et al., 2014) and (ii) thin porous membrane filters. These layers are both hydrophilic and self-adhere to each other. The porous membrane filter that supports the immobilized microalgae can be made of different polycarbonate/cellulose membranes (Schultze et al., 2015; Zhuang et al., 2014), plain printing paper (Naumann et al., 2013), or industrial textiles (Zhuang et al., 2014). Unlike suspension-based cultivation methods, the culture media is separated from the algal cells. In this system, the culture media is pumped to the top of the layer and drips down by means of gravitational flow. The immobilized cells are continuously being supplied with dissolved nutrients as the aqueous solutes permeate through the hydrophilic layers. After passing down through the biofilm panel, the culture media will be collected back into the reservoir and recirculated into the system. Gas exchange takes place on the light-exposed surface of the biofilm.

A collaboration was made with Synoxis Algae, a biotechnology start-up located in Le Cellier, France that constructs and supplies modular cultivation systems for microalgae. They provide a range of cultivation chambers ranging from the experimental scale photobioreactor to commercial production scale. As a subsidiary of the plastic company Synoxis, Synoxis Algae relies on their long-term experience in plastic production for various photobioreactor solutions. For the project, we're going to utilize their existing technology, the NANO (Figure 24) whose technical information is summarized in Table 2.

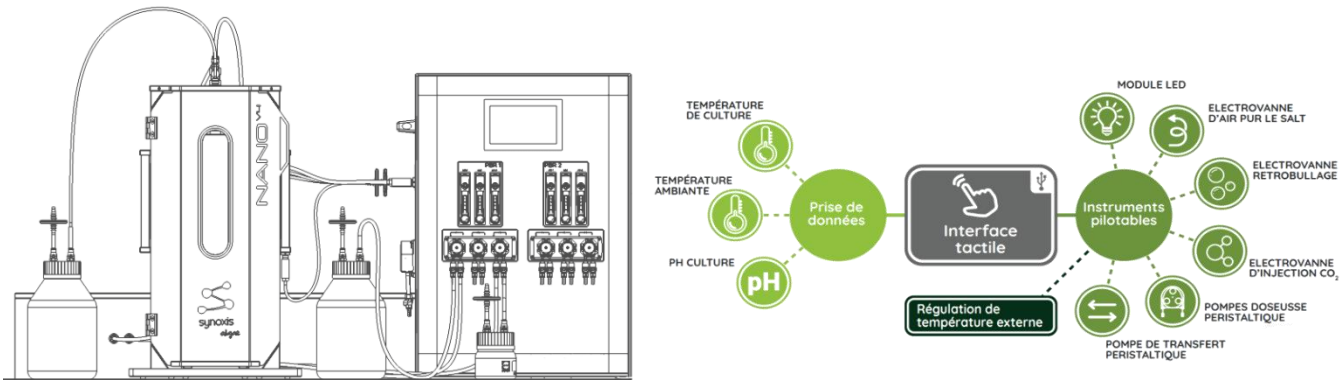

Figure 24 Functional scheme of NANO photobioreactor

Table 2 Technical data sheet of Synoxis NANO photobioreactor

CARACTÉRISTIQUES GÉNÉRALES		
Dimensions sur la paillasse (L x l x h)	2400 x 600 x 900 mm	
Poids total	25 kg	
Puissance totale installée	1300 W	
Caractéristiques électriques	220-240V 50/60 Hz	
Besoin en entrée d'air	1 à 5 bars, 6 L/min minimum	
Besoin en entrée de CO2 de la machine	1.5 à 5 bars, 2.5 L/min minimum	
CHAMBRE DE CULTURE		
Volume de chaque chambre de culture	3 L	
Volume utile	98.5%	
Ratio S/V	47 m^2/m^3	
Résistant à la corrosion	OUI	
Agréé au contact alimentaire	OUI	
2 CONFIGURATIONS POSSIBLES	**CLASSIQUE**	**AUTOCLAVABLE**
Stérilisation chimique	OUI	OUI
Stérilisation thermique	NON	OUI
LUMIÈRE (Spectre lumineux sur demande)		
2 CONFIGURATIONS POSSIBLES	**WHITE**	**COLORS**
Plage d'intensité lumineuse globale	0 à 500 µmol/m^2/s	0 à 300 µmol/m^2/s
Nombre de canaux lumineux pilotables	1	3
POMPES		
Débit des pompes doseuses péristaltiques	20 mL/min	
Débit de la pompe de transfert péristaltique	650 mL/min	
GESTION DES GAZ		
Détail sur les débitmètres	Corps en verre, indicateur à bille, molette manuelle	
Plage de débit	0 à 1.2 L/min	
SONDE PH/TEMPÉRATURE		
SONDE	**PH**	**TEMPÉRATURE**
Capteur	Sonde combinée	PT1000
Plage de mesure	0 à 14	0 à 70 °C
Résolution	0.01	0.1
Corps de la sonde	Verre résistant à 135 °C et 6 bars	
Longueur de la sonde	120 mm	
RÉGULATION THERMIQUE		
Plage de régulation	10 à 35 °C	
Puissance de l'installation froid	250 W	
Puissance de l'installation chaud	300 W	
VERRERIE		
Détails sur les flacons	Verre borosilicate, col large 80 mm, autoclavables	
Dimensions flacon 3.5 L (Diam. x h)	160 x 295 mm	
Dimensions flacon 0.25 L (Diam. x h)	95 x 130 mm	
CONNECTIQUE		
Extraction des données et mise à jour logiciel	USB	

Synoxis' tubular NANO technology is originally intended for suspension culture (Figure 25A). The culture chambers for biofilm cultivation were adapted from the design configured by Benstein et al. (2014) (Benstein et al., 2014). In the modified configuration, the biofilm photobioreactor culture chamber consists of two modular, transparent poly(methyl methacrylate) (PMMA) cylinders (diameter = 64 mm ; height = 420 mm) (Figure 25B). One of the cylinders acts as a reservoir for culture

medium while the other cylinder serves as the main container for biofilm growth. A 350 mm x 58 mm PMMA panel is secured inside the cylinder as support for the source layer. A sheet of lens cleaning tissue (Whatman, Catalog Number: 2105-918) is laid over the PMMA panel to act as a source layer. This support allows the adhesion of circular glass fiber filters (⌀25 mm, 0.7 µm pore size) that have been initially inoculated with benthic diatoms. Guillard's F/2 medium is distributed to the PMMA panel through drip method by means of a perforated tube positioned over the PMMA panel. The amount of culture medium flowing through and out of the biofilm photobioreactor is regulated by several peristaltic pumps in the control unit.

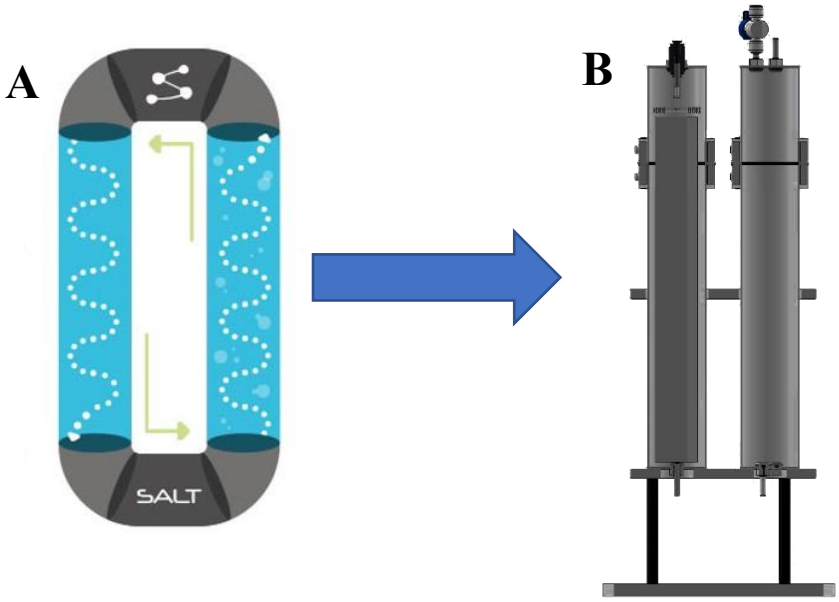

Figure 25 Schematic overview illustrating the transformation of Synoxis' NANO culture chamber from a suspension-based technology (A) to a biofilm-based system (B), highlighting the adaptation of the technology for different methods of algal cultivation.

3. Preliminary experiments using *Nitzschia laevis*

To test the feasibility of the biofilm photobioreactor, the proposed attached cultivation method was initially tested using *Nitzschia laevis,* a robust and fast-growing species of benthic diatom.

3.1 Materials and methods

Pre-combusted (400°C, 4 h) GF/C filter disks (⌀25 mm, 0.7 µm pore size) were used as substrate for the diatom biofilm. Individual filter disks were placed inside a 6-well cell culture plate and inoculated with 400 µL of *N. laevis*. The cells were carefully inoculated on the surface of the filter disks to prevent growth initiating on the underside of the disks. An additional 2 mL of natural seawater enriched with Guillard's F/2 medium was added into each cell well to keep the filter disks immersed under solution for biofilm formation. Inundation of F/2 medium was done slowly and carefully so as not to displace the diatom cells on the surface of the disks. Priorly, a circular piece of lens paper was placed between the surface of the cell well plate and the filter disk to act as a hydrophilic support for the disk and keep it from floating on the surface. The disks were left to incubate in the culture room (temperature = 16 °C, light intensity = 150 µmoles m^{-2} s^{-1}) until a stable biofilm is formed (Figure 26). Multiple culture plates were made to ensure sufficient supply for use in the experiment.

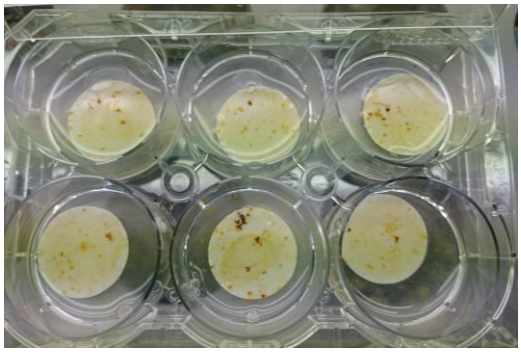

Figure 26 Thin layer of *N. laevis* biofilm forming on the filter disks nine days after inoculation, indicating successful establishment and growth of the diatom colonies

Seven filter disks were randomly taken from the cell culture plates using a number generator (www.stattrek.com). The biomass of the biofilm formed on the filter disks was measured non-destructively using normalized difference vegetation index (NDVI) (Cointet, 2019). NDVI is frequently used to evaluate the biomass of terrestrial vegetations, as well as to measure biofilm and microphytobenthos growth using satellite data (Barillé et al., 2011; Cointet, 2019; Méléder et al., 2007, 2003). The reflectance (ρ) of the cells at certain wavelengths are known to be proportional to their chlorophyll *a* content and is used as reliable proxy for biomass. Reflectance data was taken using Ocean

Optics Flame-UV-S-VIS-NIR-ES miniature spectroradiometer. The reflectance values at the maximal reflectance wavelength (λ_{750}) and the chlorophyll *a* absorption wavelength (λ_{675}) were used to calculate the NDVI following the formula:

$$NDVI = \frac{\rho_{\lambda 750} - \rho_{\lambda 675}}{\rho_{\lambda 750} + \rho_{\lambda 675}} \quad \text{(Eq. 2)}$$

The physiological stress and photosynthetic activity of the biofilms were measured through pulse-amplitude modulated (PAM) fluorometry, a method that is widely used in a lot of photosynthetic studies (Consalvey et al., 2005; Sma-Air and Ritchie, 2021). Low level non-actinic measuring light was initially applied to dark-adapted (15 minutes) samples to get the minimum fluorescence yield (F_0), followed by a strong saturating pulse to reach the maximum fluorescence level (F_m). Variable fluorescence F_v is the difference between maximal and minimal fluorescence (F_m-F_0). The maximum quantum efficiency (F_v/F_m) parameters of representative algal disks estimate the physiological stress and photosynthetic efficiency of the diatoms. The health of the photosynthetic cells is proportional to the F_v/F_m, with the optimum value set between 0.6-0.7 (Cointet, 2019).

A separate set of filter disks from the same batch of cell culture plates were harvested parallel to the ones used in the biofilm PBR to compare the status of the biofilm before and after the experiment trials.

The inoculated filter disks were arranged on top of a source panel, as illustrated in Figure 27. The panel was outlined with a grid to set the disks approximately 5 mm horizontally away from each other. The disks were identified from I to VII according to their relative position on the panel. The top section of the panel was not utilized due to the shadowing that occurs on that area of the biofilm PBR.

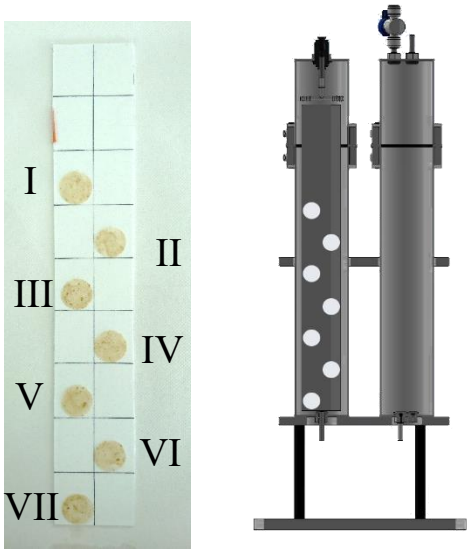

Figure 27 Strategic arrangement and layout of the filter disks on the support panel of the biofilm PSBR

Two trials were conducted using the biofilm PBR. For the first trial, the duration lasted five days, while the second one lasted 26 days. The second experiment encompassed the summer holidays, when the biofilm PBR was left to run continuously unattended. For both trials, the light was set to 150 µmoles $m^{-2}s^{-1}$, pH at 7.8, and ambient temperature at 24-30 °C. Natural seawater enriched with Guillard's F/2 medium was dripped onto the substrate at a rate of 1 mL every 10 minutes. For the second trial, an additional 10 mL of culture medium was replenished into the reservoir every 24 h by means of a peristatic pump in the control unit.

At the end of the culture cycle, all the algal disks were harvested from the biofilm photobioreactor. The biomass and photosynthetic activity of the films were measured similar to the protocol in the beginning of the experiment. The disks were individually washed with ammonium formate (68 g L^{-1}), frozen at -80 °C, and lyophilized to a constant weight.

Lipid extraction of the lyophilized samples was done using Bligh and Dyer methods (Bligh and Dyer, 1959). The disks were pooled in an Erlenmeyer flask for solvent extraction. Dichloromethane and methanol were added in a 1:1 ratio into the flask, and the flask was mechanically agitated for 1 h. The solvent extract was filtered through a Whatman phase separating filter paper (⌀15.0 cm) to remove silica

and other solid particulates resulting from the initial extraction. The extract was washed with water and mixed by means of a separatory funnel. The lower organic phase was dried over sodium sulphate. After 30 minutes, the organic phase was filtered in another flask for rotary evaporation. Once the organic solvent has evaporated off the flask, the total lipid was resuspended on a small volume of dichloromethane and transferred into a pre-weighed vial. The dichloromethane was evaporated to obtain the total lipid extract.

3.2 Results

Data obtained from Trial 1 showed very rapid biomass growth (Figure 28-Figure 29). The NDVI increased from 0.25 to over 0.7, except for filters VI and VII which are located on the bottom of the source panel. This growth corresponds to a pooled biofilm dry weight that increased from 1.17 ± 0.27 mg (Day 0) to 4.90 ± 2.5 mg (Day 5), which is significantly higher than values found in the literature (Wen and Chen, 2000). The photosynthetic efficiency of the biofilm decreased overall, but the F_v/F_m values remained strong (>0.5) indicating favorable culture conditions for the maintenance of healthy biofilm cells.

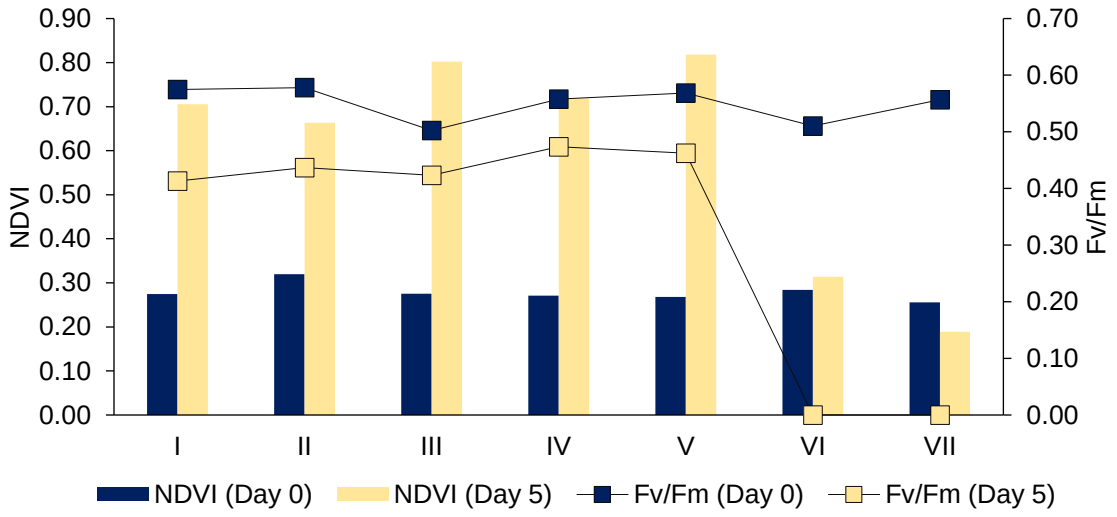

Figure 28 Preliminary result showcasing the growth dynamics and physiological status of *N. laevis* biofilm in the PSBR over a 5-day period. The left y-axis and blue bars represent the NDVI, a proxy for biomass accumulation, at the inception (Day 0) and upon the conclusion (Day 5) of the observation

period, respectively. The right y-axis and the square markers illustrate the Fv/Fm ratio, indicating photosynthetic efficiency, for the same time points. Each pair of bars and connecting line represents data collected from individual filter disks, numbered I through VII, within the PSBR setup.

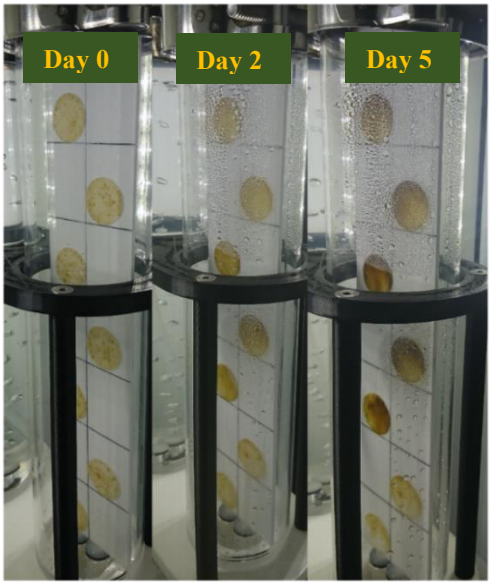

Figure 29 Progression of *N. laevis* biofilm disks in biofilm PBR following installation (Day 0), Day 2, and Day 5. The biofilms are characterized by variations in color and thickness, which indicate different stages of growth and biofilm maturation.

In the second trial, the NDVI of the biofilm has overall increased (Figure 30). However, the growth has been very heterogenous and patchy, as reflected in the appearance of the disks after 26 days (Figure 31). The photosynthetic efficiency of the biofilm has also plummeted to zero, except for disks IV and VI.

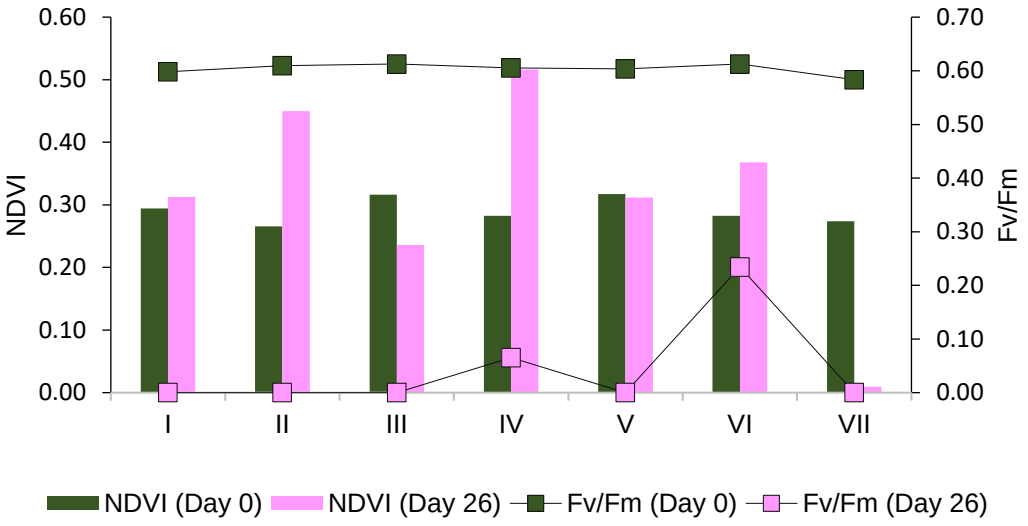

Figure 30 Biomass and photosynthetic efficiency of the *N. laevis* biofilm before the launch (Day 0) and after harvest (Day 26) from the biofilm PBR

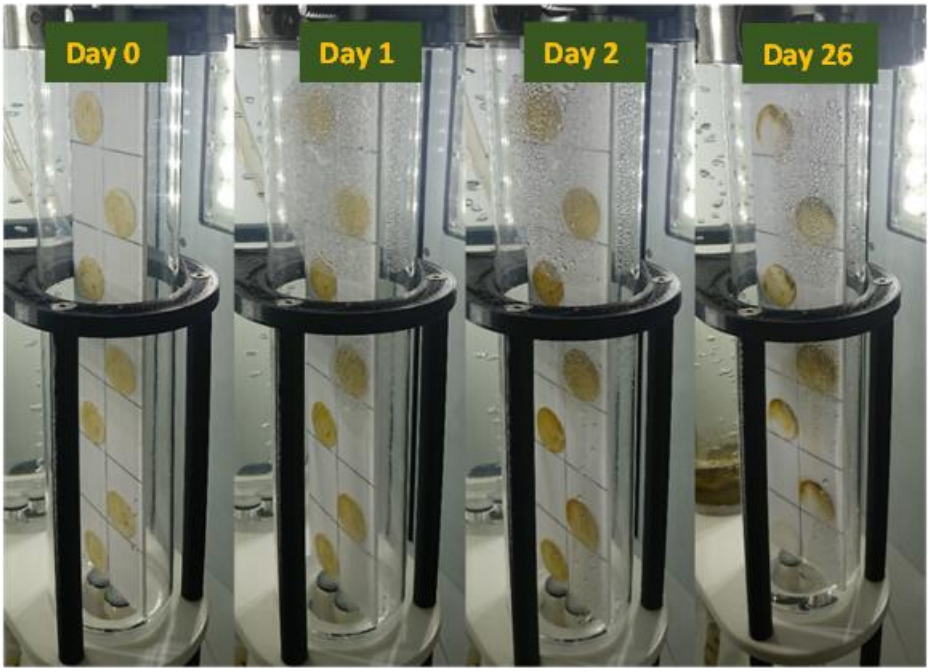

Figure 31 Progression of *N. laevis* biofilm after 0, 1, 2, and 26 days

The experiments started with an initial biomass of 1.17 ± 0.27 mg (Trial 1) and 1.12 ± 0.38 mg (Trial 2) (Figure 32). After the end of their respective culture period, the biofilms in the first trial have increased to 4.90 ± 2.54 mg while trial 2 reached 7.22 ± 3.55 mg. Trial 2 had an overall higher biomass than Trial 1, but the biofilms that formed on the disks were too heterogenous. Although the disks

appeared to be devoid cells, there could still be silica residues that contributed to the final biomass of the pooled sample.

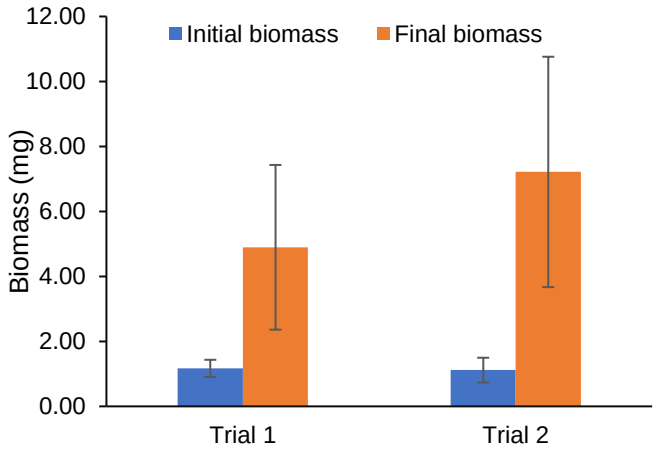

Figure 32 Increase in pooled dry biomass of *N. laevis* from the start (blue bars) to the end (orange bars) of two experimental trials, with Trial 2 showing a more pronounced increase than Trial 1. The error bars indicate variability in the biomass measurements.

At the end of culture, crude lipid made up 25% and 13% of the *N. laevis* dry biomass for Trial 1 and Trial 2, respectively (Figure 33). The lower lipid content of the biofilm in the second trial was attributable to the degradation of the cells over a significantly longer culture period.

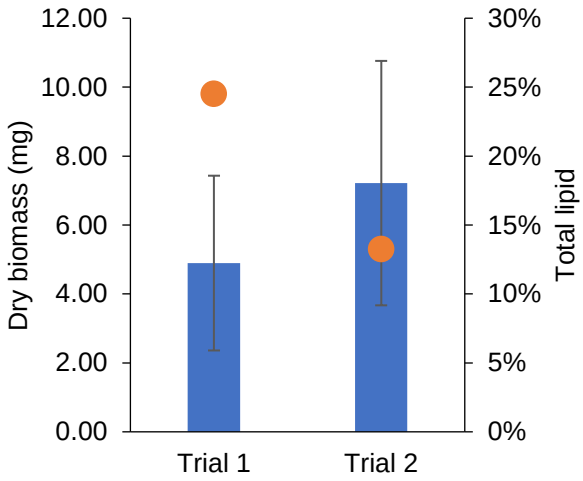

Figure 33 Comparative yield of PBR experiment trials after harvest. Dry biomass value constitutes the average of the filter disks (n=7), and total lipid is the percentage from the pooled disks.

4. Modification and new features of the PSBR

Synoxis' tubular NANO technology is originally intended for suspension culture. For this project, the culture chambers were specially modified for biofilm cultivation similar to the configuration of Benstein et al. (2014).

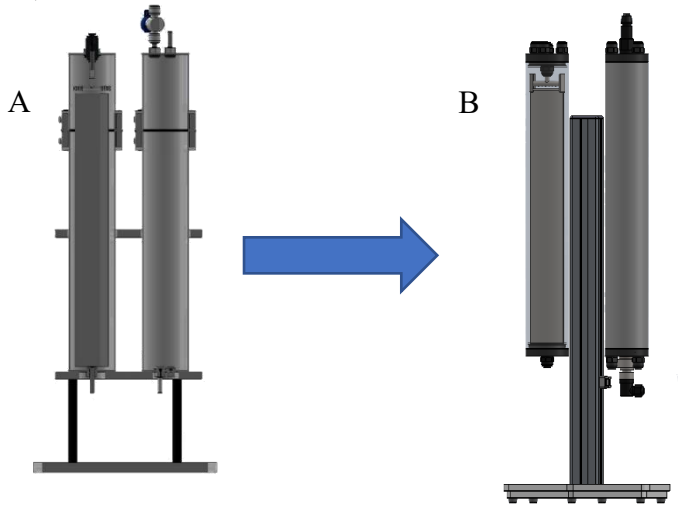

Figure 34 Schematic representation of the enhanced biofilm PSBR design, indicating the evolution from the initial configuration (A) to the optimized version (B)

Figure 34 shows the general schematic diagram of the improved biofilm PSBR. The setup is composed of two hollow vertically oriented transparent poly(methyl methacrylate) (PMMA) cylinders assembled on a PMMA stand. The cylinders both have the same height (40 cm) and diameter (inner diameter = 5.1 cm; outer diameter = 5.9 cm). Each end of the cylinders is designed with internal thread grooves for airtight screw caps. They can function either as a reservoir for culture medium or as the main culture chamber, depending on the kind of screw caps that were fitted.

Four black acetal screw caps were designed to seal the current biofilm PSBR: two caps for the reservoir, and two caps for the main culture chamber. The top and bottom caps for the reservoir are designed similarly. They have a central threaded hole for pH/temperature probe, and three supplementary holes with HPC fittings for pipe connections (Figure 35A).

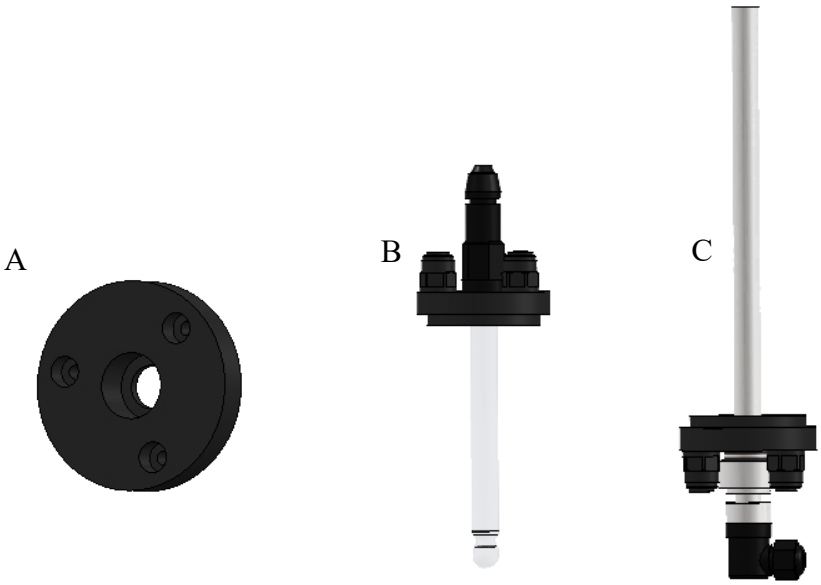

Figure 35 Reservoir cap fundamental design (A) with attached HPS fittings and pH meter on the top cap (B) and temperature sensor on the bottom cap (C)

The fundamental design of the top cap for the main culture cylinder is similar to that of the reservoir. However, the central hole is installed with male union fittings to suspend the removable T-shaped nutrient sparger (Figure 36A). The sparger itself is made of stainless steel consisting of eight equidistant ⌀1-mm diffuser holes (Figure 36B).

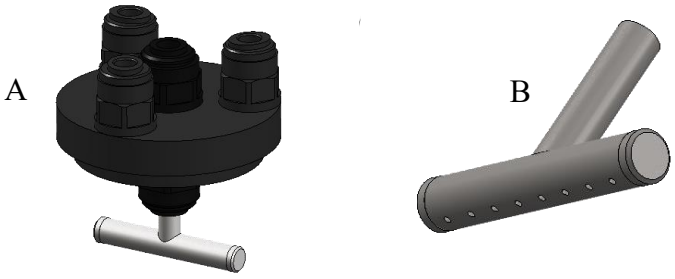

Figure 36 Complete top cap assembly (A) for culture cylinder, and sparger details (B)

The bottom cap is designed with an internal conical trough to facilitate the outflow of the culture media (Figure 37). Moreover, the bottom cap for the culture chamber is designed with narrow rectangular grooves that orient the support panel in a constant position.

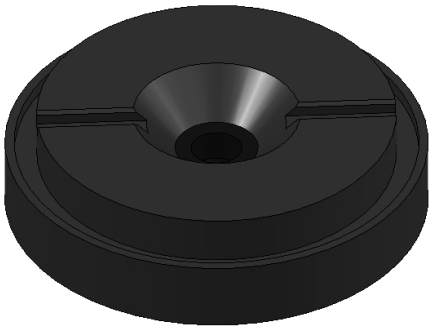

Figure 37 Bottom cap of main culture cylinder

A removable rectangular stainless-steel panel (L = 34.9 cm ; W = 4.6 cm ; thickness = 3 mm) is installed as the main physical support inside the culture chamber. Both sides of the panel can be used for biofilm culture. The lower end of the metal panel was tapered to a thickness of 1 mm to fit into the groove provided on the endcap of the cylinder (Figure 38A). The top part is similarly equipped with grooves to help keep the nutrient sparger in place (Figure 38B).

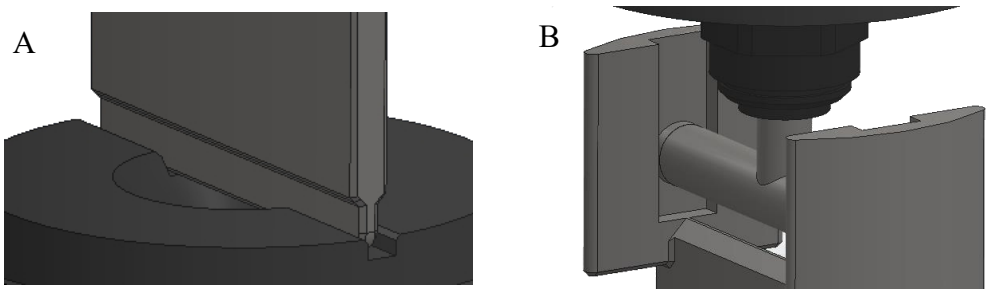

Figure 38 Support panel (A) and nutrient sparger (B) propped inside the grooves.

The culture medium is distributed on the tapered top edge of the metal panel and trickles further onto the lens paper. The liquid gets distributed to the glass fiber filter disk by absorption and gravity. The amount of culture medium flowing through and out of the biofilm photobioreactor is regulated by several peristaltic pumps in the control unit.

5. Conclusion and perspective

The construction and utilization of the PSBR represents an innovative step towards the valorization of benthic diatoms in biotechnology. The successful establishment of healthy and stable *Nitzschia laevis* biomass in the PSBR serves as a proof-of-concept, underpinning the machine's feasibility in fostering growth by leveraging the natural propensity of benthic diatoms to form biofilms. Furthermore, the increase in biomass and lipid production within a short period underscores PSBR's capacity to manipulate growth conditions favourably. The adaptations and modifications made to the PSBR highlight the system's potential for customization, potentially expanding the range of microalgae species that can be efficiently cultivated, as well as broadening the scope of possible applications.

Chapter III

Optimization of *Amphora* sp. NCC169 culturing using biofilm photobioreactor

Abstract

Chapter III directs attention towards the optimization of the PSBR and its pragmatic applications in benthic diatom culture. A rationale was presented for selecting *Amphora* sp. NCC169 as the model benthic diatom for the improved PSBR, and the experimental design was outlined to determine the most effective conditions for optimum biomass and lipid productivity. This chapter presents results from a series of optimization experiments that demonstrate the capacity of the PSBR to augment the production of biomass and lipids. The PSBR facilitated biomass productivity at 0.51 ± 0.05 $g \cdot m^{-2} \cdot day^{-1}$ and lipid productivity at 0.10 ± 0.03 $g \cdot m^{-2} \cdot day^{-1}$ at a shorter cultivation period, markedly outperforming the Fernbach flasks' production rates. These findings underscore the PSBR's efficiency in fostering conducive environments for benthic diatom growth, thus proposing a viable alternative to conventional methods with enhanced productivity and sustainability.

III.1 Comparison of different small-scale cultivation methods towards the valorization of a marine benthic diatom strain for lipid production

Mary Dianne Grace Arnaldo, Nadeeshani Dehel Gamage, Agathe Jaffrenou, Vony Rabesaotra, Aurélie Mossion, Gaëtane Wielgosz-Collin, Vona Méléder*

*Corresponding author: Vona Méléder, vona.meleder@univ-nantes.fr

Nantes Université, Institut des Substances et Organismes de la Mer, ISOMer, UR 2160, F-44000 Nantes, France

Highlights

- A commercial suspension PBR was adapted to build a vertical, tubular lab-scale porous substrate photobioreactor (PSBR) was adapted from a commercial suspension PBR for biofilm cultivation
- Marine benthic diatom *Amphora* sp. NCC169 was cultivated in Fernbach flasks and PSBR
- Diatom biomass and lipid yield in PSBR are higher than in Fernbach flasks

Abstract

Marine benthic diatoms have the capacity to produce quality biomass and bioactive compounds for various commercial applications. *Amphora* sp. NCC169 is one of such species that have high-value lipid production. However, mass-production of *Amphora* sp. NCC169 in traditional suspension photobioreactor is challenged by its sensitivity to stirring and turbulence. The aim of this study is to compare the biomass and lipid productivity of *Amphora* sp. NCC169 cultures between a Fernbach flask and a low-maintenance, laboratory-scale culture system adapted from previously described vertically oriented porous substrate bioreactor (PSBR) designs. Results revealed that cells in the PSBR could achieve significantly higher biomass productivity ($P_{biomass}$ = 0.51 ± 0.05 g·m^{-2}·day^{-1}) and lipid productivity (P_{lipid} = 0.10 ± 0.03 g·m^{-2}·day^{-1}) than those in Fernbach flasks after 20 days of cultivation ($P_{biomass}$ = 0.29 ± 0.01 g m^{-2} day^{-1} ; P_{lipid} = 0.07 ± 0.01 g·m^{-2}·day^{-1}). Cellular photosynthetic efficiency remained favorable in both culture conditions (F_v/F_m > 0.5) for the duration of the experiments.

Keywords: *Amphora* sp., immobilized photobioreactor, marine benthic diatoms, lipids

1. Introduction

Microalgae are promising candidates for biotechnological research, and they have become one of the major focus of development and innovation. Significant attention is gearing towards the study of diatoms, a major group of photosynthetic microalgae characterized by their silica cell walls. They dominate the primary production in coastal and estuarine environments, prevailing over 50% of some of the world's most productive marine food webs (Allen et al., 2011; Underwood and Kromkamp, 1999). Considerable scientific interest is given to their outstanding physical properties and their corresponding potential in biotechnology.

Diatoms are reported to have competitive advantage over other species of similarly-sized microalgae under suitable controlled conditions, given the fact that they multiply rapidly, they have more advanced carbon flux metabolism, and almost 100% of their biomass can be utilized (Furnas, 1990; Wang and Seibert, 2017). They are also highlighted for their ability to produce promising bioactive compounds with widespread industrial and pharmaceutical applications (Bozarth et al., 2009; Kroth, 2007; Lee et al., 2006; Prestegard et al., 2009). The importance of diatoms as primary producers is largely due to their high lipid content. Typical lipid fractions from diatoms were recorded to be at 15 to 25% of their dry weight, but some strains could reach lipid levels of up to 70 to 85% through regulation of the culture conditions (Cointet et al., 2019b; Kuczynska et al., 2015; Wang and Seibert, 2017). They produce copious amounts of lipids as metabolites, with the neutral fraction accounting for almost 70% of the total lipids. Diatoms have high diversity of lipid composition, such as membrane-bound polar lipids, triglycerides, and lipid-derived free fatty acids (Wang and Seibert, 2017). They were shown to possess lipids such as eicosapentaenoic acid (EPA) and phytosterols that are promising for their nutritional value and bioactivity.

Traditionally, diatoms are produced using either of the two most common methods of microalgae cultivation: (a) open system such as carboys, tanks, and ponds, or (b) closed cultivation systems using photobioreactors (PBRs). The main difference between the two systems is linked to the cost, mode of operation, and vulnerability to external factors (Pulz, 2001; Xu et al., 2009).

Classical open cultivation systems account to approximately 95% of the total global microalgae production (Cruz et al., 2018). Open culture systems have relatively inexpensive construction and

operation costs because they are almost always located outdoors and rely on natural light for illumination. They can also utilize runoffs and effluents to supply nutrients to microalgae (Carlsson et al., 2007). On the other hand, they are susceptible to prevailing external conditions such as rainfall, temperature, and light intensity for the same reasons. Contaminants and predators like ciliates and rotifers can outcompete the cultured species and wreck the entire batch of operation.

Photobioreactors are increasingly being used for microalgae research and development because of their numerous advantages over open culture systems. Among the benefits include easier control of the culture parameters (e.g., temperature, pH), reduced contamination, higher productivity, and lower harvesting cost (Zhou et al., 2020). They are mainly used to grow axenic, monospecific cultures for the production of high-value compounds (Johnson et al., 2018; Rezvani et al., 2022). Several diatom species such as *Chaetoceros calcitrans, Skeletonema costatum,* and *Phaeodactylum tricornutum* have already been cultivated successfully in PBRs (Fernández et al., 2000; Granum and Myklestad, 2002; Krichnavaruk et al., 2007).

Cultivation of planktonic microalgal species predominate both open and closed cultivation systems. Hence, high resource/energy consumption and dewatering problems arise during harvesting, which is a major bottleneck for the biomass industry. Over the past two decades, biofilm cultivation systems present a novel strategy to circumvent these issues. In this system, microalgal cells that naturally have the capacity to bind to surfaces in their own exopolysaccharides (EPS) are provided with substrates to attach and proliferate. Majority of biofilm systems use solid non-porous substrates which uniquely serve as physical support for microalgal adhesion. This facilitates the application and diffusion of all relevant growth parameters (i.e., light, nutrients, gas exchange) on the same side of the substrate. These solid substrates can either be partially or completely submerged in the culture medium. A porous substrate photobioreactor (PSBR), on contrary, is installed with a hydrophilic, microporous substrate which receives the culture media nutrients on one side while providing attachment and direct light and gas exchange to the biofilm on the opposite side. This results to minimization of light limitation and enhancement of CO_2 mass transfer between the cells and the ambient gas phase in PSBR systems. In both porous and non-porous biofilm configurations, the bulk of the culture media is separated from the biomass. Thus, biomass can be easily scraped off from the substrate and can achieve final biomass

values comparable to post-centrifuged harvest from suspension cultures (Gross et al., 2013; Johnson and Wen, 2010).

Biofilm cultivation is an attractive strategy for marine benthic diatom cultivation. Benthic diatoms are biofilm formers in nature, developing large-scale cohesive assemblages with other microorganisms. This is demonstrated by their preference for minimally disturbed conditions. Although some marine diatom species thrive in an airlift PBR, other benthic species produced higher biomass productivity and lipid rate when they were grown undisturbed in Erlenmeyer flasks (Cointet et al., 2021).

Benthic diatoms colonies greatly benefit from higher surface areas with marginal perturbation. The failure of certain species to grow in suspension leads to a potential re-evaluation of their eco-physiology and lipid production capacity under more favorable culture conditions using a biofilm photobioreactor. Research studies have shown great potential in cultivating microalgae using biofilm-based PBRs. However, since the conception of PSBR in 2003 and its successful lab-scale use on six benthic diatoms in 2005 (Nowack et al., 2005; Shi et al., 2007), the application of PSBRs for benthic diatoms studies remains scarce up to this day (Benstein et al., 2014; Berner et al., 2015; Gao et al., 2015; Naumann et al., 2013). The development and utilization of a highly controlled biofilm system could potentially enhance the growth of benthic diatoms, improve their lipid production, and valorize their bioactivities for biopharmaceuticals.

In this study, a comparative analysis for the benthic marine diatoms strain *Amphora* sp. NCC169 cultivation was conducted between (a) Fernbach flask corresponding to batch culture and (b) a vertical, tubular lab-scale biofilm PSBR corresponding to continuous culture, both allowing the natural development of biofilm. The objective of this study is to estimate if under more highly controlled conditions in the biofilm PSBR, *Amphora* sp. NCC169 biomass and lipid yield is higher than those obtained from Fernbach flasks. To reach this goal, biomass, total lipid, and nutrient assimilation were investigated between culture conditions to determine optimum conditions towards high-value lipid production.

2. Materials and methods

2.1. Strain and stock cultivation

Amphora sp. NCC169 is a strain of marine benthic diatom isolated from sediment samples collected from the French Atlantic coast, near to Piriac-sur-Mer (47°22'06"N/02°32'52"W) in 2005. It was hosted by the Nantes Culture Collection (NCC) in Nantes University, France. It is currently contained within the Roscoff Culture Collection (RCC) under an updated species code RCC5813.

Stock cultures are grown under controlled conditions in 250-mL Erlenmeyer flasks containing 150 mL of natural seawater enriched with Guillard's F/2 culture medium (Guillard, 1975). Natural seawater was strained through a 0.2 µm membrane filter to remove particulates and most of the biological contaminants. Salinity was adjusted to 28 by dilution with demineralized or distilled water, while pH was set to 7.8 using hydrochloric acid or sodium hydroxide. The solution was sterilized by autoclaving at 121 °C (14.5 psi) for 20 minutes. After cooling down, the solution was infused with heat-labile nutrients and inoculated with *Amphora* sp. NCC169 cells under axenic conditions.

After inoculation, *Amphora* sp. NCC169 is grown in culture chamber under continuous lighting (24-hour photoperiod) at 150 µmoles $m^{-2}s^{-1}$ and at 16.8 ± 0.3 °C. Stock cultures are sub-cultured every month to ensure continuous supply of healthy cells.

2.2. Fernbach experiment

Amphora sp. NCC169 was cultured in Fernbach flasks with higher surface area/volume ratio (S/V) (28.4 m^2 m^{-3}) than conventional 250-mL Erlenmeyer flasks (17.7–20.1 m^2 m^{-3}) used in laboratory stock cultures. The Fernbach flasks were filled with 800 mL of natural seawater added with Guillard's F/2 medium, submerging the resulting biofilm under 5 cm of enriched seawater. Enrichment and sterilization of culture media in Fernbach flasks follow the same protocol as those in stock Erlenmeyer flasks. Cells were sub-cultured from the stock at a starting density of 30,000 cells·mL^{-1}. Cultures were kept at constant temperature (16.8 ± 0.3 °C), light intensity (150 µmoles $m^{-2}s^{-1}$), under continuous light.

Harvesting of biomass, estimating growth parameters, and analyzing of nutrients, total lipid content, fatty acids profile and pigments composition were performed every sampling period (day 2, 4, 6, 8, 10, 12, 14, 17, 20). In order to maintain the integrity of the biofilm throughout the culture period, one unit

of Fernbach flask is allocated for every sampling day. The experiment was carried out in three trials for day 0 to day 8, and six trials for day 10 to 20.

2.2.1 Cell health and density

To initiate sampling, biofilms formed on the bottom surface of the Fernbach flask were carefully dislodged using a magnetic stirrer for two minutes until cell aggregates are disrupted, and the solution is homogenized.

A 1-mL aliquot from the homogenized culture solution was used to measure the health of the cells using Pulse Amplitude Modulated (PAM) fluorometry (Walz GmbH, Effeltrich, Germany) in the cuvette version. The aliquot was initially dark-adapted at room temperature for 15 minutes, then pipetted into a 15-mm diameter quartz glass cuvette. The minimum fluorescence (F_0) was measured with a pulse of low level non-actinic measuring light, followed by a saturating light pulse (2500 µmol photons $m^{-2} \cdot s^{-1}$ for 0.8 s) to obtain the maximum fluorescence (F_m) value. The variable fluorescence yield (F_m - F_0) was then used to calculate the maximum photosystem II (PSII) quantum yield (F_v/F_m) of the dark-adapted sample (Eq. 3).

$$\frac{F_v}{F_m} = \frac{(F_m - F_0)}{F_m} \qquad \text{Eq. 3}$$

The health of the photosynthetic cells is proportional to the F_v/F_m, with the optimum value set between 0.5–0.7 for diatoms(Büchel and Wilhelm, 1993; Rijstenbil, 2003).

The same aliquot was used to measure the culture cell density (cells mL^{-1}) using a Neubauer hemocytometer and a light optical microscope (OLYMPUS CH40, Japan, objective Olympus ×20). The relative growth rate μ was calculated according to the following equation,

$$\mu = \frac{ln\,(N_t/N_0)}{\Delta t} \qquad \text{Eq. 4}$$

where N_0 is the population size at the beginning of the time interval (*i.e.* at t_0), N_t is the density at the end of the time interval (*i.e.* at t_t), and Δt is the difference between the time intervals ($t_t - t_0$) (Michelle Wood et al., 2005).

2.2.2 Biomass

The culture solution was harvested by filtering the cells through pre-combusted and pre-weighed glass microfiber filters (Whatman™ GF/F, ⌀ 47 mm, 0.7 µm pore size). Filtered diatom biomass was washed with ammonium formate (68 $g \cdot L^{-1}$) to remove residual salt. Wet filters were frozen (-80 °C) and freeze-dried prior to dry weight estimation. Culture media samples were collected prior to the inoculation and before pre-treatment of ammonium formate for further nutrient analysis.

Total dry biomass was transformed to areal productivity corresponding to the bottom surface area of the Fernbach flask over time. Thus, biomass productivity ($P_{biomass}$) was calculated by Eq. 3,

$$P_{biomass} = m_{biomass} \,/\, \mathrm{A} \,/\, \mathrm{t} \qquad \text{Eq. 5}$$

where $m_{biomass}$ is the final dry weight (g) of *Amphora* sp. NCC169 during one sampling point, A is the area of the bottom of the Fernbach flask (0.03 m^2), and t is the culture duration (day).

2.2.3. Total lipid and nutrient analysis

Total lipid (TL) were extracted following the modified Bligh and Dyer method (Bligh and Dyer, 1959). The disks were pooled in solvent extraction composed by dichloromethane and methanol (1:1 ratio) into a flask, and mechanically agitated for 1 h. The solvent extract was filtered through a Whatman phase separating filter paper (⌀15.0 cm) to remove silica and other solid particulates resulting from the initial extraction, and subsequently added with water. The organic phase was purified using sodium sulfate and filtered for rotary evaporation. Total lipid was re-suspended on a small volume of dichloromethane and transferred into a pre-weighed vial. The residual dichloromethane was evaporated to obtain the total lipid extract by gravimetry. Final yield was expressed in percentage of the total dry weight. Total lipid productivity ($P_{total\ lipid}$) was expressed as $g \cdot m^{-2} \cdot day^{-1}$ using the formula:

$$P_{total\ lipid} = m_{total\ lipid} \text{ / A / t} \qquad \text{Eq. 6}$$

where $m_{total\ lipid}$ is the total lipid weight (g) of *Amphora* sp. NCC169 during one sampling point, A is the area of the bottom of the Fernbach flask (0.03 m^2), and t is the culture duration (day).

Water samples were taken for each sampling period to determine the nutrients present in the culture media. Continuous flow injection colorimetry was performed using SEAL Analytics AA3 HR2 Autoanalyzer to measure nitrate + nitrite ($NO_3^- + NO_2^-$), phosphate (PO_4^{3-}), and silicate (SiO_4^{4-}) (SEAL Analytical GmbH, Nordestedt, Germany) (Aminot and Kérouel, 2007). Nitrates are initially reduced to nitrites by passing the sample through a copper-treated cadmium column. The transformed nitrites, along with the pre-existing nitrites in the medium, react with sulphanilamide and *N*-naphthylethylenediamine to give a pink coloration measured at 540 nm. Phosphate and silicate ions react with molybdate to form a phosphomolybdic and β-silicomolybdic complex, respectively. These complexes are reduced by ascorbic acid to a blue compound measured at 820 nm. Ammonium (NH_4^+) levels were tested using Jasco® FP-2020 fluorometer with ADA (Seal Analytical) interface and analyzed using AACE® operating software. The method is based on the reaction of ammonium with orthophthaldialdehyde in the presence of a reducing agent in a slightly basic medium (Aminot and Kérouel, 2007). The fluorimetric analysis is performed at an excitation wavelength of 365 nm and an emission wavelength of 425 nm. The limits of quantification for these compounds are 0.2 µM ($NO_3^- + NO_2^-$), 0.06 µM (PO_4^{3-}), 0.04 µM (SiO_4^{4-}), and 0.05 µM (NH_4^+).

2.3. Porous substrate photobioreactor (PSBR) experiment

2.3.1 PSBR configuration

The PSBR used in this study is an adapted configuration for biofilm cultivation from previous designs. An existing commercial suspension PBR developed by Synoxis Algae® (Le Cellier, France) called 'Nano' was adapted to build a PSBR system (Figure 39). The adapted PSBR is composed of two cylindrical culture and reservoir chambers, and a fiberglass compartment internally embedded with two LED technology panels with three different combination of wavelengths, λ (λ_{blue} = 469 nm + 449 nm, $\lambda_{green/orange}$ = 515 nm + 598 nm, λ_{red} = 633 nm + 654 nm). This setup is completed by a central control system that programs and automatically regulates pH, light, temperature, gas, and nutrient flow using an interactive touch screen. PSBR features and accessories illustrations are available as supplemental data (S1).

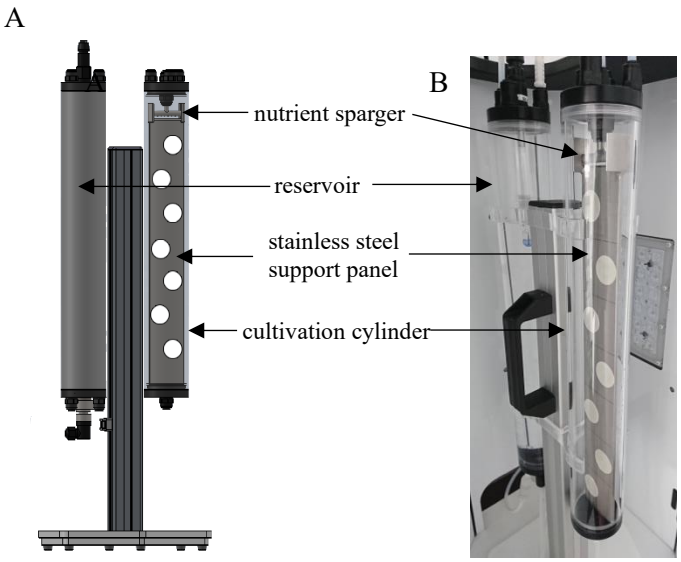

Figure 39 PSBR setup, adapted from an existing PBR for suspension cultivation, and currently composed of the cultivation (left) with steel panel covered by a lens tissue and supporting filters inoculated by diatoms; and the reservoir (right) cylinders (A)

The setup is composed of two hollow vertically oriented transparent poly(methyl methacrylate) (PMMA) cylinders assembled on a PMMA stand. The cylinders both have the same height (40 cm) and diameter (inner diameter = 5.1 cm; outer diameter = 5.9 cm).

The top cap for the main culture cylinder is installed with male union fittings to suspend the removable T-shaped stainless-steel sparger consisting of eight equidistant ⌀1-mm diffuser holes. During

culture, a sheet of lens cleaning tissue (Whatman, Catalog Number: 2105-918) is placed over the steel panel and serves as a source layer to establish the flow of the culture media. The culture medium is distributed on the tapered top edge of the metal panel and trickles further onto the lens paper. The liquid gets distributed to the glass fiber filter disk by absorption and gravity. The amount of culture medium flowing through and out of the biofilm photobioreactor is regulated by several peristaltic pumps in the control unit.

Circular glass fiber filters (Whatman™ GF/C ⌀25 mm, 0.7 µm pore size) were placed onto the source layer to act as self-adhesive substrate layer for the immobilized benthic diatoms. The substrate layer allows the passage of culture medium from the source layer into the biomass while preventing the reverse migration of the cells to the source layer and the culture medium.

2.3.2 Inoculation

Pre-combusted (400 °C, 4 h) GF/C filter disks (⌀25 mm, 0.7 µm pore size) were used as substrate for the diatom biofilm. Individual filter disks were placed inside a 6-well cell culture plate and inoculated with a total of 1 million cells of *Amphora* sp. NCC169. The cells were carefully inoculated on the surface of the filter disks to prevent growth initiating on the underside of the disks. An additional volume of natural seawater enriched with Guillard's F/2 medium was added into each cell well to reach a final volume of 2 mL. Inundation of F/2 medium was done slowly and carefully so as not to displace the diatom cells on the surface of the disks. The disks were left to incubate in the culture room (temperature = 17.6 ± 2.1 °C, light regime/intensity = continuous; 150 µmoles m^{-2} s^{-1}) until a stable biofilm is formed after three days. Five culture plates were prepared to ensure biofilm colonization on at least 14 GF/C filter disks.

2.3.3 PSBR launch

During culture, the panel was outlined with a grid to set seven disks approximately 5 mm horizontally away from each other. The same number of disks are similarly positioned on the other side of the panel for a total of 14 disks. Continuous light was provided by two panels of RGB LED channels

set at a global intensity of 150 µmoles m^{-2} s^{-1}, while external temperature was maintained at 17.6 ± 2.1 °C.

2.3.4 Sampling measurements

Growth estimation of immobilized cells in the PSBR was not possible using conventional cell counting techniques for several reasons. The developed design for the PSBR doesn't allow for sampling without opening the chambers and potentially introducing contaminants into the system. A single lab-scale photobioreactor doesn't have enough facility for multiple samplings. In the end, we have decided to sample twice—on day 0 and day 7, coinciding with the general late exponential phase of *Amphora* sp. NCC169 in the previous Fernbach experiments.

The biomass of the biofilm formed on the filter disks was measured non-destructively using normalized difference vegetation index (NDVI) (Cointet et al., 2019b). NDVI is frequently used to evaluate the biomass of terrestrial vegetation, as well as to measure biofilm and microphytobenthos growth using satellite data (Barillé et al., 2011; Cointet, 2019; Méléder et al., 2007, 2003). The reflectance (ρ) of the cells at certain wavelengths are known to be proportional to their chlorophyll *a* content and is used as reliable proxy for biomass. For each disk, 10 global reflectance values were taken at different representative points using Ocean Optics Flame-UV-S-VIS-NIR-ES miniature spectroradiometer. The reflectance values at the maximal reflectance wavelength (λ750) and the chlorophyll *a* absorption wavelength (λ675) were used to calculate the NDVI (Eq. 2). An average of 10 NDVI values were obtained for each disk every sampling period to account for potential heterogeneity.

The physiological stress and photosynthetic activity of the biofilms were measured through pulse-amplitude modulated (PAM) fluorometry (Walz GmbH, Effeltrich, Germany), but using the optical fiber version (Consalvey et al., 2005; Sma-Air and Ritchie, 2021). Similar to the Fernbach experiment, low level non-actinic measuring light was initially applied to dark-adapted (15 minutes) samples to get the minimum fluorescence yield (F_0), followed by a strong saturating pulse to reach the maximum fluorescence level (F_m) to calculate the maximum quantum efficiency (F_v/F_m) parameters (Eq. 3). Three F_v/F_m values were sampled at different points to estimate the diatoms' physiological stress and photosynthetic efficiency.

Three seven-day trials were conducted using the PSBR. At the end of the culture cycle, all the algal disks were harvested from the biofilm photobioreactor. The biomass and photosynthetic activity of the films were measured similar to the protocol in the beginning of the experiment. The disks were individually washed with ammonium formate (68 $g \cdot L^{-1}$), frozen at -80 °C, and lyophilized to a constant weight. Dry biomass estimation, lipid extraction, and nutrient analyses were done as in the Fernbach experiment.

2.4. Statistical analysis

Data obtained from the experiments both using Fernbach flasks and PSBR were expressed as mean ± standard deviation. Test for statistical significance was performed through the PAleontological STatistics (PAST) software (version 4.08). The values were evaluated for normality using the Shapiro–Wilk *W* test. Student's independent *t*-test was used to compare the means between two groups. For groups of three or more, analysis of variance (ANOVA) was used if the data was normally distributed. Percentage data of total lipid was transformed when necessary(Gomez and Gomez, 1984). However, Kruskal-Wallis was used if the assumptions of the normal distribution were violated. *Post hoc* Tukey HSD tests were used to verify the individual differences of normally distributed datasets, while Mann-Whitney U test was used otherwise.

3. Results and discussion

3.1. Fernbach flasks

In Fernbach flasks, the initial biomass density was 3.6 x 10^4 cells·mL^{-1} and gradually increased to 1.43 x 10^4 cells·mL^{-1} after 20 days of culture (Figure 40). The sigmoid growth curve does not have a prominent lag phase. There was a plateau in cell density from day 8 to day 14, following by an increase in days 18 and 20, but without any significantly difference (Tukey HSD test, $p > 0.05$). The highest growth rate was achieved between day 2 and day 4 at 0.8 ± 0.4 day^{-1}. But, average growth rate of *Amphora* sp. NCC 169 between sampling periods was 0.2 ± 0.1 day^{-1} which is comparable with the studies conducted by de la Peña (2007) on culturing *Amphora* sp. in the laboratory, reaching 0.2 ± 0.1

day^{-1}, and Indrayani *et al.* (2019) on *Amphora* sp. MUR258 in outdoor raceway ponds reaching 0.29 day^{-1}.

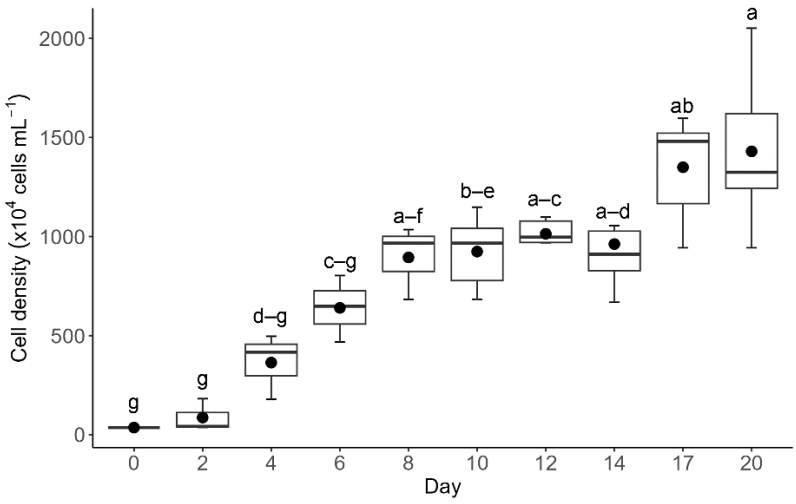

Figure 40 Box plot distribution of the average cell density across different cultivation periods using Fernbach (Day 0-8 n=3; Day 10-20 n=6). Error bars represent minimum and maximum values, whereas rectangle boundaries represent the 1st and 3rd quartile values separated by the median. Mean values were plotted as black-filled circles (●). Letters on top of error bars indicate significance of means at the 0.05 level according to an HSD test. Mean cell densities denoted by a different letter or range of letters indicate significant differences between treatments (Tukey HSD, $p < 0.05$).

The photosynthetic efficiency (F_v/F_m) of the cells remained high from day 0 to day 17 with an average value of 0.5 ± 0.1 (Tukey HSD test, p > 0.5) , and then gradually decreased to 0.3 ± 0.1 (Tukey HSD test, Q = 5.60, $p = 0.02$) (Figure 41).

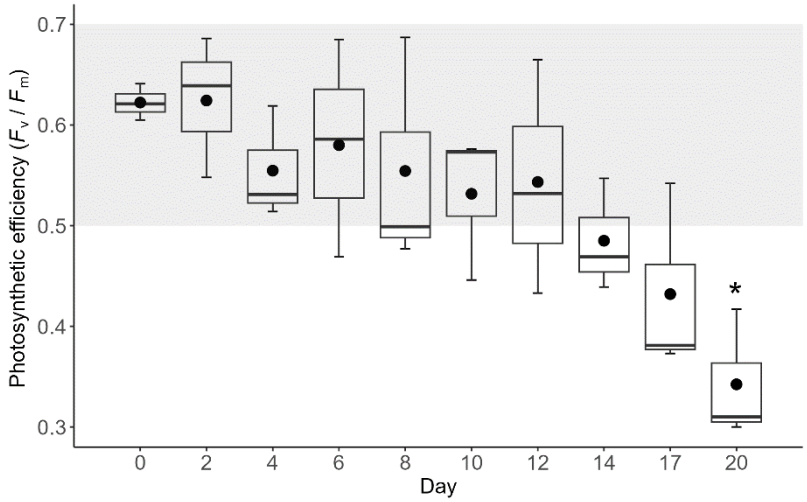

Figure 41 Variation of the average photosynthetic efficiency (F_v/F_m) of *Amphora* sp. NCC169 in Fernbach flasks over time (n=3). Error bars represent minimum and maximum values, whereas rectangle boundaries represent the 1st and 3rd quartile values separated by the median. Black-filled circles (●) represent the mean F_v/F_m of each sampling period. The optimum range of photosynthetic efficiency for diatoms (0.5–0.7) is highlighted in gray. Error bars with asterisk (*) indicate significance (Tukey HSD, $p < 0.05$).

Total dry biomass (g m^{-2}) and the total lipid (% dry weight) of *Amphora* sp. NCC 169 were directly proportional with time (Figure 42). Highest recorded value for total dry biomass was obtained on the last days of culture reached up to 158 mg (Day 17 and 20: Tukey HSD test, Q = 2.53, $p = 0.69$). Even if the total lipid reached 24.4 ± 5.6% on day 20, it remained stable from day 8 to day 20 with an average value of 20.4 ± 4.9% (Tukey HSD test, $p > 0.05$). When compared to previous study in Erlenmeyer flasks (Cointet et al., 2019b), the total lipid ratio of *Amphora* sp. NCC169 cells obtained after 13 ± 3 days (16.0 ± 2.6%) in Erlenmeyer flasks Fernbach flasks was reached after only eight days (16.2 ± 5.3%) in Fernbach flasks. By day 14, Fernbach cultures had 56% more total lipid than those in the Erlenmeyer flasks.

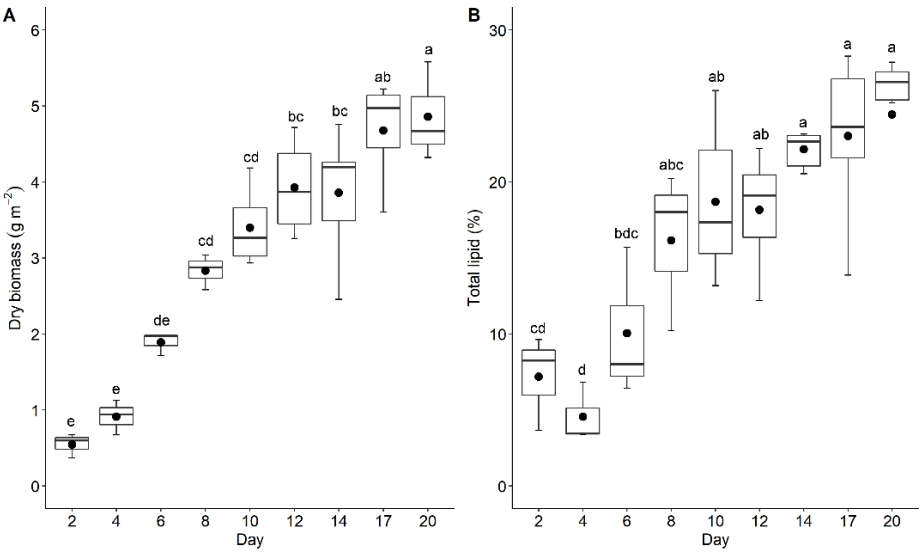

Figure 42 Box plot distribution of the average dry biomass density and total lipid rate of *Amphora* sp. NCC169 in Fernbach flasks across different cultivation periods (Day 0-8 n=3; Day 10-20 n=6). Error

bars represent minimum and maximum values, whereas rectangle boundaries represent the 1st and 3rd quartile values separated by the median. Mean values were plotted as black-filled circles (●). Letters on top of error bars indicate significance of means according to an HSD test. Mean cell densities denoted by a different letter or range of letters indicate significant differences between treatments (Tukey HSD, $p < 0.05$).

The biomass and lipid productivities of *Amphora* sp. NCC169 in Fernbach flasks were expressed as a function of area over time ($g \cdot m^{-2} \cdot day^{-1}$) to make quantitative comparisons with the PSBR, as well as to follow the common productivity growth metrics in literature (

Figure **43**). During 20 days of culture, the biomass productivity remained stable with an average of 0.30 ± 0.04 $g \cdot m^{-2} \cdot day^{-1}$ (Tukey HSD, $p > 0.05$). This value is comparatively lower than what was previously achieved in 250-mL Erlenmeyer flasks after 13 ± 3 days (75 ± 3.9 $mg \cdot L^{-1} \cdot day^{-1}$) (Cointet et al., 2019b). In this cited study, the best diatom growth rates were given by *Entomoneis paludosa* (14.4–329.6 $mg \cdot L^{-1} \cdot day^{-1}$), *Craspedostauros* spp. (120.6–265.5 $mg \cdot L^{-1} \cdot day^{-1}$), *Staurosira* sp. (244.3 $mg \cdot L^{-1} \cdot day^{-1}$), *Fallacia* spp. (174.6–238.0 $mg \cdot L^{-1} \cdot day^{-1}$), *Surirella* sp. (193.2 $mg \cdot L^{-1} \cdot day^{-1}$), (*Amphora* sp. 137 $mg \cdot L^{-1} \cdot day^{-1}$), *Brockmaniella* sp. (133.6 $mg \cdot L^{-1} \cdot day^{-1}$), *Extubocellulus* sp. (127.4 $mg \cdot L^{-1} \cdot day^{-1}$), and *Contricriba weissflogii* (126.1 $mg \cdot L^{-1} \cdot day^{-1}$). Lipid productivities were significantly higher on days 8–20 (Tukey HSD, $p \leq 0.05$), peaking at 0.1 ± 0.0 $g \cdot m^{-2} \cdot day^{-1}$ after 20 days.

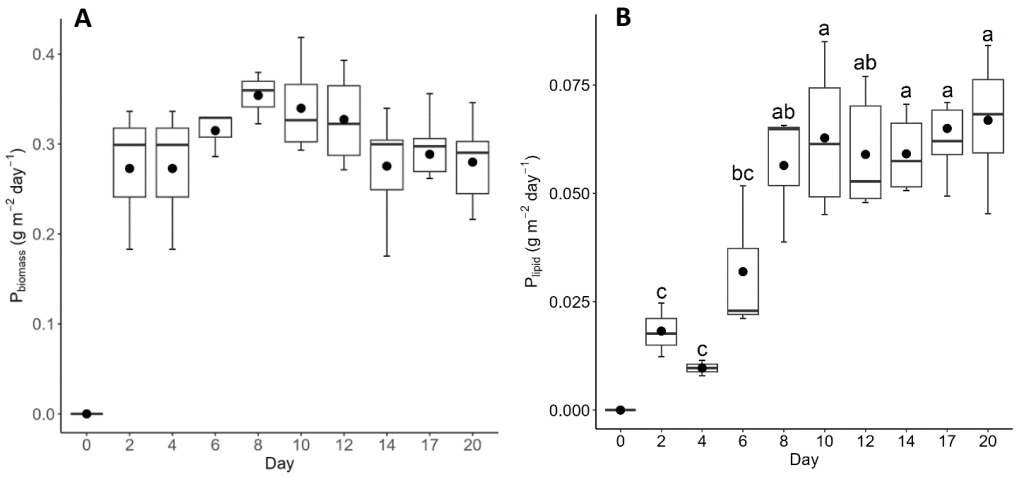

Figure 43 Average biomass (A) and lipid (B) productivities (in g m^{-2} day^{-1}) of *Amphora* sp. NCC169 over 10 different culture periods. Error bars represent minimum and maximum values, whereas

rectangle boundaries represent the 1st and 3rd quartile values separated by the median. Black-filled circles (●) represent the mean productivity of the respective sampling periods. Letters on top of error bars indicate significance of means according to an HSD test. Mean cell densities denoted by a different letter or range of letters indicate significant differences between treatments (Tukey HSD, $p < 0.05$).

The evolution of main macronutrients (nitrate + nitrite, silicate, and phosphate) as well as ammonium levels were investigated (Figure 44). All of the nutrients experienced a visible downward trend, as expected of batch cultivation systems. Nitrate and nitrite values significantly decreased by 63.8 ± 1.4% from its original concentration on the fourth day of culture (Tukey HSD test, Q = 6.26, $p = 0.07$). Silicate levels were significantly 83.6 ± 11.7% lower than their original concentration by day 6 (Tukey HSD test, Q = 5.47, $p = 0.02$), and was further reduced 0.9 ± 0.8% of their original concentrations by the end of the culture period (Tukey HSD test, Q = 5.99, $p = 0.01$). On the other hand, average phosphate concentrations remained stable during the culture (ANOVA, F = 1.32, $p = 0.29$). Ammonium levels fluctuated between 0.6 ± 0.6 µM to 5.0 ± 2.8 µM, but observed changes were not statistically significant (Tukey HSD test $p > 0.05$).

The higher surface area/volume (S/V) ratio in Fernbach flasks did not translate to better biomass growth and productivity for *Amphora* sp. NCC169. The decrease in growth rate and biomass productivity is a likely implication of photoinhibition, as more cells are spread out over a higher surface and thus exposed to high irradiances (Richmond, 1986). Cellular activities that depend on the input of light energy (e.g., nutrient consumption, CO_2 absorption) take place at a higher rate, which could have long-term detrimental effects to the growth and productivity of the cells. For example, higher photosynthetic activity without CO_2 supplementation increases the pH value, which may inhibit metabolism (Masojídek et al., 2022; Posadas et al., 2014). This is supported by the deterioration of the photosynthetic efficiency of *Amphora* sp. NCC169 in Fernbach flasks from day 14 onwards, which coincides with the decline of F_v/F_m values below the optimum threshold of 0.5 – 0.7. Furthermore, progressive pigment analysis suggests direct correlation between chlorophyll a levels and F_v/F_m values (Méléder et al., 2003).

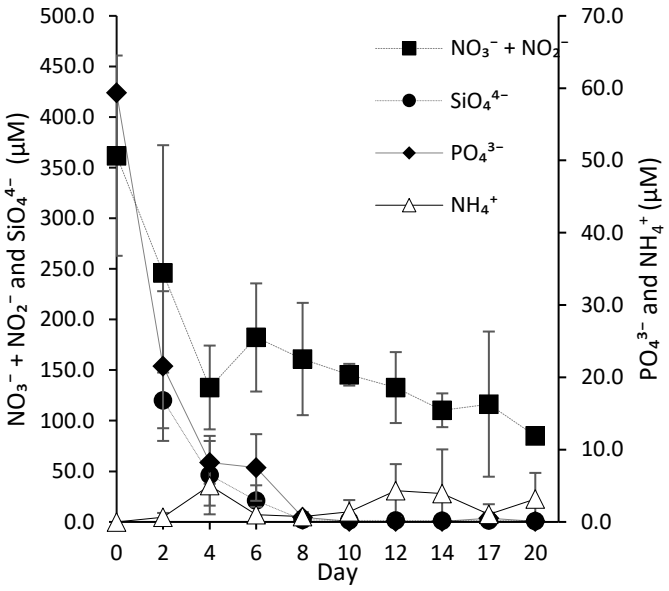

Figure 44 Average nutrient availability ($NO_3^- + NO_2^-$, PO_4^{3-}, SiO_4^{4-}, and NH_4^+) in Fernbach flasks culture media at every sampling interval (except for SiO_4^{4-} without day 0). Error bars represent standard deviation (n = 3).

3.2 PSBR

Amphora sp. NCC169 formed dense, unialgal biofilms that cover the inoculated area after seven days (Figure 45).

Figure 45 Photographic comparison of biofilm disks inoculated on the left side and right side of the PSBR support panel on the day of launch (Day 0) and after harvest (Day 7).

The culture panel supports healthy cells, as reflected by the F_v/F_m values never fall within the optimum threshold (Figure 46A) whatever the side used (Tukey HSD test, Q = 1.18, p = 0.41), and despite a small decrease on the final day (Tukey HSD test, Q = 4.12, p < 0.01). Additional pigment content investigation could elucidate the optimum S/V ratio for *Amphora* sp. NCC169 as a function of light availability at a given algal physiological state. This will enable simulations and modelling of biomass and lipid productivity, as well as optimization for subsequent scale-up technologies.

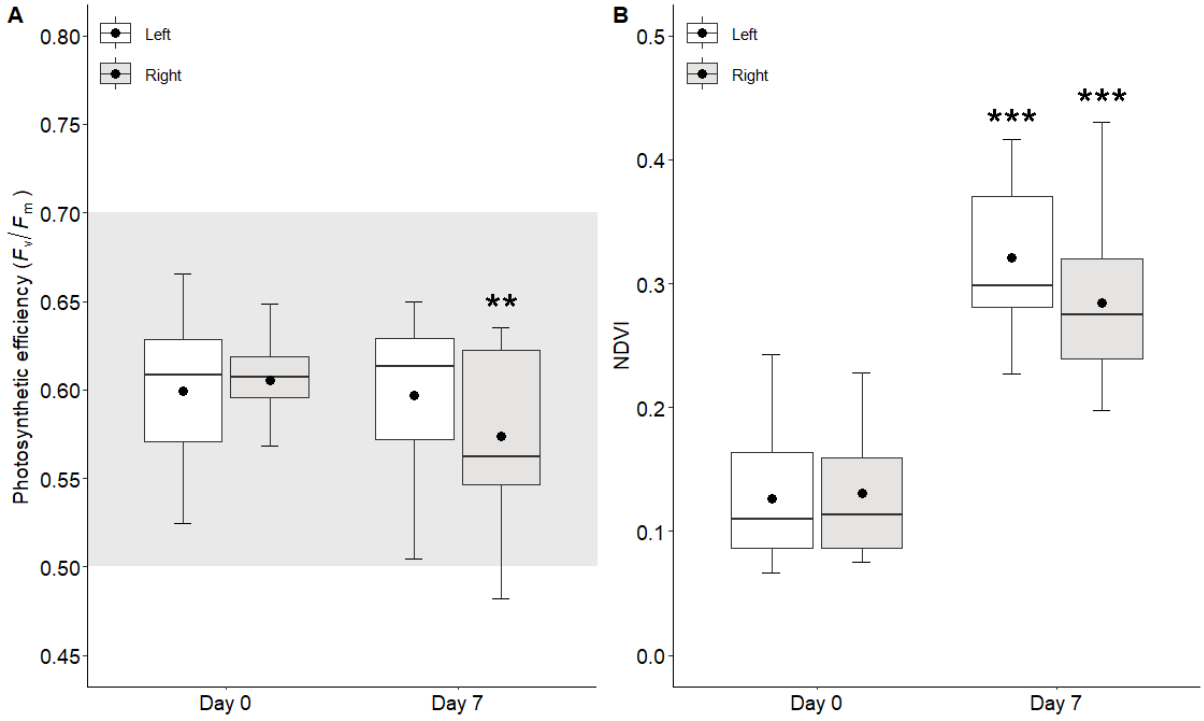

Figure 46 Average photosynthetic efficiency (F_v/F_m) (A) and NDVI (B) of *Amphora* sp. NCC169 biofilm disks in the PSBR (n = 21). Data is categorized between the location of the disks on the support panel (left and right), and sampling period (day 0 and day 7). The median line separates the 1st and 3rd quartile rectangle boundaries, while error bars represent minimum and maximum values. Black-filled circles (●) represent the population mean. The optimum range of photosynthetic efficiency for diatoms (0.5–0.7) is highlighted in gray. Asterisks show significant difference at *p < 0.05, **p < 0.01, or ***p < 0.001 (Tukey HSD).

NDVI values significantly increased from day 0 (left = 0.13 ± 0.06; right = 0.13 ± 0.06) to day 7 (left = 0.35 ± 0.07; right = 0.33 ± 0.06) without any effect due to the used side (Tukey HSD test, Q = 15.75, $p < 0.001$) (Figure 46B). This growth is further illustrated by the increase in biofilm color intensity on the day of harvest (Figure 45). NDVI values have high standard deviations that reflect the patchy biofilm development. However, data analysis shows that this heterogeneity is not significant (Tukey HSD test, Q = 0.60, $p = 0.67$).

After seven days of culture, both sides of the support panel have shown similar average pooled dry biomass reaching 11.5 ± 1.7 mg on the left side and 11.0 ± 3.0 mg on the right (Figure 47, $t = 0.07$, $p = 0.95$). Mean total lipid rate was also similar for both sides, reaching 22.0 ± 5.2% and 18.2 ± 4.5% for the left and right side, respectively ($t(4) = 0.96$, $p = 0.39$).

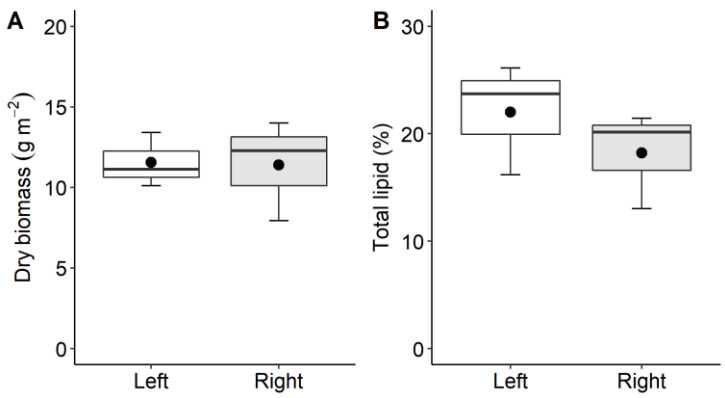

Figure 47 Box plot distribution of the average dry biomass density and total lipid content in percent dry biomass of *Amphora* sp. NCC169 on disks located on the left and right side of the PSBR upon harvest (Day 7, n=6). Error bars represent minimum and maximum values, whereas rectangle boundaries represent the 1st and 3rd quartile values separated by the median. Mean values were plotted as black-filled circles (●).

Silicate and nitrate/nitrite decreased by 21% (day 0 = 68.39 µM; day 7 = 53.79) and 25% (day 0 = 643.73 µM; day 7 = 483.60 µM) after seven days, respectively (Figure 48). On the other hand, phosphate decreased to 24% of the original concentration (day 0 = 59.35 µM; day 7 = 14.01 µM), and

ammonium to 10% (day 0 = 168.98 µM; day 7 = 16.87 µM), showing the highest consumption rate among the main macronutrients, even if the change in nutrient concentration in the culture medium is not statistically significant (Mann–Whitney, U = 3, p > 0.05).

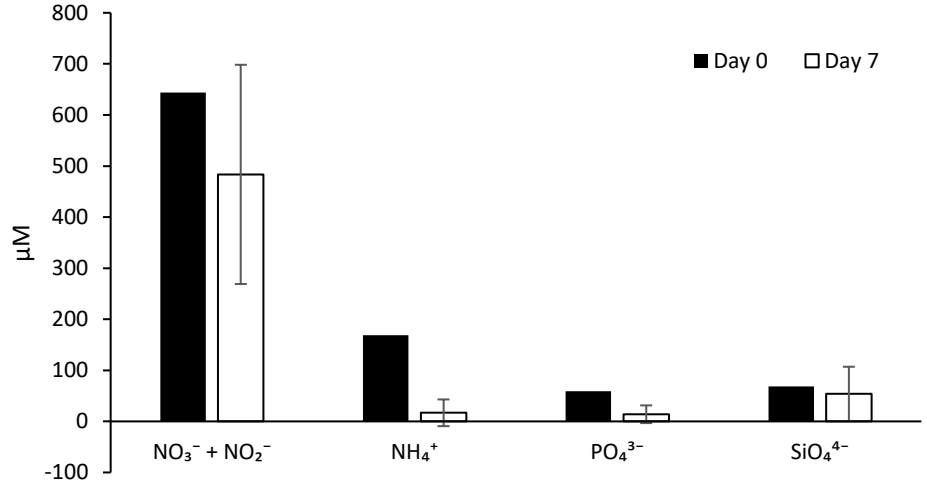

Figure 48 Nutrient analysis of *Amphora* sp. NCC169 grown in PSBR. Error bars represent standard deviation of replicates (n=3). Day 0 doesn't have replicates.

3.3 Productivity comparison between Fernbach and PSBR cultures

The PSBR has a dry biomass productivity of 0.5 ± 0.1 g m^{-2} day^{-1} after seven days of culture, which is statistically higher than the biomass productivity achieved by the Fernbach cultures at any sampling point (Tukey HSD test, $p \leq 0.05$) (Figure 49A). This supports the result of previous studies showing that attached microalgae cultivation systems are more productive than suspension methods (Lee et al., 2014; Zhuang et al., 2018). The surface biomass productivity of attached cultivation methods reported in the literature ranges between 0.04 – 80 g m^{-2} day^{-1}, depending on the influence of different factors (e.g., species, nutrient levels, temperature, light intensity, culture scale, attachment material) (Gross et al., 2013; Zhuang et al., 2018). Algae species with negative free energy of cohesion (e.g., *Ankistrodesmus falcatus*, *Botryococcus braunii*, *Botryococcus sudeticus*, *Cylindrotheca fusiformis*) indicate better adhesion to artificial substrates because of their dominating attractive acid-base and van der Waals interaction (Ozkan and Berberoglu, 2013). This determines the hydrophobicity of the cells and their superiority in forming biofilms. Additionally, the magnitude of algae-surface interactions is

directly proportional to cell size. Higher algal diameters denote higher attractive or repulsive forces. However, the influence of lift and drag forces of fluid flow must be considered in order to promote optimized adhesion of the algal cells. For example, flow rate was shown to have significantly reduced the net force acting on an adhered cell, decreasing the effective cell diameter from 10.4 to 4.3 μm (Ozkan and Berberoglu, 2013).

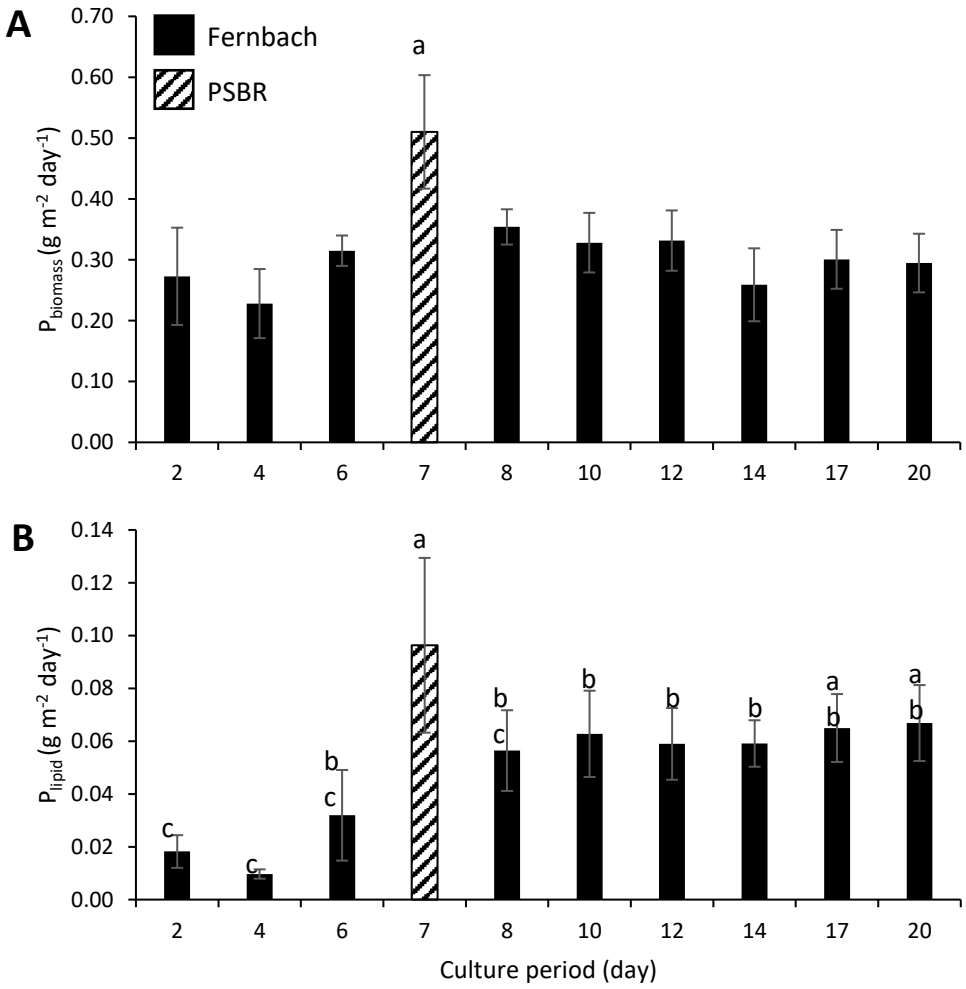

Figure 49 Average biomass (A) and lipid productivity (g m^{-2} day^{-1}) (B) of *Amphora* sp. NCC169 cultured in Fernbach flasks and in a PSBR. Error bars represent the standard deviation of the mean (n = 3 to 6). Letters represent treatments that have statistically significant difference in means (Tukey HSD test, $p \leq 0.05$). Values with the same letter are not significantly different ($p > 0.05$).

The highest recorded surface biomass productivities across different modes of attached cultivation were indeed dominated by green algae (*Scenedesmus obliquus* 50-80 g m^{-2} day^{-1} ; *Halochlorella rubescens* 31 g m^{-2} day^{-1} ; *Chlorella sorokiniana* 20.1 g m^{-2} day^{-1}) (Christenson and Sims, 2012; Gross et al., 2013). However, this could be owing to the fact that attached cultivation systems have thus far been primarily used for planktonic green algae. Benthic diatoms have the advantage to thrive in attached cultivation systems because of their ubiquitous biofilm-forming capacity (Consalvey et al., 2004; Stal and De Brouwer, 2003). Although some attached cultivation operations include diatom species like *Nitszchia* sp., *Cymbella* sp., *Melosira* sp., *Gomphonema* sp., *Synedra* sp., *Eunotia* sp., *Diatoma* sp. and *Navicula* sp., they're usually mixed in with other microalgae species (Boelee et al., 2014; Christenson and Sims, 2012; Genin et al., 2014). Research on more diatom species under similar experimental conditions is necessary for more robust comparisons.

Biomass productivity of suspended cultures was often expressed as a function of volume, hence, data on biomass productivity of microalgae in flasks as expressed in g m^{-2} day^{-1} is still wanting. However, comparison is feasible by having the same culture volume, as in the case of *Chlorella* sp. where attached cultivation generated 36% more algal biomass than its suspension counterpart (Johnson and Wen, 2010). Comparative growth performance of mixed microalgae cells in raceway ponds revealed a 2.8-times higher algal biomass when the ponds were installed with attachment substrates (Lee et al., 2014).

The higher productivity values of *Amphora* sp. NCC169 immobilized in the PSBR could be due to the higher mass-transfer efficiency of gases, nutrients, and light to support growth. In the PSBR, the biofilm cells have direct gas exchange and shorter light diffusion path through the thinner liquid membrane (PSBR = < 0.05 cm; Fernbach flask = 5 cm). This prevents the excessive accumulation of photosynthesis-generated oxygen in the biofilm, thereby reducing the negative effects of photoinhibition or photo-oxidation on net photosynthesis and keeping the F_v/F_m at optimum (Li et al., 2016; Murphy and Berberoglu, 2014). Biofilm cells can directly access and take up CO_2 from the gas phase (Wolf et al., 2007). On the other hand, in the Fernbach cultures, culture medium wasn't mixed during the period of cultivation. Hence, any available CO_2 is limiting as they must first diffuse through the gas-liquid interface prior to cellular uptake. This limitation was ameliorated using the PSBR where

the biofilm cells are directly in contact with the ambient gas phase and continuous fresh supply of culture medium. Moreover, this setup allows for better light availability than suspension cultures.

As for biomass productivity, lipid productivity was significantly higher in the PSBR (0.1 ± 0.03 g m^{-2} day^{-1}) than in Fernbach cultures harvested before day 14 (Tukey HSD test, $p \leq 0.05$) (**Figure 49**B). However, lipid productivity of *Amphora* sp. NCC169 cultured in the PSBR after 7 days and those grown in the Fernbach flasks beyond day 10 (day 17 and 20) were similar (Tukey HSD test, $p > 0.05$).

In the PSBR, *Amphora* sp. NCC169 constantly maintained optimal photosynthetic efficiency until harvest. This reflects healthy metabolic status and minimal stress to the cells. As healthy biofilm thickens, cells become self-shaded, and light limitation generally increases the F_v/F_m of low-light adapted benthic diatoms (Wulff et al., 2008). Furthermore, the dark regions contribute to the heterotrophication of the cells which subsequently foster cellular growth and lipid enrichment (Huang et al., 2022). High lipid productivity is not directly proportional to high lipid quality. The first step in this study is to improve the biomass productivity of *Amphora* sp. NCC169 and sustain the cells in good health. Afterwards, optimization of lipid accumulation and lipid quality of the cells is imperative for species valorization. These can be improved under highly controlled conditions using the PSBR. Subsequent analysis of lipid fractions obtained from PSBR is needed to investigate the feasibility of producing high-quality lipids for biotechnological applications.

Although there has been a commonly observed downward trend of F_v/F_m in benthic diatoms under laboratory conditions (Wulff et al., 2008), the decline in F_v/F_m is a potentially valuable indicator of nutrient starvation and/or degree of photoinhibition (Cointet et al., 2019a; Geider et al., 1993; Lippemeier et al., 1999; Young and Beardall, 2003). In Fernbach flasks, macronutrient concentrations were significantly reduced by 68% (NO_3^- + NO_2^-) to as much as 99% (PO_4^{3-} and SiO_4^{4-}) at day 14. Although the Redfield-Brzezinski ratios in the culture media continue to fall within the acceptable threshold for diatoms (Si:N:P = 15:16:1) (Brzezinski, 1985), the available concentrations of each macronutrient have significantly diminished at the end of the experimental period. The accumulation of several nutrient limitations (N and P) have been shown to strongly influence the F_v/F_m values of benthic diatoms *Entomoneis paludosa*, *Nitzschia alexandrina*, and *Staurosira* sp. (Cointet et al., 2019a). As these compounds are highly precipitating with other molecules in seawater (e.g., Ca^{2+}, Mg^{2+}), the

rapid decrease in media concentrations highlights subsequent enrichment to prevent any possible limitation in the system. A similar trend has been observed for the nutrients in an airlift culture of *Haslea ostrearia*, which was ameliorated by introducing a fed-batch strategy of HCO_3^-, PO_4^{3-} and SiO_3^{2-} (Xuan et al., 2021). Light stress introduced to the PSII system can also damage the photosynthetic apparatus, inhibit the light energy conversion, and eventually decrease the overall F_v/F_m (Heraud and Beardall, 2000; Wulff et al., 2008). Regardless, it has been shown that in nutrient-deficient conditions, the effect of light intensity on the PSII maximum efficiency of some species of marine benthic diatoms is negligible (Cointet et al., 2019a).The productivity of *Amphora* sp. NCC169 in the current PSBR is comparatively lower than the biomass productivities of other algal species using previously designed PSBRs (Indrayani et al., 2019; Naumann et al., 2013). This may be due to severe carbon limitation within the culture cylinder. Although the culture media reservoir was injected with CO_2 to stabilize the pH of the culture medium, the culture cylinder itself was left bereft, leaving gas exchange between the cells and the ambient air severely compromised. This could likewise explain the paltry difference in performance in comparison with the Fernbach flasks. The current PSBR design is a newly-adapted design from an existing suspension photobioreactor configuration, and not an exact replication of any of its predecessors. The PMMA cylinder that houses the support panel and reservoir were designed for planktonic algae, with which they are in direct contact. However, translated into a PSBR, this experimental adaptation still needs to undergo thorough simulation of engineering and species-specific biological factors to investigate the dynamic processes within the PSBR.

4. Conclusion and Perspective

Overall, porous substrate photobioreactor systems are promising in microalgae culture in general, and benthic diatoms in particular. The use of the PSBR enabled *Amphora* sp. NCC169 to proliferate at higher biomass and lipid productivities than those cultivated in Fernbach flasks. The results obtained in this study set a benchmark towards identifying critical knowledge gaps in benthic diatom ecophysiology and attached cultivation research.

Optimization of the PSBR design is ongoing to improve the biomass and total lipid yield of *Amphora* sp. NCC169. Subsequent experiments will focus on the selection of the best substrate material

and use the entire surface area of the support panel to obtain higher biomass yield. This will help in understanding surface physicochemical properties and determine substrate materials that promote superior biofilm characteristics for both lab-scale and commercial-scale cultivation. Additionally, choosing a durable and sustainable substrate for long-term biofilm operations is another important consideration.

Research will also have to assess the productivity of *Amphora* sp. NCC169 in the PSBR with respect to different light intensity and nutrient supply. Furthermore, the interactions between host-diatoms and their associated bacteria will be investigated in the PSBR setting to elucidate the important implications for overall diatom fitness. Most studies on bacteria-diatom co-cultures show positive influence on algal biomass by virtue of synthesized metabolites during cultivation that optimizes algal growth. Finally, life cycle analysis and overall operational costs will have to be investigated for future mass-production.

5. Acknowledgments

We are very grateful to the Pays de la Loire region (France) for financially supporting our research (via the SMIDAP grant BIOFILM, agreement n° 2021_04302). We would also like to acknowledge Synoxis Algae for the invaluable contribution to the development and engineering of the PSBR. We sincerely thank Ms. Clarisse Hubert from IFREMER (DG-ODE-PHYTOX-METALG) for her assistance in nutrient analyses of the samples and also Philippe Rosa and Alexandra Petit for their technical help in ISOMer lab.

III.2 Assess light quality effect on the biomass and total lipid rate of *Amphora* sp. NCC169 cultivated in a porous substrate photobioreactor *(Supplemental Result)*

1. Introduction

Given their importance as primary producers, marine benthic diatoms are highly sensitive to light (Underwood & Kromkamp 1999; Cartaxana et al. 2016; Lehmuskero et al. 2018; Hope et al. 2020). Their specialized, three-dimensional silica frustules act as protective covering for the cells. The porous architecture of the frustules also influences the scattering and distribution of light by acting as a scaffold that influences light absorption efficiency (Noyes et al. 2008; De Tommasi et al. 2010, 2014, 2021; Kieu et al. 2014; Romann et al. 2015; Ellegaard et al. 2016). Moreover, intricately patterned frustules provide a framework for spatial deposition and organization of various pigments found within the diatoms (e.g., chlorophylls, carotenoids, fucoxanthin) that utilize light energy during photosynthesis (Su et al. 2015, 2017). The structural support conferred by diatom frustules also reduces the potential for pigment self-shading that can limit the cells' photosynthetic efficiency and nutrient uptake.

Marine benthic diatoms efficiently harvest light energy through a variety of photosynthetic pigments that act as antennae to efficiently harvest and funnel light energy into the cells' photosynthetic units (Mirkovic et al. 2017). Diatoms generally contain two major categories of pigment: chlorophylls and carotenoids. Chlorophyll a absorbs light in the blue (440 nm) and red (675 nm) portions of the electromagnetic spectrum and plays a central role in photosynthesis. Additionally, diatoms possess supplemental chlorophyll c pigments (c1, c2, and c3) that participate effectively as accessory photosynthetic pigments. Carotenoids include light harvesting pigment fucoxanthin and photoprotective pigments such as diadinoxanthin, diatoxanthin, violaxanthin, and zeaxanthin that absorb a broader range of light in the spectrum (400-500 nm). These pigments allow diatoms to efficiently capture light energy in environments with fluctuating lighting intensities and regimes, as well as to protect the cells from deleterious light-induced photodamage (Méléder et al. 2003; Kuczynska et al. 2015). The specific combination of these pigments gives the characteristic color to the diatoms. The abundance of each pigment significantly varies relative to the species, physiological status, and environmental parameters involved.

When the total pigments of *Amphora* sp. NCC169 at different sampling periods were quantified by HPLC, there are mainly five pigment peaks: chlorophyll a (380 – 450 nm ; 600 – 670 nm), chlorophyll c1 (447 – 452 nm), fucoxanthin (450 – 540 nm), and diadinoxanthin (450 – 500 nm) . Blue light and red/far-red light receptors have been encoded in sequenced diatom genomes, but no green light photoreceptors have been assessed so far. Additionally, red and blue light are both absorbed at shallower depths compared to green light, which reflects the species' genomic adaptation to shallower, turbid environments. Theoretically, the red wavelength would provide sufficient energy to be used in photosynthesis, and the blue light photons could be used to increase overall photosynthesis in *Amphora* sp. NCC169. The mixture of red and blue (50:50) LED irradiance is also used to derive adaptive laboratory evolution in diatoms. The effect of light on diatom lipid production involves a complex process that ultimately depends on the quality, intensity, and duration of exposure. Optimizing these conditions is vital in the investigation of eco-physiological processes that take place among benthic diatom communities, as well as the inherent effects of light on the biochemical characteristics of the cells. By understanding the mechanisms that govern the photosynthetic properties of benthic diatoms through light manipulation, production of high-value compounds such as EPA and DHA can be more productive and cost-effective.

The intention of the current study is to investigate the effect of applying only red (620 – 780 nm) and blue (440 – 490 nm) wavelengths to the laboratory-scale culture of *Amphora* sp. NCC169 in a porous substrate photobioreactor. The cell health, density, and lipid productivity of the cells are measured and compared with datasets obtained from cells grown under white light conditions with green wavelength (495 – 570 nm).

2. Materials and methods

The materials and methods used in this experiment are similar to the ones used in chapter III.1. Additionally, some disks were left to incubate in the Fytoscope culture chamber under similar condition of the culture stock (i.e., blue (448 nm) and red (638 nm) light at 150 μmoles m^{-2} s^{-1}, and at 16 °C) until a visible and stable biofilm is formed. Multiple culture plates were made to ensure sufficient supply for use in the experiment.

In the PSBR, red (620 – 780 nm) and blue (440 – 490 nm) wavelengths were continuously activated to reach a final intensity of 150 µmoles m^{-2} s^{-1} (red=75 µmoles m^{-2} s^{-1}; blue=75 µmoles m^{-2} s^{-1}). Continuous light was provided by two panels of RGB LED channels set at a global intensity of 150 µmoles m^{-2} s^{-1} was used as control. Medium pH was set at 7.8 ± 0.1 , and external temperature at 17.6 ± 2.1 °C. Artificial seawater enriched with Guillard's F/2 medium was dripped onto the substrate at a rate of 2 mL every 3 minutes by means of a peristatic pump in the control unit (Wolfstein and Stal, 2002).

Data obtained were expressed as mean ± standard deviation. The test for statistical significance was performed through the PAleontological STatistics (PAST) software (version 4.12). Percentage data was transformed when necessary [43]. The values were evaluated for normality using the Shapiro–Wilk W test. Student's independent t-test was used to compare the means between two groups if the data was normally distributed, while non-parametric Mann-Whitney U test was used otherwise. The level of statistical significance was indicated by asterisks, where single asterisk (*) represents $p \leq 0.05$, double asterisks (**) represents $p \leq 0.01$, and triple asterisks (***) represents $p \leq 0.001$.

3. Results and discussion

After 10 days of acclimating the cells inside the Fytoscope culture chamber, the disks had negligible biomass (NDVI) values (Figure 50A) but were still used to launch the PSBR. After seven days of culture in the PSBR, NDVI values in the RB treatment increased to 0.2 ± 0.1 as translated by the vivid browning of the biofilm on the disks (Figure 50B).

A B

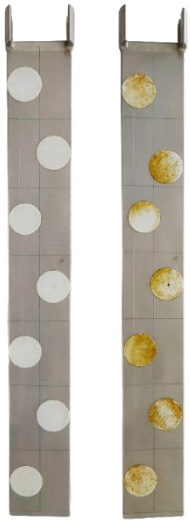

Figure 50 Biofilm progression from Day 0 (A) to Day 7 (B)

Photosynthetic efficiency values were optimum at the launch of the experiment (RGB = 0.6 ± 0.0; RB = 0.5 ± 0.3) (p = 0.8). This status remained throughout the duration of the experiment for both RB (0.6 ± 0.1) and RGB (0.6 ± 0.1) treatments (p = 0.4) (Figure 51).

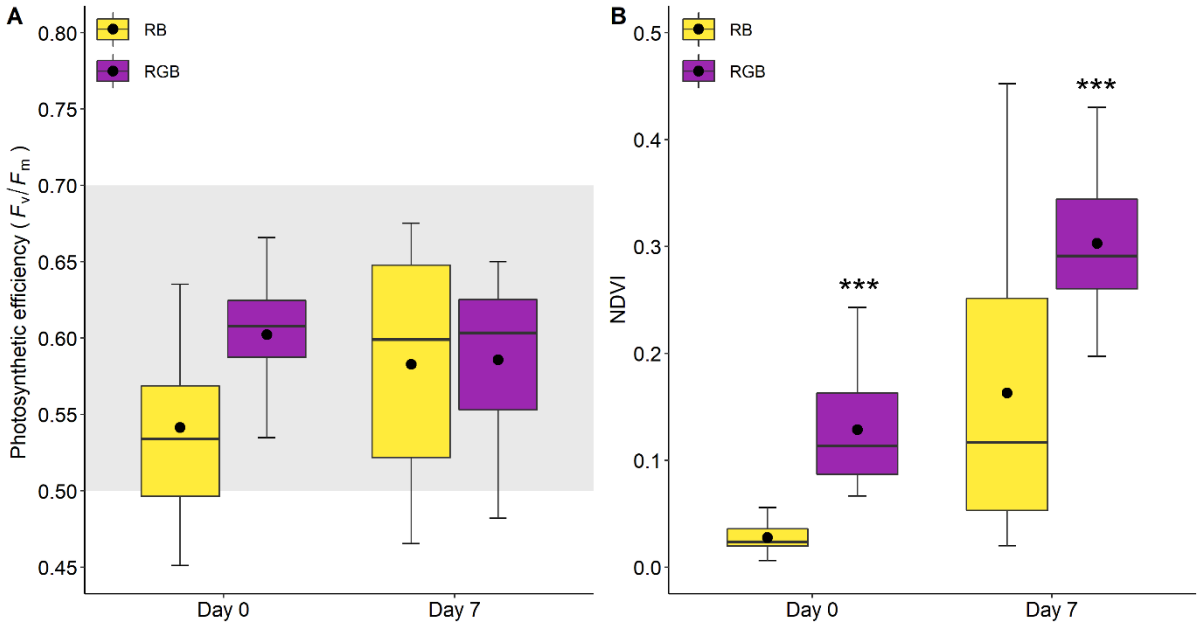

Figure 51 Average photosynthetic efficiency (F_v/F_m) (A) and NDVI (B) of *Amphora* sp. NCC169 biofilm disks in the PSBR (n = 42). Data is categorized between disks exposed to different light wavelengths (RGB = red, green, and blue; RB = red and blue) and sampling period (Day 0 and Day 7). The median line separates the 1st and 3rd quartile rectangle boundaries, while error bars represent minimum and maximum values. Black-filled circles (●) represent the population mean. The optimum range of photosynthetic efficiency for diatoms (0.5–0.7) is highlighted in gray. Asterisks show significant difference at *p < 0.05, **p < 0.01, or ***p < 0.001 (Mann-Whitney U test).

After seven days of culture, both light treatments have shown similar average pooled dry biomass reaching 11.5 ± 2.2 mg on the RGB treatment and 9.2 ± 4.4 mg on the RB treatment (Figure 52, p = 0.3). Mean total lipid rate was similar for variables, reaching 20.1 ± 4.8% and 23.8 ± 2.1% for the RGB and RB wavelengths, respectively (p = 0.12).

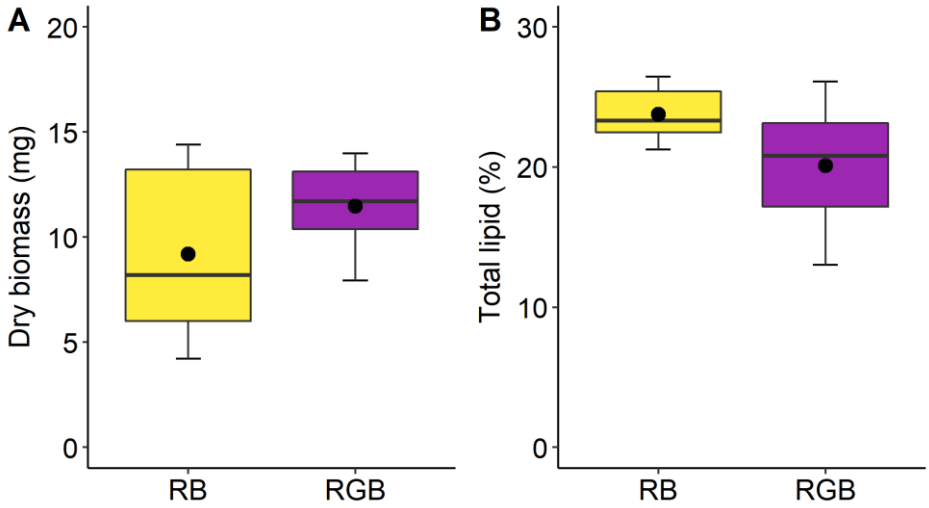

Figure 52 Box plot distribution of the average dry biomass density and total lipid content in percent dry biomass of *Amphora* sp. NCC169 on disks located on the left and right side of the PSBR upon harvest (Day 7, n=6). Error bars represent minimum and maximum values, whereas rectangle boundaries represent the 1st and 3rd quartile values separated by the median. Mean values were plotted as black-filled circles (●).

Diatoms possess chlorophylls a and c which absorb light in the blue and red regions of the electromagnetic spectrum. They require a sufficient amount of light to carry out photosynthesis effectively and fulfill their energy requirements. In this experiment, blue and red lights didn't have any significant influence on the biomass of *Amphora* sp. NCC169 after seven days of cultivation in the PSBR in comparison to the yield obtained from cells exposed to RGB. This is contrary to previous studies supporting the use of blue light to enhance the growth of *Amphora* sp. (Kwon et al., 2013; Romero-Romero and del Pilar Sánchez-Saavedra, 2017). While blue and red light are necessary components of the spectrum, specific positive or negative effects to the cells are highly dependent on the balance in the light spectrum. The unexpected low growth of *Amphora* sp. NCC169 under blue and red-light conditions could be due to reduced photosynthetic efficiency caused by an imbalance in photosynthetic pigments. The intensities used in the study might have also generated excess energy that weren't efficiently utilized for photosynthesis, which eventually led to inefficiencies in energy conversion and reduced growth.

Amphora sp. NCC169 cells fostered under blue and red light had higher lipid productivity (23.78 ± 2.08%) than when the cells were previously cultured under white light conditions (20.11 ± 4.83%), however insignificant (t = 1.72, p = 0.12). Blue light was shown to have significant effect on the cell size of certain species of benthic diatoms (Mercado et al., 2004). The was a dramatic change in the biomass of *Amphora* sp. NCC169 after 7 days, as quantified by the NDVI, similar to results obtained by (Mercado et al., 2004). The rapid growth rate resulted in differences in cell size and, consequently, in lipid content. The increase in lipid content could also be a consequence of storage products in the cells due to the spectral composition of light (Vadiveloo et al., 2015).

General Conclusion and Perspective

This dissertation principally aimed to explore the potential of using a porous substrate photobioreactor (PSBR) in the cultivation of *Amphora* sp. NCC169 to valorize its lipid content for various biotechnological applications.

Through rigorous experimentation and analysis, we demonstrated the PSBR's efficacy in enhancing biomass and lipid productivity. Results revealed the potential of the PSBR in producing healthy, dense microalgal biomass. *N. laevis*' pooled dry weight significantly increased from 1.17 ± 0.27 mg to 4.90 ± 2.5 mg in a matter of five (5) days. The growth rate and total lipid rate observed in this study are notably higher than previously recorded values in similar investigations. Photosynthetic efficiency of the biofilm decreased overall, but the F_v/F_m values remained strong (>0.5) indicating robust biofilm growth and favorable culture conditions for photosynthesis. The findings of the study indicate that cells cultivated in the PSBR have indeed exhibited significantly higher biomass and lipid productivity compared to those grown in Fernbach flasks over a 20-day cultivation period. Photosynthetic efficiency of the cells remained favourable in both PSBR and Fernbach systems, as indicated by the constant $F_v/F_m \geq 0.5$ values throughout the duration of the experiments. Experiments conducted on two distinct light qualities demonstrate that the total biomass yield and total lipid rate for both RB and RGB are similar to each other. Both treatments also yielded a satisfactory physiological cell health throughout the entire culture period. Nonetheless, the biomass density of *Amphora* sp. NCC169 biofilm is significantly higher in cells receiving the RGB treatment after 7 days. This suggests that although benthic diatoms primarily utilize RB wavelengths for photosynthesis, they may also have the capacity to capture some energy from green light to an extent. Moreover, this would imply that their capacity to thrive in various ecological conditions and adjust to new circumstances is more extensive than previously believed.

The adaptability and resilience of *Amphora* sp. NCC169 biofilms under PSBR conditions were demonstrated by noteworthy enhancements in growth rates and lipid accumulation. This success is attributed to the PSBR's design, which provided a controlled and stable environment for the cultivation of the benthic diatoms. By immobilizing the cells on a substrate, the natural benthic conditions in their

habitats are mimicked and allows for the simulation of different benthic conditions and environmental factors, such as light quality and intensity, nutrient availability, and temperature.

Although the results of the research show promise, it is crucial to recognize the limitations that were encountered. Several issues during the *N. laevis* trials revolve around the design and engineering of the crude PSBR. Significant challenges include light shading, nutrient sparger positioning, and support panel placement. These problems were addressed through a process of reimagining and redesigning specific features of the PSBR. The construction of an optimized PSBR adapted more stable and more efficient modular elements. However, the design of the PSBR is still in its infancy, and there is still plenty of room for improvement, both in terms of engineering and experimental design. Since the PSBR was manufactured from scratch, there has been a constant and inevitable need to troubleshoot, revise, and retest hypotheses and variables. Unanticipated problems and challenges also arose, which led to several delays in project timelines. To mitigate barriers, ongoing research and development focus on mastering the operation of the PSBR, rigorous testing and validation of performance data, as well as developing solutions to address engineering issues.

The promising outcomes of employing PSBR for the cultivation of *Amphora* sp. NCC169 underscore the need for an expansive and multidisciplinary approach to fully realize the potential of benthic diatoms. Future endeavors should prioritize scalability and operational optimization of the PSBR to transition from laboratory efficacy to industrial viability. This entails dedicating attention to advancing material innovation (e.g., substrate material, sparger design), optimizing light regimes, and effectively managing nutrient uptake and availability. Simultaneously, a rigorous economic and environmental impact analysis will be paramount to help in identifying key areas for improvement and ensuring that the technology is both economically viable and environmentally sustainable.

The construction of a PSBR expands the scope of benthic diatom research to include a wider range of microorganisms like bacteria and fungi. These microorganisms play a pivotal role in the complex dynamics of benthic diatom communities in a wide range of aquatic habitats. Investigating their growth dynamics in the PSBR will provide valuable insights into their synergistic potential that may further valorize bioactive compounds. In addition, the association between benthic diatoms and bacteria is

sensitive to environmental changes, underscoring the importance of understanding how these microbial communities respond to future shifts in climate and nutrient regimes.

The full extent of the potential of benthic diatoms is an ongoing field of research and is still being explored. Their unique properties and ecophysiology make them fascinating subjects for interdisciplinary investigations between ecology, biochemistry, materials science, and nanotechnology. The shift towards biofilm-based culture systems for benthic diatoms presents opportunities for addressing prevailing bottlenecks in microalgae cultivation. As our understanding of benthic diatoms grows, so does the potential for innovative and sustainable solutions for both scientific and practical applications.

References

Allen, A.E., Dupont, C.L., Oborník, M., Horák, A., Nunes-Nesi, A., McCrow, J.P., Zheng, H., Johnson, D.A., Hu, H., Fernie, A.R., 2011. Evolution and metabolic significance of the urea cycle in photosynthetic diatoms. Nature 473, 203–207.

Almeida, S.F.P., Feio, M.J.D., n.d. Present and future perspectives for bioassessment of running water using diatoms, in: Goessling, J.W., Serôdio, J., Lavaud, J. (Eds.), Diatom Photosynthesis: From Primary Production to High Value Molecules. Wiley Scrivener, Beverly, Mass.

Amer, L., Adhikari, B., Pellegrino, J., 2011. Technoeconomic analysis of five microalgae-to-biofuels processes of varying complexity. Bioresour. Technol. 102, 9350–9359.

Aminot, A., Kérouel, R., 2007. , in: Dosage automatique des nutriments dans les eaux marines: méthodes en flux continu. Quae Ifremer, pp. 77–132.

Antunes, J., Pereira, S., Ribeiro, T., Plowman, J.E., Thomas, A., Clerens, S., Campos, A., Vasconcelos, V., Almeida, J.R., 2019. A multi-bioassay integrated approach to assess the antifouling potential of the cyanobacterial metabolites portoamides. Mar. Drugs 17, 111.

Arnaldo, M.D.G., n.d. Eco-physiological study of *Amphora* sp. NCC169 for the optimization of culture conditions to find way of valorization in health, cosmetics and food (unpublished doctoral dissertation). Nantes Université, Nantes, France.

Austic, R.E., Mustafa, A., Jung, B., Gatrell, S., Lei, X.G., 2013. Potential and limitation of a new defatted diatom microalgal biomass in replacing soybean meal and corn in diets for broiler chickens. J. Agric. Food Chem. 61, 7341–7348.

Babenko, I., Friedrich, B.M., Kröger, N., 2022. Structure and morphogenesis of the frustule, in: Falciatore, A., Mock, T. (Eds.), The Molecular Life of Diatoms. Springer, pp. 287–312.

Badel, S., Callet, F., Laroche, C., Gardarin, C., Petit, E., El Alaoui, H., Bernardi, T., Michaud, P., 2011. A new tool to detect high viscous exopolymers from microalgae. J. Ind. Microbiol. Biotechnol. 38, 319–326.

Baker, L.-A., Biron, D.G., Millan, F., Voldoire, O., Breton, V., Allain, E., Wetzel, C.E., Ector, L., Beauger, A., 2022. The substrate, a key factor or not, to explain the species diversity of diatom communities in mineral springs. Bot. Lett. 1–11.

Balamurugan, S., Wang, X., Wang, H.-L., An, C.-J., Li, H., Li, D.-W., Yang, W.-D., Liu, J.-S., Li, H.-Y., 2017. Occurrence of plastidial triacylglycerol synthesis and the potential regulatory role of AGPAT in the model diatom *Phaeodactylum tricornutum*. Biotechnol. Biofuels 10, 1–14.

Bally, R., McQuaid, C., Pierce, S., 1985. Primary productivity of the Bot river estuary, South Africa. Trans. R. Soc. South Afr. 45, 333–345.

Barillé, L., Mouget, J.-L., Méléder, V., Rosa, P., Jesus, B., 2011. Spectral response of benthic diatoms with different sediment backgrounds. Remote Sens. Environ. 115, 1034–1042.

Bayu, A., Rachman, A., Noerdjito, D., Putra, M., Widayatno, W., 2020. High-value chemicals from marine diatoms: A biorefinery approach. Presented at the IOP Conference Series: Earth and Environmental Science, IOP Publishing, p. 012012.

Behrenfeld, M.J., Halsey, K.H., Boss, E., Karp-Boss, L., Milligan, A.J., Peers, G., 2021. Thoughts on the evolution and ecological niche of diatoms. Ecol. Monogr. 91, e01457.

Benoiston, A.-S., Ibarbalz, F.M., Bittner, L., Guidi, L., Jahn, O., Dutkiewicz, S., Bowler, C., 2017. The evolution of diatoms and their biogeochemical functions. Philos. Trans. R. Soc. B Biol. Sci. 372, 20160397. https://doi.org/10.1098/rstb.2016.0397

Benstein, R.M., Çebi, Z., Podola, B., Melkonian, M., 2014. Immobilized growth of the peridinin-producing marine dinoflagellate *Symbiodinium* in a simple biofilm photobioreactor. Mar. Biotechnol. 16, 621–628.

Berhe, N., Tefera, Y., Tintagu, T., 2017. Review on biofilm formation and its control options. Int. J. Adv. Res. Biol. Sci. 8, 122–133.

Berner, F., Heimann, K., Sheehan, M., 2015. Microalgal biofilms for biomass production. J. Appl. Phycol. 27, 1793–1804.

Bernstein, H.C., Kesaano, M., Moll, K., Smith, T., Gerlach, R., Carlson, R.P., Miller, C.D., Peyton, B.M., Cooksey, K.E., Gardner, R.D., 2014. Direct measurement and characterization of active

photosynthesis zones inside wastewater remediating and biofuel producing microalgal biofilms. Bioresour. Technol. 156, 206–215.

Bertrand, M., 2010. Carotenoid biosynthesis in diatoms. Photosynth. Res. 106, 89–102.

Blanken, W., Janssen, M., Cuaresma, M., Libor, Z., Bhaiji, T., Wijffels, R., 2014. Biofilm growth of *Chlorella sorokiniana* in a rotating biological contactor based photobioreactor. Biotechnol. Bioeng. 111, 2436–2445.

Bligh, E.G., Dyer, W.J., 1959. A rapid method of total lipid extraction and purification. Can. J. Biochem. Physiol. 37, 911–917.

Blommaert, L., Lavaud, J., Vyverman, W., Sabbe, K., 2018. Behavioural versus physiological photoprotection in epipelic and epipsammic benthic diatoms. Eur. J. Phycol. 53, 146–155.

Body, A.G., 1987. Abalone culture in Japan. Mar. Fish. Rev. 49, 75–76.

Boelee, N., Janssen, M., Temmink, H., Shrestha, R., Buisman, C., Wijffels, R., 2014. Nutrient removal and biomass production in an outdoor pilot-scale phototrophic biofilm reactor for effluent polishing. Appl. Biochem. Biotechnol. 172, 405–422.

Bojko, M., Olchawa-Pajor, M., Goss, R., Schaller-Laudel, S., Strzałka, K., Latowski, D., 2019. Diadinoxanthin de-epoxidation as important factor in the short-term stabilization of diatom photosynthetic membranes exposed to different temperatures. Plant Cell Environ. 42, 1270–1286.

Bolhuis, H., Fillinger, L., Stal, L.J., 2013. Coastal microbial mat diversity along a natural salinity gradient. PLOS One 8, e63166.

Borowitzka, M.A., 2018. Biology of microalgae, in: Microalgae in Health and Disease Prevention. Elsevier, pp. 23–72.

Bozarth, A., Maier, U.-G., Zauner, S., 2009. Diatoms in biotechnology: modern tools and applications. Appl. Microbiol. Biotechnol. 82, 195–201.

Brembu, T., Mühlroth, A., Alipanah, L., Bones, A.M., 2017. The effects of phosphorus limitation on carbon metabolism in diatoms. Philos. Trans. R. Soc. B Biol. Sci. 372, 20160406.

Brzezinski, M.A., 1985. The Si: C: N ratio of marine diatoms: interspecific variability and the effect of some environmental variables. J. Phycol. 21, 347–357.

Büchel, C., Goss, R., Bailleul, B., Campbell, D.A., Lavaud, J., Lepetit, B., 2022. Photosynthetic light reactions in diatoms. I. The lipids and light-harvesting complexes of the thylakoid membrane, in: The Molecular Life of Diatoms. Springer, pp. 397–422.

Büchel, C., Wilhelm, C., 1993. In vivo analysis of slow chlorophyll fluorescence induction kinetics in algae: progress, problems and perspectives. Photochem. Photobiol. 58, 137–148.

Carlsson, A.S., van Beilen, J.B., Möller, R., Clayton, D., 2007. Micro-and macro-algae: utility for industrial applications: outputs from the EPOBIO project. CPL Press, University of York.

Carolina Biological Supply Company, n.d. Mixed diatom frustules.

Castilla-Gavilán, M., Reznicov, M., Turpin, V., Decottignies, P., Cognie, B., 2020. Sea urchin recruitment: Effect of diatom based biofilms on *Paracentrotus lividus* competent larvae. Aquaculture 515, 734559.

Cavicchioli, R., Ripple, W.J., Timmis, K.N., Azam, F., Bakken, L.R., Baylis, M., Behrenfeld, M.J., Boetius, A., Boyd, P.W., Classen, A.T., 2019. Scientists' warning to humanity: microorganisms and climate change. Nat. Rev. Microbiol. 17, 569–586.

Chang, Y., Chen, J., 2008. The status of mariculture in northern China, in: Lovatelli, A., Phillips, M., Arthur, J., Yamamoto, K. (Eds.), FAO/NACA Regional Workshop on the Future of Mariculture: A Regional Approach for Responsible Development in the Asia-Pacific Region. pp. 271–284.

Chavant, P., Gaillard-Martinie, B., Talon, R., Hébraud, M., Bernardi, T., 2007. A new device for rapid evaluation of biofilm formation potential by bacteria. J. Microbiol. Methods 68, 605–612.

Cheah, Y.T., Chan, D.J.C., 2021. Physiology of microalgal biofilm: a review on prediction of adhesion on substrates. Bioengineered 12, 7577–7599.

Cheng, K.-C., Demirci, A., Catchmark, J.M., 2010. Advances in biofilm reactors for production of value-added products. Appl. Microbiol. Biotechnol. 87, 445–456.

Cheng, P., Wang, J., Liu, T., 2014. Effects of nitrogen source and nitrogen supply model on the growth and hydrocarbon accumulation of immobilized biofilm cultivation of *B. braunii*. Bioresour. Technol. 166, 527–533.

Choudhary, P., Malik, A., Pant, K.K., 2017. Algal biofilm systems: an answer to algal biofuel dilemma, in: Algal Biofuels: Recent Advances and Future Prospects. Springer, pp. 77–96.

Christenson, L.B., Sims, R.C., 2012. Rotating algal biofilm reactor and spool harvester for wastewater treatment with biofuels by-products. Biotechnol. Bioeng. 109, 1674–1684.

Cointet, E., 2019. Diatomées marines benthiques : une ressource originale de souches “oléagineuses” pour une application en santé et nutrition [dissertation]. Université de Nantes.

Cointet, E., Séverin, E., Couzinet-Mossion, A., Méléder, V., Gonçalves, O., Wielgosz-Collin, G., 2021. Assessment of the lipid production potential of six benthic diatom species grown in airlift photobioreactors. J. Appl. Phycol. 1–11.

Cointet, E., Wielgosz-Collin, G., Bougaran, G., Rabesaotra, V., Goncalves, O., Meleder, V., 2019a. Effects of light and nitrogen availability on photosynthetic efficiency and fatty acid content of three original benthic diatom strains. PLoS One 14.

Cointet, E., Wielgosz-Collin, G., Méléder, V., Gonçalves, O., 2019b. Lipids in benthic diatoms: A new suitable screening procedure. Algal Res. 39, 101425.

Consalvey, M., Paterson, D.M., Underwood, G.J., 2004. The ups and downs of life in a benthic biofilm: migration of benthic diatoms. Diatom Res. 19, 181–202.

Consalvey, M., Perkins, R.G., Paterson, D.M., Underwood, G.J., 2005. PAM fluorescence: a beginners guide for benthic diatomists. Diatom Res. 20, 1–22.

Costerton, J.W., Lewandowski, Z., Caldwell, D.E., Korber, D.R., Lappin-Scott, H.M., 1995. Microbial biofilms. Annu. Rev. Microbiol. 49, 711–745.

Coutaud, M., Méheut, M., Viers, J., Rols, J.-L., Pokrovsky, O.S., 2019. Copper isotope fractionation during excretion from a phototrophic biofilm. Chem. Geol. 513, 88–100.

Croteau, D., Guérin, S., Bruyant, F., Ferland, J., Campbell, D.A., Babin, M., Lavaud, J., 2021. Contrasting nonphotochemical quenching patterns under high light and darkness aligns with light niche occupancy in Arctic diatoms. Limnol. Oceanogr. 66, S231–S245.

Cruz, Y.R., Aranda, D., Seidl, P.R., Diaz, G.C., Carliz, R.G., Fortes, M.M., da Ponte, D., de Paula, R., 2018. Cultivation systems of microalgae for the production of biofuels, in: Biofuels - State of Development. Intech Open London, UK, pp. 199–218.

Daboussi, F., Leduc, S., Maréchal, A., Dubois, G., Guyot, V., Perez-Michaut, C., Amato, A., Falciatore, A., Juillerat, A., Beurdeley, M., 2014. Genome engineering empowers the diatom *Phaeodactylum tricornutum* for biotechnology. Nat. Commun. 5, 1–7.

Davidovich, N.A., Davidovich, O.I., Podunay, Y.A., Gastineau, R., Kaczmarska, I., Poulíčková, A., Witkowski, A., 2017. *Ardissonea crystallina* has a type of sexual reproduction that is unusual for centric diatoms. Sci. Rep. 7, 14670.

Davidovich, O., Davidovich, N., Mouget, J.-L., 2018. The effect of temperature on vegetative growth and sexual reproduction of two diatoms from the genus *Haslea* Simonsen. Russ. J. Mar. Biol. 44, 8–13.

De Angelis, R., Melino, S., Prosposito, P., Casalboni, M., Lamastra, F.R., Nanni, F., Bruno, L., Congestri, R., 2016. The diatom *Staurosirella pinnata* for photoactive material production. PLoS One 11, e0165571.

De Godos, I., González, C., Becares, E., García-Encina, P.A., Muñoz, R., 2009. Simultaneous nutrients and carbon removal during pretreated swine slurry degradation in a tubular biofilm photobioreactor. Appl. Microbiol. Biotechnol. 82, 187–194.

de la Peña, M.R., 2007. Cell growth and nutritive value of the tropical benthic diatom, *Amphora* sp., at varying levels of nutrients and light intensity, and different culture locations. J. Appl. Phycol. 19, 647–655.

De Tommasi, E., De Luca, A.C., 2022. Diatom biosilica in plasmonics: applications in sensing, diagnostics and therapeutics. Biomed. Opt. Express 13, 3080–3101.

De Tommasi, E., Rea, I., Ferrara, M.A., De Stefano, L., De Stefano, M., Al-Handal, A.Y., Stamenković, M., Wulff, A., 2021. Underwater light manipulation by the benthic diatom *Ctenophora pulchella*: From PAR efficient collection to UVR screening. Nanomaterials 11, 2855.

De Tommasi, E., Rea, I., Mocella, V., Moretti, L., De Stefano, M., Rendina, I., De Stefano, L., 2010. Multi-wavelength study of light transmitted through a single marine centric diatom. Opt. Express 18, 12203–12212.

de Viçose, G.C., Viera, M., Huchette, S., Izquierdo, M., 2012. Improving nursery performances of *Haliotis tuberculata coccinea*: nutritional value of four species of benthic diatoms and green macroalgae germlings. Aquaculture 334, 124–131.

Delalat, B., Sheppard, V.C., Rasi Ghaemi, S., Rao, S., Prestidge, C.A., McPhee, G., Rogers, M.-L., Donoghue, J.F., Pillay, V., Johns, T.G., 2015. Targeted drug delivery using genetically engineered diatom biosilica. Nat. Commun. 6, 8791.

Di Pippo, F., Ellwood, N.T., Gismondi, A., Bruno, L., Rossi, F., Magni, P., De Philippis, R., 2013. Characterization of exopolysaccharides produced by seven biofilm-forming cyanobacterial strains for biotechnological applications. J. Appl. Phycol. 25, 1697–1708.

Dobretsov, S., Rittschof, D., 2020. Love at first taste: induction of larval settlement by marine microbes. Int. J. Mol. Sci. 21, 731.

Donlan, R.M., Costerton, J.W., 2002. Biofilms: survival mechanisms of clinically relevant microorganisms. Clin. Microbiol. Rev. 15, 167–193.

Du Clos, K.T., Karp-Boss, L., Gemmell, B.J., 2021. Diatoms rapidly alter sinking behavior in response to changing nutrient concentrations. Limnol. Oceanogr. 66, 892–900.

Duarte, B., Feijão, E., Goessling, J.W., Caçador, I., Matos, A.R., 2021. Pigment and fatty acid production under different light qualities in the diatom *Phaeodactylum tricornutum*. Appl. Sci. 11, 2550.

Dunstan, G.A., Volkman, J.K., Barrett, S.M., Leroi, J.-M., Jeffrey, S., 1993. Essential polyunsaturated fatty acids from 14 species of diatom (Bacillariophyceae). Phytochemistry 35, 155–161.

Dutkiewicz, S., Hickman, A., Jahn, O., Gregg, W., Mouw, C., Follows, M., 2015. Capturing optically important constituents and properties in a marine biogeochemical and ecosystem model. Biogeosciences 12, 4447–4481.

Ediz, N., Bentli, İ., Tatar, İ., 2010. Improvement in filtration characteristics of diatomite by calcination. Int. J. Miner. Process. 94, 129–134.

Eich, A., Mildenberger, T., Laforsch, C., Weber, M., 2015. Biofilm and diatom succession on polyethylene (PE) and biodegradable plastic bags in two marine habitats: early signs of degradation in the pelagic and benthic zone? PLoS One 10, e0137201.

Fan, J., Andre, C., Xu, C., 2011. A chloroplast pathway for the de novo biosynthesis of triacylglycerol in *Chlamydomonas reinhardtii*. FEBS Lett. 585, 1985–1991.

Fernández, F.A., Perez, J.S., Sevilla, J.F., Camacho, F.G., Grima, E.M., 2000. Modeling of eicosapentaenoic acid (EPA) production from *Phaeodactylum tricornutum* cultures in tubular photobioreactors. Effects of dilution rate, tube diameter, and solar irradiance. Biotechnol. Bioeng. 68, 173–183.

Fontana, A., d'Ippolito, G., Cutignano, A., Miralto, A., Ianora, A., Romano, G., Cimino, G., 2007. Chemistry of oxylipin pathways in marine diatoms. Pure Appl. Chem. 79, 481–490.

Forehead, H.I., Kendrick, G.A., Thompson, P.A., 2012. Effects of shelter and enrichment on the ecology and nutrient cycling of microbial communities of subtidal carbonate sediments. FEMS Microbiol. Ecol. 80, 64–76.

Furnas, M.J., 1990. In situ growth rates of marine phytoplankton: approaches to measurement, community and species growth rates. J. Plankton Res. 12, 1117–1151.

Fusco, G., Minelli, A., 2019. Chapter 7: Reproduction: a Taxonomic Survey, in: The Biology of Reproduction. Cambridge University Press.

Gadelmawla, E.S., Koura, M.M., Maksoud, T.M., Elewa, I.M., Soliman, H.H., 2002. Roughness parameters. J. Mater. Process. Technol. 123, 133–145.

Gao, F., Yang, Z.-H., Li, C., Zeng, G.-M., Ma, D.-H., Zhou, L., 2015. A novel algal biofilm membrane photobioreactor for attached microalgae growth and nutrients removal from secondary effluent. Bioresour. Technol. 179, 8–12.

Geider, R.J., La Roche, J., Greene, R.M., Olaizola, M., 1993. Response of the photosynthetic apparatus of *Phaeodactylum tricornutum* (Bacillariophyceae) to nitrate, phosphate, or iron starvation. J. Phycol. 29, 755–766.

Genin, S.N., Aitchison, J.S., Allen, D.G., 2014. Design of algal film photobioreactors: material surface energy effects on algal film productivity, colonization and lipid content. Bioresour. Technol. 155, 136–143.

Ghobara, M., Maibohm, C., Reissig, L., Goessling, J.W., in press. Diatom applications in space: from oxygen production to nanomaterials, in: Goessling, J.W., Serôdio, J., Lavaud, J. (Eds.), Diatom

Photosynthesis: From Primary Production to High Value Molecules. Wiley Scrivener, Beverly, Mass.

Ghobara, M.M., Mazumder, N., Vinayak, V., Reissig, L., Gebeshuber, I.C., Tiffany, M.A., Gordon, R., 2019. On light and diatoms: A photonics and photobiology review, in: Seckbach, J., Gordon, R. (Eds.), Diatoms: Fundamentals and Applications. Wiley Online Library, pp. 129–189.

Gilmore, B.F., 2011. Antimicrobial ionic liquids. INTECH Open Access Publisher London, UK.

Gismondi, A., Pippo, F.D., Bruno, L., Antonaroli, S., Congestri, R., 2016. Phosphorus removal coupled to bioenergy production by three cyanobacterial isolates in a biofilm dynamic growth system. Int. J. Phytoremediation 18, 869–876.

Goeres, D.M., Hamilton, M.A., Beck, N.A., Buckingham-Meyer, K., Hilyard, J.D., Loetterle, L.R., Lorenz, L.A., Walker, D.K., Stewart, P.S., 2009. A method for growing a biofilm under low shear at the air–liquid interface using the drip flow biofilm reactor. Nat. Protoc. 4, 783–788.

Goessling, J.W., Su, Y., Cartaxana, P., Maibohm, C., Rickelt, L.F., Trampe, E.C., Walby, S.L., Wangpraseurt, D., Wu, X., Ellegaard, M., 2018. Structure-based optics of centric diatom frustules: modulation of the *in vivo* light field for efficient diatom photosynthesis. New Phytol. 219, 122–134.

Goessling, J.W., Su, Y., Maibohm, C., Ellegaard, M., Kühl, M., 2019. Differences in the optical properties of valve and girdle band in a centric diatom. J. R. Soc. Interface Focus 9, 20180031.

Gomez, K.A., Gomez, A.A., 1984. Statistical procedures for agricultural research. John Wiley & sons.

Gordon, R., Losic, D., Tiffany, M.A., Nagy, S.S., Sterrenburg, F.A.S., 2008. The glass menagerie: diatoms for novel applications in nanotechnology. Trends Biotechnol. 27. https://doi.org/10.1016/j.tibtech.2008.11.003

Granum, E., Myklestad, S.M., 2002. A photobioreactor with pH control: demonstration by growth of the marine diatom *Skeletonema costatum*. J. Plankton Res. 24, 557–563.

Grenier, J., Bonnefond, H., Lopes, F., Bernard, O., 2019. The impact of light supply to moving photosynthetic biofilms. Algal Res. 44, 101674.

Gross, M., Henry, W., Michael, C., Wen, Z., 2013. Development of a rotating algal biofilm growth system for attached microalgae growth with in situ biomass harvest. Bioresour. Technol. 150, 195–201.

Gross, M., Jarboe, D., Wen, Z., 2015. Biofilm-based algal cultivation systems. Appl. Microbiol. Biotechnol. 99, 5781–5789.

Gross, M., Wen, Z., 2014. Yearlong evaluation of performance and durability of a pilot-scale revolving algal biofilm (RAB) cultivation system. Bioresour. Technol. 171, 50–58.

Gross, M., Zhao, X., Mascarenhas, V., Wen, Z., 2016. Effects of the surface physico-chemical properties and the surface textures on the initial colonization and the attached growth in algal biofilm. Biotechnol. Biofuels 9, 1–14.

Gross-Wen Technologies, 2022. Cattlemen's Heritage selects Iowa company, Gross-Wen Technologies, to provide wastewater treatment technology to its new processing facility in Western Iowa [WWW Document]. Cision. URL https://www.prnewswire.com/news-releases/cattlemens-heritage-selects-iowa-company-gross-wen-technologies-to-provide-wastewater-treatment-technology-to-its-new-processing-facility-in-western-iowa-301520088.html

Guillard, R.R., 1975. Culture of phytoplankton for feeding marine invertebrates, in: Culture of Marine Invertebrate Animals. Springer, pp. 29–60.

Guillou, L., Chrétiennot-Dinet, M., Medlin, L.K., Claustre, H., Goër, S.L., Vaulot, D., 1999. Bolidomonas: a new genus with two species belonging to a new algal class, the Bolidophyceae (Heterokonta). J. Phycol. 35, 368–381.

Hajnal, É., Stenger-Kovács, C., Ács, É., Padisák, J., 2009. DILSTORE software for ecological status assessment of lakes based on benthic diatoms. Fottea 9, 351–354.

Hamm, C.E., Merkel, R., Springer, O., Jurkojc, P., Maier, C., Prechtel, K., Smetacek, V., 2003. Architecture and material properties of diatom shells provide effective mechanical protection. Nature 421, 841–843.

Harder, T., Lam, C., Qian, P.-Y., 2002. Induction of larval settlement in the polychaete *Hydroides elegans* by marine biofilms: an investigation of monospecific diatom films as settlement cues. Mar. Ecol. Prog. Ser. 229, 105–112.

Harding, I.C., Chant, L.S., 2000. Self-sedimented diatom mats as agents of exceptional fossil preservation in the Oligocene Florissant lake beds, Colorado, United States. Geology 28, 195–198.

Harrison, J.J., Ceri, H., Turner, R.J., 2007. Multimetal resistance and tolerance in microbial biofilms. Nat. Rev. Microbiol. 5, 928–938.

Hassard, F., Biddle, J., Cartmell, E., Jefferson, B., Tyrrel, S., Stephenson, T., 2015. Rotating biological contactors for wastewater treatment–a review. Process Saf. Environ. Prot. 94, 285–306.

He, S., Xue, G., 2010. Algal-based immobilization process to treat the effluent from a secondary wastewater treatment plant (WWTP). J. Hazard. Mater. 178, 895–899.

Hendrarto, I.B., Nitisuparjo, M., 2011. Biodiversity of benthic diatom and primary productivity of benthic micro-flora in mangrove forests on central Java. J. Coast. Dev. 14, 131–140.

Heraud, P., Beardall, J., 2000. Changes in chlorophyll fluorescence during exposure of *Dunaliella tertiolecta* to UV radiation indicate a dynamic interaction between damage and repair processes. Photosynth. Res. 63, 123–134.

Hildebrand, M., Davis, A.K., Smith, S.R., Traller, J.C., Abbriano, R., 2012. The place of diatoms in the biofuels industry. Biofuels 3, 221–240.

Hoagland, K.D., Rosowski, J.R., Gretz, M.R., Roemer, S.C., 1993. Diatom extracellular polymeric substances: function, fine structure, chemistry, and physiology. J. Phycol. 29, 537–566.

Hofmann, A.M., Geist, J., Nowotny, L., Raeder, U., 2020. Depth-distribution of lake benthic diatom assemblages in relation to light availability and substrate: implications for paleolimnological studies. J. Paleolimnol. 64, 315–334.

Hoh, D., Watson, S., Kan, E., 2016. Algal biofilm reactors for integrated wastewater treatment and biofuel production: a review. Chem. Eng. J. 287, 466–473.

Holland, A., Zingmark, R., Dean, J., 1974. Quantitative evidence concerning the stabilization of sediments by marine benthic diatoms. Mar. Biol. 27, 191–196.

Huang, B., Marchand, J., Blanckaert, V., Lukomska, E., Ulmann, L., Wielgosz-Collin, G., Rabesaotra, V., Moreau, B., Bougaran, G., Mimouni, V., 2019. Nitrogen and phosphorus limitations induce carbon partitioning and membrane lipid remodelling in the marine diatom *Phaeodactylum tricornutum*. Eur. J. Phycol. 54, 342–358.

Huang, Yun, Li, P., Huang, Yong, Xia, A., Zhu, X., Liao, Q., 2022. A synchronous photoautotrophic-heterotrophic biofilm cultivation mode for *Chlorella vulgaris* biomass and lipid simultaneous accumulation. J. Clean. Prod. 336, 130453.

Indrayani, I., Moheimani, N.R., Borowitzka, M.A., 2019. Long-term reliable culture of a halophilic diatom, *Amphora* sp. MUR258, in outdoor raceway ponds. J. Appl. Phycol. 31, 2771–2778.

Jeremiason, J.D., Eisenreich, S.J., Baker, J.E., Eadie, B.J., 1998. PCB decline in settling particles and benthic recycling of PCBs and PAHs in Lake Superior. Environ. Sci. Technol. 32, 3249–3256.

Jha, P.K., Dallagi, H., Richard, E., Deleplace, M., Benezech, T., Faille, C., 2022. Does the vertical vs horizontal positioning of surfaces affect either biofilm formation on different materials or their resistance to detachment? Food Control 133, 108646.

Johnson, M.B., Wen, Z., 2010. Development of an attached microalgal growth system for biofuel production. Appl. Microbiol. Biotechnol. 85, 525–534.

Johnson, T.J., Katuwal, S., Anderson, G.A., Gu, L., Zhou, R., Gibbons, W.R., 2018. Photobioreactor cultivation strategies for microalgae and cyanobacteria. Biotechnol. Prog. 34, 811–827.

Johnson, V.R., Brownlee, C., Milazzo, M., Hall-Spencer, J.M., 2015. Marine microphytobenthic assemblage shift along a natural shallow-water CO_2 gradient subjected to multiple environmental stressors. J. Mar. Sci. Eng. 3, 1425–1447.

Jones, M.D., 2005. Overview of the Calvin Cycle pathway [WWW Document]. URL https://commons.wikimedia.org/wiki/File:Calvin-cycle3.png

Kaczmarska, I., Poulíčková, A., Sato, S., Edlund, M.B., Idei, M., Watanabe, T., Mann, D.G., 2013. Proposals for a terminology for diatom sexual reproduction, auxospores and resting stages. Diatom Res. 28, 263–294.

Katarzyna, L., Sai, G., Singh, O.A., 2015. Non-enclosure methods for non-suspended microalgae cultivation: literature review and research needs. Renew. Sustain. Energy Rev. 42, 1418–1427.

Kawamura, T., 1996. The role of benthic diatoms in the early life stages of the Japanese abalone (*Haliotis discus hannai*). Surviv. Strateg. Early Life Stages Mar. Resour. 355–367.

Kesaano, M., Gardner, R.D., Moll, K., Lauchnor, E., Gerlach, R., Peyton, B.M., Sims, R.C., 2015. Dissolved inorganic carbon enhanced growth, nutrient uptake, and lipid accumulation in wastewater grown microalgal biofilms. Bioresour. Technol. 180, 7–15.

Kesaano, M., Sims, R.C., 2014. Algal biofilm based technology for wastewater treatment. Algal Res. 5, 231–240.

Kim, B., Lee, J., Noh, J., Bae, H., Lee, C., Ha, H.J., Hwang, K., Kim, D.-U., Kwon, B.-O., Ha, H.K., 2021. Spatiotemporal variation of extracellular polymeric substances (EPS) associated with the microphytobenthos of tidal flats in the Yellow Sea. Mar. Pollut. Bull. 171, 112780.

Kirsten, K.L., Fell, J., Frenzel, P., Meschner, S., Kasper, T., Wündsch, M., Meadows, M., Haberzettl, T., 2018. The spatial heterogeneity of micro-and meio-organisms and their significance in understanding coastal system dynamics. Estuar. Coast. Shelf Sci. 213, 98–107.

Koizumi, I., Yamamoto, H., 2018. Diatom ooze and diatomite–diatomaceous sediments in and around the North Pacific Ocean. JAMSTEC Rep. Res. Dev. 27, 26–46.

Kolbe, F., Brunner, E., 2022. Silicic acid uptake and storage by diatoms, in: Falciatore, A., Mock, T. (Eds.), The Molecular Life of Diatoms. Springer, pp. 345–365.

Kooistra, W.H., Gersonde, R., Medlin, L.K., Mann, D.G., 2007. The origin and evolution of the diatoms: their adaptation to a planktonic existence, in: Evolution of Primary Producers in the Sea. Elsevier.

Korsunsky, A.M., Bedoshvili, Y.D., Cvjetinovic, J., Aggrey, P., Dragnevski, K.I., Gorin, D.A., Salimon, A.I., Likhoshway, Y.V., 2020. Siliceous diatom frustules–A smart nanotechnology platform. Mater. Today Proc. 33, 2032–2040.

Krichnavaruk, S., Powtongsook, S., Pavasant, P., 2007. Enhanced productivity of *Chaetoceros calcitrans* in airlift photobioreactors. Bioresour. Technol. 98, 2123–2130.

Kroth, P., 2007. Molecular biology and the biotechnological potential of diatoms, in: Transgenic Microalgae as Green Cell Factories. Springer, pp. 23–33.

Kuczynska, P., Jemiola-Rzeminska, M., Strzalka, K., 2015. Photosynthetic pigments in diatoms. Mar. Drugs 13, 5847–5881.

Kuehl, L.M., 2020. Survival, growth, and radula morphology of postlarval pinto abalone (*Haliotis kamtschatkana*) when fed six species of benthic diatoms [master's thesis]. Western Washington University.

Kumar, S., Baweja, P., Sahoo, D., 2015. Diatoms: Yellow or golden brown algae, in: The Algae World. Springer, pp. 235–258.

Kwon, H.K., Oh, S.J., Yang, H.-S., 2013. Growth and uptake kinetics of nitrate and phosphate by benthic microalgae for phytoremediation of eutrophic coastal sediments. Bioresour. Technol. 129, 387–395.

Lain, L.R., Bernard, S., 2018. The fundamental contribution of phytoplankton spectral scattering to ocean colour: implications for satellite detection of phytoplankton community structure. Appl. Sci. 8, 2681.

Laviale, M., Beaussart, A., Allen, J., Quilès, F., El-Kirat-Chatel, S., 2019. Probing the adhesion of the common freshwater diatom *Nitzschia palea* at nanoscale. ACS Appl. Mater. Interfaces 11, 48574–48582.

Lebeau, T., Robert, J.-M., 2003a. Diatom cultivation and biotechnologically relevant products. Part II: Current and putative products. Appl. Microbiol. Biotechnol. 60, 624–632.

Lebeau, T., Robert, J.-M., 2003b. Diatom cultivation and biotechnologically relevant products. Part I: Cultivation at various scales. Appl. Microbiol. Biotechnol. 60, 612–623.

Leblanc, K., Queguiner, B., Diaz, F., Cornet, V., Michel-Rodriguez, M., Durrieu de Madron, X., Bowler, C., Malviya, S., Thyssen, M., Grégori, G., 2018. Nanoplanktonic diatoms are globally overlooked but play a role in spring blooms and carbon export. Nat. Commun. 9, 953.

Lecointe, C., Coste, M., Prygiel, J. 1, 1993. "Omnidia": software for taxonomy, calculation of diatom indices and inventories management. Hydrobiologia 269, 509–513.

Lee, J.-B., Hayashi, K., Hirata, M., Kuroda, E., Suzuki, E., Kubo, Y., Hayashi, T., 2006. Antiviral sulfated polysaccharide from *Navicula directa*, a diatom collected from deep-sea water in Toyama Bay. Biol. Pharm. Bull. 29, 2135–2139.

Lee, R., Nevenzel, J., Paffenhöfer, G.-A., 1971. Importance of wax esters and other lipids in the marine food chain: phytoplankton and copepods. Mar. Biol. 9, 99–108.

Lee, Seung-Hoon, Oh, H.-M., Jo, B.-H., Lee, S.-A., Shin, S.-Y., Kim, H.-S., Lee, Sang-Hyup, Ahn, C.-Y., 2014. Higher biomass productivity of microalgae in an attached growth system, using wastewater. J. Microbiol. Biotechnol. 24, 1566–1573.

Leng, X., Hsu, K.-N., Austic, R.E., 2014. Effect of dietary defatted diatom biomass on egg production and quality of laying hens. J. Anim. Sci. Biotechnol. 5, 1–7.

Li, H.-Y., Lu, Y., Zheng, J.-W., Yang, W.-D., Liu, J.-S., 2014. Biochemical and genetic engineering of diatoms for polyunsaturated fatty acid biosynthesis. Mar. Drugs 12, 153–166.

Li, T., Piltz, B., Podola, B., Dron, A., de Beer, D., Melkonian, M., 2016. Microscale profiling of photosynthesis-related variables in a highly productive biofilm photobioreactor. Biotechnol. Bioeng. 113, 1046–1055.

Li, Y., Gao, J., Meng, F., Chi, J., 2015. Enhanced biodegradation of phthalate acid esters in marine sediments by benthic diatom *Cylindrotheca closterium*. Sci. Total Environ. 508, 251–257.

Lippemeier, S., Hartig, P., Colijn, F., 1999. Direct impact of silicate on the photosynthetic performance of the diatom *Thalassiosira weissflogii* assessed by on-and off-line PAM fluorescence measurements. J. Plankton Res. 21.

Liu, T., Wang, J., Hu, Q., Cheng, P., Ji, B., Liu, J., Chen, Y., Zhang, W., Chen, X., Chen, L., 2013. Attached cultivation technology of microalgae for efficient biomass feedstock production. Bioresour. Technol. 127, 216–222.

Liu, Y., El Masoudi, A., Pronk, J.T., van Gulik, W.M., 2019. Quantitative physiology of non-energy-limited retentostat cultures of *Saccharomyces cerevisiae* at near-zero specific growth rates. Appl. Environ. Microbiol. 85, e01161-19.

Lobo, E.A., Heinrich, C.G., Schuch, M., Wetzel, C.E., Ector, L., 2016. Diatoms as bioindicators in rivers, in: Necchi Jr., O. (Ed.), River Algae. Springer International Publishing, pp. 245–271.

Lohrer, A.M., Thrush, S.F., Gibbs, M.M., 2004. Bioturbators enhance ecosystem function through complex biogeochemical interactions. Nature 431, 1092–1095.

Losic, D., Korunic, Z., 2017. Diatomaceous earth, a natural insecticide for stored grain protection: Recent progress and perspectives, in: Losic, D. (Ed.), Diatom Nanotechnology: Progress and Emerging Applications, Nanoscience & Nanotechnology. p. 270.

Lu, H., Roeder, L.B., Powers, J.M., 2003. Effect of polishing systems on the surface roughness of microhybrid composites. J. Esthet. Restor. Dent. 15, 297–304.

Lupette, J., Jaussaud, A., Seddiki, K., Morabito, C., Brugière, S., Schaller, H., Kuntz, M., Putaux, J.-L., Jouneau, P.-H., Rébeillé, F., 2019. The architecture of lipid droplets in the diatom *Phaeodactylum tricornutum*. Algal Res. 38, 101415.

Mann, D.G., Droop, S.J.M., 1996. Biodiversity, biogeography and conservation of diatoms, in: Kristiansen, J. (Ed.), Biogeography of Freshwater Algae. Springer Netherlands, Dordrecht, pp. 19–32. https://doi.org/10.1007/978-94-017-0908-8_2

Mann, D.G., Vanormelingen, P., 2013. An inordinate fondness? The number, distributions, and origins of diatom species. J. Eukaryot. Microbiol. 60, 414–420.

Mannix-Fisher, E., 2021. Exploring the antimicrobial efficacy of silver acetate against *Acinetobacter baumannii* and development of an in vitro biofilm model.

Marchan, S., Rajhbeharrysingh, A., Bascombe, K., Smith, W., 2023. Qualitative Characterization of the Abrasive Component of Charcoal-Containing Toothpastes and the Effect on Dentin Roughness. Int. J. Odontostomatol. 17, 346–355.

Marella, T.K., López-Pacheco, I.Y., Parra-Saldívar, R., Dixit, S., Tiwari, A., 2020. Wealth from waste: Diatoms as tools for phycoremediation of wastewater and for obtaining value from the biomass. Sci. Total Environ. 724, 137960.

Marshall, K., Stout, R., Mitchell, R., 1971. Mechanism of the initial events in the sorption of marine bacteria to surfaces. Microbiology 68, 337–348.

Masojídek, J., Gómez-Serrano, C., Ranglová, K., Cicchi, B., Encinas Bogeat, Á., Câmara Manoel, J.A., Sanches Zurano, A., Silva Benavides, A.M., Barceló-Villalobos, M., Robles Carnero, V.A., 2022. Photosynthesis monitoring in microalgae cultures grown on municipal wastewater as a nutrient source in large-scale outdoor bioreactors. Biology 11, 1380.

McCoy, W., Bryers, J., Robbins, J., Costerton, J., 1981. Observations of fouling biofilm formation. Can. J. Microbiol. 27, 910–917.

McGee, D., Laws, R.A., Cahoon, L.B., 2008. Live benthic diatoms from the upper continental slope: extending the limits of marine primary production. Mar. Ecol. Prog. Ser. 356, 103–112.

McNair, H.M., Brzezinski, M.A., Till, C.P., Krause, J.W., 2018. Taxon-specific contributions to silica production in natural diatom assemblages. Limnol. Oceanogr. 63, 1056–1075.

Medlin, L., 2014. Evolution of the diatoms: VIII. Re-Exam. SSU-Rrna Gene Using Mult. Outgroups Cladistic Anal. Valve Featur. J Biodivers Bioprospect Dev 50, 129.

Medlin, L.K., 2016. Evolution of the diatoms: major steps in their evolution and a review of the supporting molecular and morphological evidence. Phycologia 55, 79–103.

Medlin, L.K., 2009. The use of the terms centric and pennate. Diatom Res. 24, 499–501.

Méléder, V., Barillé, L., Launeau, P., Carrère, V., Rincé, Y., 2003. Spectrometric constraint in analysis of benthic diatom biomass using monospecific cultures. Remote Sens. Environ. 88, 386–400.

Méléder, V., Rincé, Y., Barillé, L., Gaudin, P., Rosa, P., 2007. Spatiotemporal changes in microphytobenthos assemblages in a macrotidal flat (Bourgneuf Bay, France) 1. J. Phycol. 43, 1177–1190.

Mercado, J.M., del Pilar Sánchez-Saavedra, M., Correa-Reyes, G., Lubián, L., Montero, O., Figueroa, F.L., 2004. Blue light effect on growth, light absorption characteristics and photosynthesis of five benthic diatom strains. Aquat. Bot. 78, 265–277.

Michelle Wood, A., Everroad, R., Wingard, L., 2005. Measuring growth rates in microalgal cultures, in: Andersen, R.A. (Ed.), Algal Culturing Techniques. Elsevier, p. 269.

Milagros, R., Bautista, J.I., Buen-Ursua, S.M., Bayona, N., Tupaz, S., Tigbauan, I., 2010. Settlement, growth and survival of the donkey's ear abalone *Haliotis asinina* (Linne) in response to diatom diets and attachment substrate. Philipp. J. Sci. 139, 27–34.

Miranda, A.F., Ramkumar, N., Andriotis, C., Höltkemeier, T., Yasmin, A., Rochfort, S., Wlodkowic, D., Morrison, P., Roddick, F., Spangenberg, G., 2017. Applications of microalgal biofilms for wastewater treatment and bioenergy production. Biotechnol. Biofuels 10, 120.

Mitchell, J.G., Seuront, L., Doubell, M.J., Losic, D., Voelcker, N.H., Seymour, J., Lal, R., 2013. The role of diatom nanostructures in biasing diffusion to improve uptake in a patchy nutrient environment. PLoS One 8.

Molino, P.J., Wetherbee, R., 2008. The biology of biofouling diatoms and their role in the development of microbial slimes. Biofouling 24, 365–379.

Moore, E.R., Bullington, B.S., Weisberg, A.J., Jiang, Y., Chang, J., Halsey, K.H., 2017. Morphological and transcriptomic evidence for ammonium induction of sexual reproduction in *Thalassiosira pseudonana* and other centric diatoms. PLoS One 12, e0181098.

Morales, M., Bonnefond, H., Bernard, O., 2020. Rotating algal biofilm versus planktonic cultivation: LCA perspective. J. Clean. Prod. 257, 120547.

Mouget, J.-L., Gastineau, R., Davidovich, O., Gaudin, P., Davidovich, N.A., 2009. Light is a key factor in triggering sexual reproduction in the pennate diatom *Haslea ostrearia*. FEMS Microbiol. Ecol. 69, 194–201.

Moxley, K., Coyne, V.E., 2020. Improved growth and survival of post-larval *Haliotis midae* in response to probiotic biofilm diets. Aquaculture 519, 734929.

Mulbry, W.W., Wilkie, A.C., 2001. Growth of benthic freshwater algae on dairy manures. J. Appl. Phycol. 13, 301–306.

Murdock, J.N., Dodds, W.K., 2007. Linking benthic algal biomass to stream substratum topography. J. Phycol. 43, 449–460.

Murphy, T.E., Berberoglu, H., 2014. Flux balancing of light and nutrients in a biofilm photobioreactor for maximizing photosynthetic productivity. Biotechnol. Prog. 30, 348–359.

Naumann, T., Çebi, Z., Podola, B., Melkonian, M., 2013. Growing microalgae as aquaculture feeds on twin-layers: a novel solid-state photobioreactor. J. Appl. Phycol. 25, 1413–1420.

Nicklisch, A., 1998. Growth and light absorption of some planktonic cyanobacteria, diatoms and Chlorophyceae under simulated natural light fluctuations. J. Plankton Res. 20, 105–119.

Niu, Y.-F., Zhang, M.-H., Li, D.-W., Yang, W.-D., Liu, J.-S., Bai, W.-B., Li, H.-Y., 2013. Improvement of neutral lipid and polyunsaturated fatty acid biosynthesis by overexpressing a type 2

diacylglycerol acyltransferase in marine diatom *Phaeodactylum tricornutum*. Mar. Drugs 11, 4558–4569.

Not, F., Siano, R., Kooistra, W.H., Simon, N., Vaulot, D., Probert, I., 2012. Diversity and ecology of eukaryotic marine phytoplankton, in: Advances in Botanical Research. Elsevier, pp. 1–53.

Nowack, E.C., Podola, B., Melkonian, M., 2005. The 96-well twin-layer system: a novel approach in the cultivation of microalgae. Protist 156, 239–251.

Oakes, J.M., Eyre, B.D., 2014. Transformation and fate of microphytobenthos carbon in subtropical, intertidal sediments: potential for long-term carbon retention revealed by ^{13}C-labeling. Biogeosciences 11, 1927–1940.

Orandi, S., Lewis, D., Moheimani, N., 2012. Biofilm establishment and heavy metal removal capacity of an indigenous mining algal-microbial consortium in a photo-rotating biological contactor. J. Ind. Microbiol. Biotechnol. 39, 1321–1331.

Orefice, I., Di Dato, V., Sardo, A., Lauritano, C., Romano, G., 2022. Lipid mediators in marine diatoms. Aquat. Ecol. 56, 377–397.

Osorio, J.H.M., Pollio, A., Frunzo, L., Lens, P.N.L., Esposito, G., 2021. A review of microalgal biofilm technologies: definition, applications, settings and analysis. Front. Chem. Eng. 3, 737710.

Osuna-Cruz, C.M., Bilcke, G., Vancaester, E., De Decker, S., Bones, A.M., Winge, P., Poulsen, N., Bulankova, P., Verhelst, B., Audoor, S., 2020. The *Seminavis robusta* genome provides insights into the evolutionary adaptations of benthic diatoms. Nat. Commun. 11, 1–13.

Ozkan, A., Berberoglu, H., 2013. Cell to substratum and cell to cell interactions of microalgae. Colloids Surf. B Biointerfaces 112, 302–309.

Ozkan, A., Kinney, K., Katz, L., Berberoglu, H., 2012. Reduction of water and energy requirement of algae cultivation using an algae biofilm photobioreactor. Bioresour. Technol. 114, 542–548.

Palma, H., Killoran, E., Sheehan, M., Berner, F., Heimann, K., 2017. Assessment of microalga biofilms for simultaneous remediation and biofuel generation in mine tailings water. Bioresour. Technol. 234, 327–335.

Paterson, D., 1995. Biogenic structure of early sediment fabric visualized by low-temperature scanning electron microscopy. J. Geol. Soc. 152, 131–140.

Pavarina, A.C., Dovigo, L.N., Sanitá, P.V., Machado, A.L., Giampaolo, E.T., Vergani, C.E., 2011. Dynamic models for in vitro biofilm formation, in: Bailey, W.C. (Ed.), Biofilms: Formation, Development and Properties. Nova Science Publishers, Inc., Hauppauge, NY, pp. 125–162.

Philippe, H., Sörhannus, U., Baroin, A., Perasso, R., Gasse, F., Adoutte, A., 1994. Comparison of molecular and paleontological data in diatoms suggests a major gap in the fossil record. J. Evol. Biol. 7, 247–265.

Podola, B., Li, T., Melkonian, M., 2017. Porous substrate bioreactors: a paradigm shift in microalgal biotechnology? Trends Biotechnol. 35, 121–132.

Posadas, E., Bochon, S., Coca, M., García-González, M., García-Encina, P., Muñoz, R., 2014. Microalgae-based agro-industrial wastewater treatment: a preliminary screening of biodegradability. J. Appl. Phycol. 26, 2335–2345.

Posadas, E., García-Encina, P.-A., Soltau, A., Domínguez, A., Díaz, I., Muñoz, R., 2013. Carbon and nutrient removal from centrates and domestic wastewater using algal–bacterial biofilm bioreactors. Bioresour. Technol. 139, 50–58.

Poulíčková, A., Mann, D.G., 2019. Diatom sexual reproduction and life cycles, in: Seckbach, J., Gordon, R. (Eds.), Diatoms: Fundamentals and Applications. Scrivener Publishing LLC, Hoboken, New Jersey, pp. 245–272.

Prestegard, S.K., Oftedal, L., Coyne, R.T., Nygaard, G., Skjærven, K.H., Knutsen, G., Døskeland, S.O., Herfindal, L., 2009. Marine benthic diatoms contain compounds able to induce leukemia cell death and modulate blood platelet activity. Mar. Drugs 7, 605–623.

Pulz, O., 2001. Photobioreactors: production systems for phototrophic microorganisms. Appl. Microbiol. Biotechnol. 57, 287–293.

Qureshi, N., Annous, B.A., Ezeji, T.C., Karcher, P., Maddox, I.S., 2005. Biofilm reactors for industrial bioconversion processes: employing potential of enhanced reaction rates. Microb. Cell Factories 4, 1–21.

Rabiee, N., Khatami, M., Jamalipour Soufi, G., Fatahi, Y., Iravani, S., Varma, R.S., 2021. Diatoms with invaluable applications in nanotechnology, biotechnology, and biomedicine: recent advances. ACS Biomater. Sci. Eng. 7, 3053–3068.

Ragni, R., Cicco, S.R., Vona, D., Farinola, G.M., 2017. Nanostructured silica from diatoms microalgae: smart materials for photonics and electronics, in: Irimia-Vladu, M., Glowacki, E.D., Sariciftci, N.S., Bauer, S. (Eds.), Green Materials for Electronics. John Wiley & Sons, pp. 287–313.

Rezvani, S., Saadaoui, I., Al Jabri, H., Moheimani, N.R., 2022. Techno-economic modelling of high-value metabolites and secondary products from microalgae cultivated in closed photobioreactors with supplementary lighting. Algal Res. 65, 102733.

Richmond, A., 1986. Outdoor mass cultures of microalgae, in: Handbook of Microalgal Mass Culture. CRC Press, pp. 285–330.

Rijstenbil, J., 2003. Effects of UVB radiation and salt stress on growth, pigments and antioxidative defence of the marine diatom *Cylindrotheca closterium*. Mar. Ecol. Prog. Ser. 254, 37–48.

Rimet, F., Gusev, E., Kahlert, M., Kelly, M.G., Kulikovskiy, M., Maltsev, Y., Mann, D.G., Pfannkuchen, M., Trobajo, R., Vasselon, V., 2019. Diat. barcode, an open-access curated barcode library for diatoms. Sci. Rep. 9, 15116.

Rodolfi, L., Chini Zittelli, G., Bassi, N., Padovani, G., Biondi, N., Bonini, G., Tredici, M.R., 2009. Microalgae for oil: Strain selection, induction of lipid synthesis and outdoor mass cultivation in a low-cost photobioreactor. Biotechnol. Bioeng. 102, 100–112.

Roeselers, G., Van Loosdrecht, M.C., Muyzer, G., 2008. Phototrophic biofilms and their potential applications. J. Appl. Phycol. 20, 227–235.

Romero-Romero, C.C., del Pilar Sánchez-Saavedra, M., 2017. Effect of light quality on the growth and proximal composition of *Amphora* sp. J. Appl. Phycol. 29, 1203–1211.

Round, F.E., Crawford, R.M., Mann, D.G., 1990. Diatoms: biology and morphology of the genera. Cambridge university press.

Russo, E., Ianora, A., Carotenuto, Y., 2019. Re-shaping marine plankton communities: Effects of diatom oxylipins on copepods and beyond. Mar. Biol. 166, 1–11.

Rynearson, T.A., Bishop, I.W., Collins, S., 2022. The population genetics and evolutionary potential of diatoms, in: Falciatore, A., Mock, T. (Eds.), The Molecular Life of Diatoms. Springer, pp. 29–57.

Sabir, J.S., Theriot, E.C., Manning, S.R., Al-Malki, A.L., Khiyami, M.A., Al-Ghamdi, A.K., Sabir, M.J., Romanovicz, D.K., Hajrah, N.H., El Omri, A., 2018. Phylogenetic analysis and a review of the history of the accidental phytoplankter, *Phaeodactylum tricornutum* Bohlin (Bacillariophyta). PLOS One 13, e0196744.

Salmaso, F., Quadroni, S., Compare, S., Gentili, G., Crosa, G., 2019. Benthic diatoms as bioindicators of environmental alterations in different watercourses of northern Italy. Environ. Monit. Assess. 191, 1–17.

Sansone, C., Del Mondo, A., Pistelli, L., Smerilli, A., Saggiomo, M., Brunet, C., n.d. Opportunities and challenges of diatom cell factory for human health, in: Goessling, J.W., Serôdio, J., Lavaud, J. (Eds.), Diatom Photosynthesis: From Primary Production to High Value Molecules. Wiley Scrivener, Beverly, Mass.

Sapieha, P., Stahl, A., Chen, J., Seaward, M.R., Willett, K.L., Krah, N.M., Dennison, R.J., Connor, K.M., Aderman, C.M., Liclican, E., 2011. 5-Lipoxygenase metabolite 4-HDHA is a mediator of the antiangiogenic effect of ω-3 polyunsaturated fatty acids. Sci. Transl. Med. 3, 69ra12-69ra12.

Sato, S., Nanjappa, D., Dorrell, R.G., Vieira, F.R.J., Kazamia, E., Tirichine, L., Veluchamy, A., Heilig, R., Aury, J.-M., Jaillon, O., 2020. Genome-enabled phylogenetic and functional reconstruction of an araphid pennate diatom *Plagiostriata* sp. CCMP470, previously assigned as a radial centric diatom, and its bacterial commensal. Sci. Rep. 10, 9449.

Scarsini, M., Marchand, J., Manoylov, K.M., Schoefs, B., 2019. Photosynthesis in diatoms, in: Seckbach, J., Gordon, R. (Eds.), Diatoms: Fundamentals and Applications. Scrivener Publishing LLC, pp. 191–211.

Schnurr, P.J., Espie, G.S., Allen, D.G., 2013. Algae biofilm growth and the potential to stimulate lipid accumulation through nutrient starvation. Bioresour. Technol. 136, 337–344.

Schultze, L.K., Simon, M.-V., Li, T., Langenbach, D., Podola, B., Melkonian, M., 2015. High light and carbon dioxide optimize surface productivity in a Twin-Layer biofilm photobioreactor. Algal Res. 8, 37–44.

Sebestyén, P., Blanken, W., Bacsa, I., Tóth, G., Martin, A., Bhaiji, T., Dergez, Á., Kesserű, P., Koós, Á., Kiss, I., 2016. Upscale of a laboratory rotating disk biofilm reactor and evaluation of its performance over a half-year operation period in outdoor conditions. Algal Res. 18, 266–272.

Sharma, K.K., Garg, S., Li, Y., Malekizadeh, A., Schenk, P.M., 2013. Critical analysis of current microalgae dewatering techniques. Biofuels 4, 397–407.

Sharma, N., Simon, D.P., Diaz-Garza, A.M., Fantino, E., Messaabi, A., Meddeb-Mouelhi, F., Germain, H., Desgagné-Penix, I., 2021. Diatoms biotechnology: various industrial applications for a greener tomorrow. Front. Mar. Sci. 8, 636613.

Shen, Y., Zhu, W., Chen, C., Nie, Y., Lin, X., 2016. Biofilm formation in attached microalgal reactors. Bioprocess Biosyst. Eng. 39, 1281–1288.

Shi, J., Podola, B., Melkonian, M., 2014. Application of a prototype-scale Twin-Layer photobioreactor for effective N and P removal from different process stages of municipal wastewater by immobilized microalgae. Bioresour. Technol. 154, 260–266.

Shi, J., Podola, B., Melkonian, M., 2007. Removal of nitrogen and phosphorus from wastewater using microalgae immobilized on twin layers: an experimental study. J. Appl. Phycol. 19, 417–423.

Shi, P., Shen, H., Wang, W., Yang, Q., Xie, P., 2016. Habitat-specific differences in adaptation to light in freshwater diatoms. J. Appl. Phycol. 28, 227–239.

Singh, G., Patidar, S., 2018. Microalgae harvesting techniques: a review. J. Environ. Manage. 217, 499–508.

Singh, P.K., Saxena, A., Tiwari, A., in press. Diatom-based bioproducts, and the potential of frustules in drug delivery, in: Goessling, J.W., Serôdio, J., Lavaud, J. (Eds.), Diatom Photosynthesis: From Primary Production to High Value Molecules. Wiley Scrivener, Beverly, Mass.

Sma-Air, S., Ritchie, R.J., 2021. Spectrofluorometric Insights into the Application of PAM Fluorometry in Photosynthetic Research. Photochem. Photobiol. 97, 991–1000.

Smetacek, V., 1985. Role of sinking in diatom life-history cycles: ecological, evolutionary and geological significance. Mar. Biol. 84, 239–251.

Snoeijs, P., Busse, S., Potapova, M., 2002. The importance of diatom cell size in community analysis. J. Phycol. 38, 265–281.

Stal, L., De Brouwer, J., 2003. Biofilm formation by benthic diatoms and their influence on the stabilization of intertidal mudflats. Berichte-Forschungszentrum Terramare 12, 109–111.

Tanaka, T., Yoneda, K., Maeda, Y., 2022. Lipid Metabolism in Diatoms, in: Falciatore, A., Mock, T. (Eds.), The Molecular Life of Diatoms. Springer, pp. 493–527.

Teughels, W., Van Assche, N., Sliepen, I., Quirynen, M., 2006. Effect of material characteristics and/or surface topography on biofilm development. Clin. Oral Implants Res. 17, 68–81.

Tong, C., Chang, Y.S., Ooi, B.S., Chan, D.J.C., 2021. Physico-chemistry and adhesion kinetics of algal biofilm on polyethersulfone (PES) membrane with different surface wettability. J. Environ. Chem. Eng. 9, 106531.

Tong, C., Derek, C., 2022. Membrane surface roughness promotes rapid initial cell adhesion and long term microalgal biofilm stability. Environ. Res. 206, 112602.

Toyofuku, M., Inaba, T., Kiyokawa, T., Obana, N., Yawata, Y., Nomura, N., 2016. Environmental factors that shape biofilm formation. Biosci. Biotechnol. Biochem. 80, 7–12.

Underwood, G., Perkins, R.G., Consalvey, M.C., Hanlon, A., Oxborough, K., Baker, N., Paterson, D., 2005. Patterns in microphytobenthic primary productivity: Species-specific variation in migratory rhythms and photosynthetic efficiency in mixed-species biofilms. Limnol. Oceanogr. 50, 755–767.

Underwood, G.C., Kromkamp, J., 1999. Primary production by phytoplankton and microphytobenthos in estuaries. Adv. Ecol. Res. 29, 93–153.

Underwood, G.J.C., n.d. Extracellular polymeric substance production by benthic pennate diatoms, in: Goessling, J.W., Serôdio, J., Lavaud, J. (Eds.), Diatom Photosynthesis: From Primary Production to High Value Molecules. Wiley Scrivener, Beverly, Mass.

Vadiveloo, A., Moheimani, N.R., Cosgrove, J.J., Bahri, P.A., Parlevliet, D., 2015. Effect of different light spectra on the growth and productivity of acclimated *Nannochloropsis* sp. (Eustigmatophyceae). Algal Res. 8, 121–127.

Van Loosdrecht, M., Heijnen, J., Eberl, H., Kreft, J., Picioreanu, C., 2002. Mathematical modelling of biofilm structures. Antonie Van Leeuwenhoek 81, 245–256.

Van Oss, C., 1993. Acid—base interfacial interactions in aqueous media. Colloids and Surfaces A: Physicochemical and Engineering Aspects 78, 1–49.

Vázquez-Nion, D., Fuentes, E., Prieto, B., 2020. Effect of inorganic carbon concentration on the development of subaerial phototrophic biofilms on granite. Coatings 10, 1049.

Viana, M.T., Correa, G., Lazo, J.P., Frías-Díaz, R., Durazo-Beltrán, E., Vasquez-Pelaez, C., 2007. Digestive physiology and metabolism of green abalone *Haliotis fulgens* from postlarvae to juvenile, fed three different diatoms. Aquaculture 271, 449–460.

Vinayak, V., Joshi, K.B., Sarma, P.M., 2019. Diafuel™(diatom biofuel) vs electric vehicles, a basic comparison: a high potential renewable energy source to make India energy independent, in: Seckbach, J., Gordon, R. (Eds.), Diatoms: Fundamentals and Applications. Wiley Online Library, pp. 537–582.

Virta, L., Gammal, J., Järnström, M., Bernard, G., Soininen, J., Norkko, J., Norkko, A., 2019. The diversity of benthic diatoms affects ecosystem productivity in heterogeneous coastal environments. Ecology 100, e02765.

Wan, M., Hou, D., Li, Y., Fan, J., Huang, J., Liang, S., Wang, W., Pan, R., Wang, J., Li, S., 2014. The effective photoinduction of *Haematococcus pluvialis* for accumulating astaxanthin with attached cultivation. Bioresour. Technol. 163, 26–32.

Wang, J., Liu, Q., Zhao, X., Borthwick, A.G., Liu, Y., Chen, Q., Ni, J., 2019. Molecular biogeography of planktonic and benthic diatoms in the Yangtze River. Microbiome 7, 1–15.

Wang, J., Liu, W., Liu, T., 2017. Biofilm based attached cultivation technology for microalgal biorefineries—a review. Bioresour. Technol. 244, 1245–1253.

Wang, J.-K., Seibert, M., 2017. Prospects for commercial production of diatoms. Biotechnol. Biofuels 10, 16.

Wang, Y., Zhang, D., Cai, J., Pan, J., Chen, M., Li, A., Jiang, Y., 2012. Biosilica structures obtained from *Nitzschia*, *Ditylum*, *Skeletonema*, and *Coscinodiscus* diatom by a filtration-aided acid cleaning method. Appl. Microbiol. Biotechnol. 95, 1165–1178.

Wehr, J.D., Sheath, R.G., Kociolek, J.P., 2015. Freshwater algae of North America: ecology and classification. Elsevier.

Wen, Z.-Y., Chen, F., 2000. Production potential of eicosapentaenoic acid by the diatom *Nitzschia laevis*. Biotechnol. Lett. 22, 727–733.

Westall, F., de Wit, M.J., Dann, J., van der Gaast, S., de Ronde, C.E., Gerneke, D., 2001. Early Archean fossil bacteria and biofilms in hydrothermally-influenced sediments from the Barberton greenstone belt, South Africa. Precambrian Res. 106, 93–116.

Wiktorowska-Owczarek, A., Berezinska, M., Nowak, J.Z., 2015. PUFAs: structures, metabolism and functions. Adv. Clin. Exp. Med. 24, 931–941.

Williams, D.M., Kociolek, J.P., 2011. An overview of diatom classification with some prospects for the future, in: Seckbach, J., Kociolek, J.P. (Eds.), The Diatom World. Springer, pp. 47–91.

Williams, D.M., Kociolek, J.P., 2007. Pursuit of a natural classification of diatoms: History, monophyly and the rejection of paraphyletic taxa. Eur. J. Phycol. 42, 313–319.

Winogradsky, S., 1928. The direct method in soil microbiology and its application to the study of nitrogen fixation. Soil Sci. 25, 37–44.

Wolf, G., Picioreanu, C., van Loosdrecht, M.C., 2007. Kinetic modeling of phototrophic biofilms: the PHOBIA model. Biotechnol. Bioeng. 97, 1064–1079.

Wolfstein, K., Stal, L.J., 2002. Production of extracellular polymeric substances (EPS) by benthic diatoms: effect of irradiance and temperature. Mar. Ecol. Prog. Ser. 236, 13–22.

Wood, J.L., Takemoto, J.Y., Sims, R.C., 2022. Rotating algae biofilm reactor for management and valorization of produced wastewater. Front. Energy Res. 10.

Wulff, A., Zacher, K., Hanelt, D., Al-Handal, A., Wiencke, C., 2008. UV radiation-a threat to Antarctic benthic marine diatoms? Antarct. Sci. 20, 13–20.

Xu, L., Weathers, P.J., Xiong, X., Liu, C., 2009. Microalgal bioreactors: challenges and opportunities. Eng. Life Sci. 9, 178–189.

Xuan, R.N., Mouget, J.-L., Turpin, V., Jaouen, P., Pruvost, J., 2021. Optimization of the growth and marennine production by the diatom *Haslea ostrearia* in photobioreactor. Algal Res. 55, 102251.

Young, E.B., Beardall, J., 2003. Photosynthetic function in *Dunaliella tertiolecta* (Chlorophyta) during a nitrogen starvation and recovery cycle. J. Phycol. 39, 897–905.

Zamalloa, C., Boon, N., Verstraete, W., 2013. Decentralized two-stage sewage treatment by chemical–biological flocculation combined with microalgae biofilm for nutrient immobilization in a roof installed parallel plate reactor. Bioresour. Technol. 130, 152–160.

Zhang, L., Chen, L., Wang, J., Chen, Y., Gao, X., Zhang, Z., Liu, T., 2015. Attached cultivation for improving the biomass productivity of *Spirulina platensis*. Bioresour. Technol. 181, 136–142.

Zhou, W., Lu, Q., Han, P., Li, J., 2020. Microalgae cultivation and photobioreactor design, in: Microalgae Cultivation for Biofuels Production. Elsevier, pp. 31–50.

Zhuang, L.-L., Hu, H.-Y., Wu, Y.-H., Wang, T., Zhang, T.-Y., 2014. A novel suspended-solid phase photobioreactor to improve biomass production and separation of microalgae. Bioresour. Technol. 153, 399–402.

Zhuang, L.-L., Yu, D., Zhang, J., Liu, F., Wu, Y.-H., Zhang, T.-Y., Dao, G.-H., Hu, H.-Y., 2018. The characteristics and influencing factors of the attached microalgae cultivation: A review. Renew. Sustain. Energy Rev. 94, 1110–1119.

Zimmermann, J., Abarca, N., Enk, N., Skibbe, O., Kusber, W.-H., Jahn, R., 2014. Taxonomic reference libraries for environmental barcoding: a best practice example from diatom research. PLoS One 9, e108793.

Zobell, C., Allen, E.C., 1933. Attachment of marine bacteria to submerged slides. Proc. Soc. Exp. Biol. Med. 30, 1409–1411.

COLLEGE VEGETAL
DOCTORAL ANIMAL, ALIMENT
PAYS DE LA LOIRE MER, ENVIRONNEMENT

Nantes Université

Titre : Etude eco-physiologique de la diatomée benthique *Amphora* sp. : optimisation des conditions de culture, pour une valorisation en santé, cosmétique et nutrition

Mots clés : *Amphora* sp., photobioréacteur à substrat poreux, diatomées benthiques marines, lipides

Résumé : Les diatomées benthiques marines ont la capacité de produire une biomasse de qualité et des composés bioactifs pour diverses applications commerciales. *Amphora* sp. NCC169 est l'une de ces espèces qui produisent des lipides de grande valeur. Cependant, la production de masse d'*Amphora* sp. NCC169 dans un photobioréacteur traditionnel à suspension est rendue difficile par sa sensibilité à l'agitation et aux turbulences. Des cultures d'*Amphora* sp NCC169 ont été mise en place au sein d'un phtobioréacteur de substrat poreux (PSBR) à orientation verticale afin de produire de la biomasse et des lipides. Les résultats ont été comparés à ceux obtenus par une technique plus classique de culture en batch dans des fioles de type Fernbach. Il apparaît une productivité de croissance ($P_{biomasse}$ = 0.5 ± 0.03 g·m^{-2}·j^{-1}) et une production de lipide (P_{lipide} = 0.10 ± 0.02 g·m^{-2}·j^{-1}) plus importante en PSBR. L'étude a également démontré l'impact positif d'une combinaison de longueurs d'onde de lumière rouge (620 - 780 nm) et bleue (440 - 490 nm) sur le taux de production de lipides d'*Amphora* sp. NCC169 en utilisant le PSBR (23,8 ± 2,3 %). Cette recherche met en exergue le succès des cultures en biofilm, et souligne l'importance de respecter la physiologie des Diatomées benthiques afin de générer de la biomasse et des lipides d'intérêt.

Title : Eco-physiological study of the marine benthic diatom *Amphora* sp. : optimization of culture conditions for health, cosmetic and food applications

Keywords : *Amphora* sp., porous substrate photobioreactor, marine benthic diatoms, lipids

Abstract : Marine benthic diatoms have the capacity to produce quality biomass and bioactive compounds for various commercial applications. *Amphora* sp. NCC169 is one of such species that have high-value lipid production. However, mass-production of *Amphora* sp. NCC169 in traditional suspension photobioreactor is challenged by its sensitivity to stirring and turbulence. Cultures of *Amphora* sp. NCC169 were set up in a vertically oriented porous substrate photobioreactor (PSBR) to produce biomass and lipids. Results were compared with those obtained using a more conventional batch culture technique in Fernbach-type flasks. Growth productivity ($P_{biomass}$ = 0.5 ± 0.03 g·m^{-2}·day^{-1}) and lipid production (P_{lipid} = 0.1 ± 0.02 g·m^{-2}·day^{-1}) were higher in PSBR. The study also demonstrated the positive impact of a combination of red (620 - 780 nm) and blue (440 - 490 nm) light wavelengths on the lipid production rate of *Amphora* sp. NCC169 using PSBR (23.8 ± 2.3%). This research highlights the success of biofilm cultures and underlines the importance of respecting the physiology of benthic diatoms in order to generate biomass and lipids of interest.